UNIVERSITY OF CALIFORNIA
RIVERSIDE

Exploring Neural Circuit Development with Reverse Genetics and Intersectional Viral Approaches

A Dissertation submitted in partial satisfaction
of the requirements for the degree of

Doctor of Philosophy

in

Neuroscience

by

Tyler Alexander Vahedi-Hunter

December 2020

Dissertation Committee:
Dr. Martin M. Riccomagno, Chairperson
Dr. Michael E. Adams
Dr. Kelly J. Huffman

The Dissertation of Tyler A. Vahedi-Hunter is approved:

_____

_____

_____

Committee Chairperson

University of California, Riverside

Acknowledgments

The text of this dissertation, in part, is a reprint of the material as it appears in Vahedi-Hunter et al., 2018. The co-author, Martin M. Riccomagno, directed and supervised the research. Co-authors Jason Estep, Kylee A. Rosette, Michael L. Rutlin, and Kevin M. Wright contributed experimental data and suggested edits to the manuscript. Chapter 2 is reproduced in its entirety from the publication, Vahedi-Hunter, T.A., Estep, J.A., Rosette, K.A. *et al.* (2018). Cas adaptor proteins coordinate sensory axon fasciculation. *Scientific Reports, 8***,** 5996. https://doi.org/10.1038/s41598-018-24261-x, under the Creative Commons license.

ABSTRACT OF THE DISSERTATION

Exploring Neural Circuit Development with Reverse Genetics and Intersectional Viral Approaches

by

Tyler A. Vahedi-Hunter

Doctor of Philosophy, Graduate Program in Neuroscience
University of California, Riverside, December 2020
Dr. Martin M. Riccomagno, Chairperson

Proper establishment of connectivity in the nervous system is essential for higher cognitive functions. Progressive and regressive developmental events build and sculpt these circuits to reach functional maturity. A key progressive step during the assembly of neural circuits is the guidance of growing axons. The direction that an axon grows is largely influenced by the degree of adhesion to the extracellular matrix (ECM) substrate, which is locally regulated in response to guidance cues. Adhesion must also be regulated during fasciculation into axon bundles and dissociation for innervation of individual targets. The modulation of adhesion by guidance cues is mediated by intracellular cascades of signaling proteins, of which very little is known. In Aim 1, we provide genetic evidence for the requirement of Cas signaling adaptor proteins in guidance and fasciculation of DRG projections

in mice. Our results demonstrate that Cas proteins play important roles in allowing sensory axons to distinguish between adhesion to the substrate and to other axons.

A critical regressive event during the refinement of neural circuits is the pruning of exuberant synapses and projections. Activity-dependent pruning ensures that only the most functional connections are maintained. Although clearly important for proper connectivity, this developmental process is understudied. An apparent roadblock in the investigation of these refinement events is the need for tools that are able to reversibly modulate neuronal activity for a protracted period of time. In Aim 2, we offer a solution with the design and characterization of the Expression by Boolean Exclusion (ExBoX) system, a simple AAV-based approach to control expression by exclusion logic (AND NOT). This ExBoX system encodes for a gene of interest which is turned ON by a particular recombinase (Cre or FlpO) and turned OFF by another. We show the ability of the ExBoX system to tightly regulate expression of fluorescent reporters both *in vitro* and *in vivo*, and demonstrate the adaptability of the system by achieving expression of a variety of virally-delivered functional manipulations in the mouse brain. This simple strategy will expand the molecular toolkit available for cell- and time-specific gene expression.

Table of Contents

Chapter 4

List of Tables

List of Figures

Chapter 2: Cas Adaptor Proteins Coordinate Sensory Axon Fasciculation

Abbreviations:

Dorsal Root Ganglia (DRG)

Extracellular matrix (ECM)

Dorsal Root Entry Zone (DREZ)

Crk-associated substrate (Cas)

Drosophila Cas (dCas)

Retinal Ganglia Cell (RGC)

Cortico spinal tract (CST)

Infrapyramidal bundle (IFB)

Peripheral nervous system (PNS)

Neuromuscular junction (NMJ)

Central nervous system (CNS)

Climbing fiber (CF)

Purkinje cell (PC)

Lateral geniculate nucleus (LGN)

Designer Receptors Exclusively Activated by Designer Drugs (DREADDs)

Clozapine N-oxide (CNO)

Expression by Boolean Exclusion (ExBoX)

Adeno-Associated Virus (AAV)

Neural crest cells (NCCs)

Focal adhesion kinase (Fak)

Src Homology 2 (SH2)

Ras-related C3 botulinum toxin substrate 1 (Rac1)

Cell division control protein 42 homolog (Cdc42)

Spinal cord (SC)

Gene Expression Nervous System Atlas (GENSAT)

Bacterial artificial chromosome (BAC)

Green fluorescent protein (EGFP)

Wild-type (WT)

Phosphotyrosine-p130Cas (PY-Cas)

Triple conditional knock-out (TcKO)

Small interference RNA (siRNA)

Basement membrane (BM)

Wingless-related integration site (Wnt)

Human tissue plasminogen activator promoter (Ht-PA)

Analysis of variance (Anova)

Honestly significant difference (HSD)

Institutional Animal Care and Use Committee (IACUC)

Neuronal growth factor (NGF)

Hemagglutinin (HA)

Double-floxed Inverse Orientation (DIO)

Dentate Gyrus (DG)

Gene of interest (GOI)

Coding sequence (CDS)

Flippase recognition target (FRT)

Days in vitro (DIV)

Phosphate buffer solution (PBS)

Hanks' balanced salt solution (HBBS)

Paraformaldehyde (PFA)

Red fluorescent protein (RFP)

Region of interest (ROI

Mediodorsal Thalamus (MD)

Medial prefrontal cortex (mPFC)

Chapter 1

Introduction

Development of the Nervous system

Proper establishment of connectivity in the nervous system is essential for higher cognitive functions, including perception, learning and memory. The initial assembly of neural circuitry is carried out by progressive developmental events such as cell proliferation and migration, axon growth and guidance, and synapse formation. These mechanisms must be tightly controlled to ensure cells and their projections reach their proper destinations and targets, respectively. Improper migration that fails to deliver cells to their designated destination often results in severe developmental defects, including embryonic lethality (Rakic et al., 1988; Hirotsune et al., 1998; Sasaki et al., 2005). The consequences of improper axon guidance and synaptogenesis can be just as severe (Bin et al., 2015). However, proper assembly of the nervous system is not the only requirement for functional neural circuitry. As a byproduct of progressive circuit building events, more neurons, projections, and connections than required in the mature system are generated. For this reason, to understand the development of the nervous system requires investigation of not only progressive, but of regressive events as well (Riccomagno & Kolodkin, 2015).

Regressive events, such as programmed cell death, axon and synapse pruning, control the refinement of the nervous system by removing extraneous

neurons, axonal projections, and synaptic connections. These events are indispensable for proper structural organization, the efficient wiring of neural circuitry, and functional maturity of synaptic connections. The importance of cell refinement is demonstrated by the gross morphological defects and embryonic lethality of mice with mutations to the cell death pathway (Kuida et al., 1996; Kuida et al., 1998). Though not usually lethal, improper refinement of neural connectivity has been linked to severe cognitive dysfunction (Lewis and Levitt, 2002; Pardo and Eberhart, 2007; Van Battum et al., 2015). The progressive and regressive events employed to construct a functional neural circuit require participation of a myriad of proteins, signals and cellular interactions. Understanding the key components and interactions that are required for proper establishment and maturation of neural circuitry will be of utmost importance in understanding the etiology of such neurodevelopmental defects. My thesis work focused on examining the mechanisms underlying the establishment and refinement of axonal connectivity.

Axon Guidance

A key step during the assembly of neural circuitry is the guidance of growing axons. As the emerging axon extends towards targets that may be a considerable distance away, it will encounter a variety of guidance signals to dictate the correct pathway to its destination (Tessier-Lavigne & Goodman, 1996). Upon binding to their cognate receptors, guidance cues trigger cytoskeletal remodeling that results

in steering of the axon's growth in the appropriate direction. This response takes place in the specialized process known as the growth cone, which is located at the leading tip of the axon and houses the receptors capable of detecting the ligand guidance signals from the surrounding environment (Dent et al., 2011).

Axon Guidance cues can be found in the form of long-range molecules that act via secretion into the extracellular space, or short-range molecules that require cell-to-cell contact (Raper & Mason, 2010). Furthermore, these ligand cues can exert either attractive or repulsive effects on the navigating growth cone when encountering their cognate receptors. More than half a century of investigation has uncovered four prominent families of guidance cues: Netrins, Ephrins, Semaphorins, and Slits (Kolodkin & Tessier-Lavigne, 2011; Kozalin & Richards, 2016). As demonstrated with loss of function mutations, failure to express these guidance ligands or their receptors during growth of dependent axons has been demonstrated to result in defects of axonal targeting and circuit assembly that are often detrimental to nervous system functionality. For example, disruptions in the *Sema3A* gene in mice produce axon guidance defects in DRG peripheral projections (Kitsukawa et al., 1997); disruptions in Ephrin signaling result in retinal ganglia cell wiring deficits and improper topographic map formation (Feldheim & O'Leary, 2010); and removal of Netrin signaling results in loss of commissural axon attraction to the floorplate and inability to cross the midline of the neural tube (Kennedy et al., 1994; Serafini et al., 1994). Further highlighting the robust

applicability of guidance cues, it has been observed that while some ligands are specialized to confer only one type of directional cue, others like Netrins, Semaphorins and Ephrins, have multiple receptor variants and can have attractive or repulsive effects depending on the type of receptor expressed in the navigating growth cone (Colamarino & Tessier-Lavigne, 1995; Hong et al., 1999; Hindges et al., 2002; Dickson, 2003; Zhou et al., 2008).

Upon encountering guidance cues, the growth cone must respond appropriately by navigating towards or away from the source of the signal. The direction that a growth cone steers is largely influenced by degree of adhesion to the extracellular matrix (ECM) substrate (Kolodkin & Tessier-Lavigne, 2011). Attractive cues have the ability to strengthen growth cone adhesion to the substrate, anchoring the axon in the appropriate orientation for growth towards the attractive source. Degree of attachment to the substrate is regulated by cytoskeletal remodeling of the growth cone's actin (Lowery & Van Vactor, 2009). Actin is locally strengthened where attractive cues are encountered, enhancing the connection between the growth cone and the substrate. In contrast, repulsive cues cause growth cone disassembly and detachment from the substrate, leading to retraction. Actin is locally destabilized by repulsive signaling, weakening the growth cone's hold on the substrate and facilitating growth in a direction with greater affinity.

The processes of axon guidance as described thus far are predominantly applicative for pioneering axons, the leading axons of a particular pathway which act as the pathfinders for the follower axons in waiting. In comparison to the follower axons, pioneers have more complex growth cones and move more slowly through the environment to their target in order to detect and respond to the incoming guidance cues (LoPresti et al., 1973; Bastiani et al., 1984). Loss of pioneer axons will cause the pioneer fate to be adopted by one of the follower axons, which will be influenced by environmental signals to develop the growth cone complexity necessary to detect and respond to environmental guidance cues (Bak & Frasier, 2003; Lim et al., 2015).

Axon Fasciculation

The follower axons of a growing pathway do not require the same specialization for detecting environmental guidance cues because they are able to follow the path established by the pioneers through a process known as axon fasciculation (Van Vactor, 1998; Bak & Frasier, 2003). Axon fasciculation refers to the aggregation of axons into nerve bundles or axon tracts, and aids to ensure that projections traveling towards a particular location arrive without being misled towards a wrong target. The opposing process whereby axons un-bundle from one another is referred to as defasciculation. When axons arrive in their target region, defasciculation is necessary for axons to innervate their independent targets. Improper defasciculation imposed via gain of function mutations of positive

fasciculation regulators has been shown to prevent proper sensory innervation of the periphery (Huang et al., 2007).

The fasciculation of axons does not occur only among axons projecting from a similar source that travel together until target innervation; axons can be observed coalescing with and switching between different stereotyped axon pathways before arriving at their final destination (Goodman et al., 1984). It can be appreciated from these observations that fasciculation is a complex process requiring a variety of signals to selectively alter the affinity of subsets of axons without exerting effects on others located in the same vicinity. The decision to continue adherence with a particular nerve bundle or to separate and adhere to a different nerve pathway or substrate is made at particular locations along the growth of an axon commonly referred to as choice points. One particular example is the Dorsal Root Entry Zone (DREZ), whereby dorsal root ganglia (DRG) axons projecting into the spinal cord must fasciculate before journeying into the CNS (Ozaki & Snider, 1997; Masuda & Shida, 2005). At these choice points, axons must simultaneously detect signals from other axons and the ECM, and make the decision to fasciculate or defasciculate based on the balance of attraction between axons and substrate.

The adhesion of an axon to the ECM substrate is largely dependent on receptors for cell adhesion molecules. A classical example of adhesion receptors are integrins. Integrins are a family of heterodimeric receptors expressed on the

membrane of the growth cone, that act as a physical linkage to the substrate when ligand-receptor interaction occurs (Hynes, 1996; Hynes, 2002). Integrin receptors are activated by protein ligands embedded within the ECM such as laminin, collagen, and fibronectin (Myers et al., 2011). Integrins appear to be particularly important as effectors of axon affinity for the substrate. Integrins can also be activated by guidance cues, or recruited downstream of guidance receptors (Stevens & Jacobs, 2002; Nakamoto et al., 2004). Activation of integrin receptors not only creates a physical adhesion of the axon to the substrate, but can also activate signaling within the growth cone to regulate actin remodeling dynamics (Hynes, 2002; Myers et al., 2011). By mediating these signaling functions, integrins have been shown to play functional roles in axon guidance throughout the CNS (Becker et al., 2003; Harper et al., 2010).

One known process by which fasciculation occurs is axon-axon interactions employing cell adhesion molecules (CAMs). Cell adhesion molecules belonging to the immunoglobulin (Ig) superfamily of proteins are expressed externally on axons, and have specific affinity for homophilic or heterophilic counterparts (Landmesser et al. 1988). A classic demonstration of fasciculation induced by CAMs can be observed in Drosophila motor axons, where overexpression of Fasciclin II (FasII), a Drosophila paralog for Ig CAMs, is sufficient to induce hyperfasciculation (Lin & Goodman, 1994). Adhesion molecule affinity can be modulated at particular times of axon growth, allowing for fasciculation or defasciculation of particular axon

subsets at choice points (Lin et al., 1994; Van Vactor, 1998).

Guidance signals producing surrounding-repulsion can also exert fasciculation on growing axons (Cloutier et al., 2004; Jaworski & Tessier-Lavigne, 2012; Luxey et al., 2013). The very same guidance ligands responsible for axon repulsion have been shown to confer this external influence on axons; however, this application can be observed as a distinct mechanism to effect fasciculation independently as interruption of these guidance events impairs fasciculation without disturbing the appropriate innervation of the target. One such example can be observed in vomeronasal projections where Sema3F interaction with the Neuropilin-2 receptor mediates fasciculation (Cloutier et al., 2004). Genetic loss of the Sema3F ligand disrupts fasciculation, but innervation of the appropriate target is unaffected. Similar observations have been documented with peripheral motor axons requiring EfnB1 and Slit2 for proper fasciculation, but not guidance (Luxey et al., 2013; Jaworski & Tessier-Lavigne, 2012).

IV. Cytoplasmic Effectors of Guidance Cues

Although much is known of the ligand-receptor pairs that govern axon guidance and fasciculation, the cytoplasmic effector proteins that act downstream of receptor activation remain largely undiscovered. As described thus far, guidance cues have a wide-range of applications on growing axons. The axon's ultimate interpretation of attraction or repulsion to axons or the substrate relies on these effector proteins to mediate the response (Lowery & Vactor, 2004). Therefore,

defining effector proteins with key roles during guidance and fasciculation is of great significance.

The actin stabilization dynamics in response to attractive and repulsive guidance cues require contributions from a cascade of signaling transduction molecules (Lowery & Vactor, 2004). While the identities and/or roles of many of these molecules are incompletely understood, the role of the Rho family of GTPases during navigation of the growth cone has been extensively studied (Govek, 2005; Koh, 2006). Rho GTPases, specifically RhoA, Rac1, and Cdc42, have been demonstrated to act downstream of the major guidance cue receptors, and play key roles in regulating the actin dynamics for steering of the growth cone. Intriguingly, Rho GTPases have been demonstrated to play antagonistic roles in steering of the growth cone. In general, Rac1 and Cdc42 are known to promote extension and adherence of the axon, whereas RhoA activity promotes disassembly and retraction (Koh et al., 2006). For example, Rac1 and Cdc42 have been shown to act downstream of Netrin-1 signaling to induce actin polymerization and anchoring of the growth cone to the substrate during attractive guidance of rat commissural axons (Shekarabi & Kennedy, 2002). Alternatively, inhibition of RhoA during Netrin-1 signaling has been shown to promote outgrowth in rat commissural explants (Li et al., 2002). A similar role can be observed in repulsion of mouse RGC axons with Ephrin signaling, where EphA receptor activation triggers preferential downstream activation of RhoA instead of Cdc42 and Rac1 in order to

induce growth cone disassembly (Sahin et al., 2005). Considering the importance of these effectors in mediating cytoskeletal remodeling in response to guidance cues, elucidating the proteins that modulate Rho GTPases will be vital to our understanding of axon guidance and fasciculation.

The Cas (Crk-associated substrate) family of adaptor proteins has been shown to interact with various classes of signaling proteins, and upon phosphorylation, can provide docking sites for effectors to stimulate Rac1-mediated actin remodeling (Defilippi et al., 2006). Roles for Cas proteins in cell migration and cell morphology have been documented (O'Neill et al., 2000; Riccomagno et al., 2014), yet little is known of their function during mammalian axon pathfinding. One example of Cas proteins in mediating the signaling response to guidance cues can be observed in the chick spinal cord, where p130CAS is required for Netrin guidance signaling. Axons mutant for p130Cas fail to induce Rac1 activation in response to Netrin signaling, and attraction of commissural axons towards the floorplate is notably reduced (Liu, G. et al., 2007). Cas adaptor proteins have also been demonstrated to act downstream of integrin signaling to mediate cell adhesion to the ECM substrate in a variety of cell lines (O'Neill et al., 2000). Interestingly, in Drosophila, the paralog *dCas* is required for proper integrin signaling during motor axon guidance, and *dCas* mutants display axon defasciculation defects (Huang et al., 2007). Thus, Cas adaptor proteins may provide an important link between guidance signals and cytoskeletal regulation in

growing axons. In Chapter 2, we set out to investigate the requirement of Cas adaptor proteins during fasciculation of peripheral neural projections in mice.

V. Regressive Development - Refinement Theories

After the initial phases of progressive development have generated a “draft” for neural circuits, exuberant connectivity requires refinement to achieve proper functional maturity. Why is a strategy of exuberant connectivity and subsequent refinement employed in the first place? Functional significance, limited signaling cue availability, and functional refinement are three possible explanations for the initial exuberant growth (Riccomagno & Kolodkin, 2015):

- *Functional Significance:* It is possible that exuberant connections serve a functional role during early development. For instance, they may supply factors or activity to the innervated region that is necessary in early development, but not later.
- *Limited availability of unique queues to establish myriad of specific mature circuits:* During the early development of the brain, there is a limited availability of resources such as the variety of unique signaling cues that will express later in development. Given these limitations, strategies to establish mature circuits must proceed in sequential steps to ensure connections are finely tuned. Starting with an exuberant number of neurons and connections between them gives the developmental refinement and specification processes a large enough slab of marble to chisel down.

- *Functional Refinement:* Exuberant growth and connectivity could be intended to allow for activity-dependent sculpting and refinement of connections via competition. This type of strategy is fit to ensure that only the strongest, most functional connections are supported.

These potential explanations lay a theoretical foundation for the significance of circuit refinement as a whole. However, we must survey refinement events across the nervous system to truly understand the functional roles for these strategies. Developing circuits have been shown to employ very similar mechanistic strategies, allowing for the classification of refinement events into a number of defined categories. The first of these classifications differentiates between stereotyped pruning of long axons and competition-based pruning of short axons.

VI. Axon Pruning

Stereotyped pruning of long axons

Stereotyped pruning of long axons occurs mostly in the CNS. This form of pruning eliminates axons based on a genetic predetermination, rendering the axons to be pruned identifiable before the onset of the pruning event. Of those identified, stereotyped pruning events effect entire populations of axons, not subsets.

A classic example of a pruning event controlled by genetic programs is that of the cortical spinal tract (CST) during early postnatal development. After initial

circuit formation, layer V neurons of the visual and sensorimotor cortices both project collaterals to the pons (sensory and motor control), spinal cord (motor control), and superior colliculus (visual processing) (O'Leary and Stanfield, 1985; Stanfield and O'Leary, 1985). By adulthood, the neurons in these cortical regions connect to overlapping but distinct targets in a functionally appropriate way: the visual cortex maintains connections to the superior colliculus and pons, but those to the spinal cord are removed. On the contrary, the motor cortex maintains connections to the spinal cord and the pons, but loses those to the superior colliculus. Despite the same initial projection scheme, the divergence observed in the mature circuitry arises from selective pruning of functionally inappropriate projections. For axons of the visual CST, Sema3F (a member of the Semaphorin family) expression in the dorsal spinal cord has been shown to direct the synaptic removal and activate retraction of the inappropriate projections (Low et al. 2008). Visual CST projections are pruned while motor CST projections remain because the visual projections express the plexin and neuropilin co-receptors required for detection of the Sema3F signal, while motor axons do not express these receptors. Intriguingly, this Sema3F-dependent mechanism is not similarly used for pruning of the inappropriate motor CST projections as genetic mutants for the Plexin A3/A4 and neuropilin receptors demonstrate failure to remove the visual CST, but no change in motor projection pruning can be observed.

Another example of stereotyped pruning is the retraction of hippocampal

infrapyramidal bundle (IFB) connections during mouse postnatal development (Bagri et al., 2003). During establishment of the hippocampal circuit, two bundles of mossy fibers emerge from the dentate gyrus (DG): the suprapyramidal bundle that travels above the pyramidal layer, and the IFB which travels below. In early postnatal development (P10), the IFB extends to reach CA3 and makes synaptic connections to CA3 neurons (Chen et al., 2000, Liu et al., 2005). However, these connections are progressively pruned back to the DG until P45, when the shortened IFB crosses the pyramidal layer to join the suprapyramidal bundle. Synaptic pruning and subsequent axon regression of the IFB is genetically determined by the timely expression of Sema3F in CA3 dendrites (Bagri et al., 2003). Sema3F in the hippocampal circuit acts to repel axons back to the DG through a Chn2-mediated signaling pathway (Riccomagno et al., 2012), rather than promoting their degeneration as was shown in the visual CST. Thus, Sema3F mediated pruning provides an example of similar mechanisms incorporating different tactics.

Short axon pruning: Competition for limited resources

Short axon pruning refers to the local pruning of subsets of branches that occurs within target regions to regulate terminal arborization. This strategy for circuit refinement involves integration of environmental factors, such as trophic support or neuronal activity, in order to select “winner” axons that will be maintained.

It has long been established that developing neurons require target-derived survival factors for growth and support (Hamburger & Levi-Montalcini, 1949; Levi-Montalcini, 1987). Stemming from this discovery came the Neurotrophic factor hypothesis, which posited that survival factors such as neuronal growth factors or neurotrophins are available in limited quantities. Due to these limitations, neurons must compete with each other in order to secure survival. The classic example of such a pruning event is that of sensory and motor nerve innervation of the periphery (Levi-Mantalcini, 1987). Neurons that successfully innervate close to neurotrophin-producing targets receive an advantage for survival over their counterparts, which will lose their axons and are targeted for apoptosis (Openheim, 1989, Luo & O'Leary, 2005). This ensures that only the cells that innervate targets as desired are maintained.

In addition to refinement strategies that reward axons for securing survival factors, there also exist examples whereby axons compete for survival through activity. The classic example of an activity-dependent pruning event in the PNS is that of motor axon innervation at the neuromuscular junction (NMJ). Upon initial assembly of this circuit, motor neurons exuberantly innervate the NMJ (Balice-Gordon & Lichtman 1994). In order to refine these connections to only those that are most functionally relevant, "loser" axons that generate less activity than their counterparts are selected for removal via synapse elimination.

Activity-driven circuit refinement can also be observed in the CNS during

cerebellar postnatal development (Crepel et al. 1976, Mariani & Changeux 1981). Initially, the inferior olivary nucleus projects an exuberant number of climbing fiber (CF) axons to their Purkinje cell (PC) targets. However, when this circuit is mature, each PC is innervated by only one CF. The removal of extraneous innervating CFs is orchestrated via a series of events which enable the translocation of only the most active innervating CF from the soma of the PC to its dendrites (Watanabe & Kano 2011). Once the winner has been selected and translocated to the dendrites, all CFs that remain on the soma are targeted for synaptic pruning and axonal degeneration. From these examples, activity-driven strategies of selection can be seen to ensure that only the most functional connections are maintained (Coleman et al., 1997, Lanuza et al., 2018).

One reason that activity-driven pruning strategies are so intriguing is that they can provide insight into windows of heightened plasticity during which experience-driven activity is influential for circuit refinement. These windows are referred to as critical periods if the environmental input is required, or sensitive periods if this window is when experiences have their greatest impact on circuit development (Berardi et al., 2000; Hensch, 2005; Hensch and Bilimoria, 2012). Learning in humans is thought to be an example of a sensitive period, where heightened circuit plasticity is theorized to underly the advantages in learning experienced during youth (Wilson et al., 2006). To gain a better understanding of these activity-driven windows of plasticity, research has focused on critical

windows during sensory circuit refinement in animals (Hensch, 2005; Berardi et al., 2000). The classical example of experience-influenced refinement during sensory development is that of ocular dominance columns made famous by Hubert and Weisel (1962). Ocular dominance columns refer to the eye-specific termination zones of visual lateral geniculate nucleus (LGN) thalamic projections that are formed in layer IV primary visual cortex during postnatal development. In these classical experiments, depriving the stimulation of one eye (monocular deprivation) demonstrated that competitive activity is necessary for proper innervation of the ocular dominance columns by their respective inputs, whereby absence of competing input allowed the uncovered eye to take over termination zones at the cost of the covered eye (Hubert and Weisel, 1962; Antonini and Stryker, 1996; Antonini et al., 1999). However, monocular deprivation only produces this effect during a particular window of development during which these connections are actively refined. Attempts to unilaterally block visual input after this critical window do not result in any changes to circuit wiring, and altered connectivity cannot be rescued. Understanding the mechanics and modulating factors that mediate events with such significant and irreversible impacts on circuit connectivity carries implications in improving learning and memory, and recovering proper circuit connectivity after injury or neurodevelopmental abnormality.

Although the examples of pruning provided are some of the most investigated of known events, many of the molecules and specific mechanisms

used to refine these circuits still remain largely unknown (Riccomagno & Kolodkin, 2015). This is especially true of the activity-dependent mechanisms for winner selection. It is therefore apparent that the field of circuit refinement requires further investigation. However, an apparent limitation in the investigation of activity-dependent circuit refinement mechanisms is the need for tools that can manipulate activity of a specific subset of projections with temporal control. Circuit refinement events occur during defined developmental windows or critical periods (Wiesel & Hubel,1963, Berardi et al., 2000). These windows can span days or weeks, and any manipulations must be temporally controlled to occur during their duration. Virally-expressed DREADDs (Designer Receptors Exclusively Activated by Designer Drugs) offer a possible solution to this problem in that they can confer activity manipulations for limited durations, only when supplied the exogenous ligand CNO (Roth, 2016). However, manipulations induced by DREADDs require frequent pharmacological dosing in order to maintain expression. Furthermore, when dealing with developmental events at very young postnatal ages, establishing effective dosing parameters can be a challenge. Optogenetics offer another possible solution for temporally controlled activity manipulation without the need for pharmacological dosing, but must also be maintained via continuous light stimulation (Yizhar et al., 2011). Furthermore, application of light stimulation to neurons often requires invasive headgear, which would be extremely challenging in the young animals in which these events take place. Both of these strategies

require continued pharmacological or light-evoked activation of the channels or receptors of interest, which is unviable for protracted periods of time. Furthermore, the physiological level of activation/inactivation required to exert an effect on a particular system is not known a priori. This is a critical issue due to the largely unknown mechanisms of activity-dependent refinement events. If, for example, reaching a particular activity threshold is a metric for winning projections, any lapse in activity reduction could allow these thresholds to be met, resulting in potentially significant manipulations to be overlooked. It can therefore be observed that the need for more consistent strategies of obtaining temporally controlled manipulations is an impediment to future investigations of activity-dependent pruning. Aim 2 (Chapter 3) of my doctoral thesis addresses this need with the design of ExBoX, a novel AAV-based intersectional approach using Boolean AND-NOT logic to drive cell type specific and temporally controllable manipulations.

VII. Investigating the Development of Neural Circuitry

The review of literature hitherto provided demonstrates the requirement of both progressive and regressive developmental events for functional maturation of neural circuitry to be achieved. While many fundamental properties of these events are known, there is still much to be discovered. In order to investigate processes of circuit development, the labeling of axons based on region of origination and innervation targets becomes a requirement. To achieve this labeling, genetic and viral strategies have been used to trace circuitry and assess dynamics of guidance

and refinement. Such techniques will be described for the investigations henceforth provided.

Aim 1: Within the field of axon guidance, a particular need for investigation is warranted by the intracellular signaling proteins that help transduce the response in actin regulation conferred by guidance cues. Of particular interest are the Cas family of adaptor proteins. We examined the requirement for Cas adaptor proteins during DRG axon pathfinding in mice. Our genetic data supports a novel role for Cas adaptor proteins during the fasciculation and guidance of central DRG projections in the DREZ. These data provide insight into the interplay between adhesion to the substrate and axon fasciculation.

Aim 2: Within the field of axon refinement, much still needs to be discovered about the events and mechanics of activity-dependent axon pruning. Investigation of such events can be especially difficult because of the discrete timeline that refinement events occupy, and need for spatially and temporally controlled manipulations of neural activity. The ability to turn ON or OFF an activity manipulation at discrete timepoints of circuit development is not always feasibly achieved by genetic means. To address these difficulties, the second part of my studies described the generation and characterization of a novel viral tool for controlled and reversible expression of genes of interest governed by recombinase-dependent Boolean logic. This will ultimately allow us to manipulate neuronal activity (among other things) during protracted periods of time in a

reversible manner.

References

Antonini, A., Fagiolini, M., & Stryker, M. P. (1999). Anatomical correlates of functional plasticity in mouse visual cortex. *The Journal of neuroscience : the official journal of the Society for Neuroscience, 19*(11), 4388–4406. https://doi.org/10.1523/JNEUROSCI.19-11-04388.1999

Antonini, A., & Stryker, M. P. (1996). Plasticity of geniculocortical afferents following brief or prolonged monocular occlusion in the cat. *The Journal of comparative neurology, 369*(1), 64–82. https://doi.org/10.1002/(SICI)1096-9861(19960520)369:1<64::AID-CNE5>3.0.CO;2-I

Bak, M., & Fraser, S. E. (2003). Axon fasciculation and differences in midline kinetics between pioneer and follower axons within commissural fascicles. *Development*, *130*(20), 4999–5008. https://doi.org/10.1242/dev.00713

Balice-Gordon, R. J., & Lichtman, J. W. (1994). Long-term synapse loss induced by focal blockade of postsynaptic receptors. Nature, 372(6506), 519–524. https://doi.org/10.1038/372519a0

Bagri, A., Cheng, H. J., Yaron, A., Pleasure, S. J., & Tessier-Lavigne, M. (2003). Stereotyped pruning of long hippocampal axon branches triggered by retraction inducers of the semaphorin family. *Cell*, *113*(3), 285–299.

Bastiani, M. J., Raper, J. A., & Goodman, C. S. (1984). Pathfinding by neuronal growth cones in grasshopper embryos. III. Selective affinity of the G growth cone for the P cells within the A/P fascicle. *Journal of Neuroscience*, *4*(9), 2311–2328. https://doi.org/10.1523/jneurosci.04-09-02311.1984

Becker, T., McLane, M. A., & Becker, C. G. (2003). Integrin antagonists affect growth and pathfinding of ventral motor nerves in the trunk of embryonic zebrafish. *Molecular and Cellular Neuroscience*, *23*(1), 54–68. https://doi.org/10.1016/S1044-7431(03)00018-6

Berardi, N., Pizzorusso, T., & Maffei, L. (2000). Critical periods during sensory development. *Current Opinion in Neurobiology*, *10*(1), 138–145. https://doi.org/10.1016/S0959-4388(99)00047-1

Bin, J. M., Han, D., Lai Wing Sun, K., Croteau, L. P., Dumontier, E., Cloutier, J. F., Kania, A., & Kennedy, T. E. (2015). Complete Loss of Netrin-1 Results in Embryonic Lethality and Severe Axon Guidance Defects without Increased Neural Cell Death. *Cell Reports*, *12*(7), 1099–1106. https://doi.org/10.1016/j.celrep.2015.07.028

Chen, H., Bagri, A., Zupicich, J.A., Zou, Y., Stoeckli, E., Pleasure, S.J., Lowenstein, D.H., Skarnes, W.C., Chedotal, A., and Tessier- Lavigne, M. (2000). Neuropilin-2 regulates the development of selective cranial and sensory nerves and hippocampal mossy fiber projections. *Neuron 25*, 43–56.

Cloutier, J.-F., Giger, R. J., Koentges, G., Dulac, C., Kolodkin, A. L., & Ginty, D. D. (2002). Neuropilin-2 mediates axonal fasciculation, zonal segregation, but not axonal convergence. *Neuron*, *33*, 877–892.

Colamarino, S. A., & Tessier-Lavigne, M. (1995). The axonal chemoattractant netrin-1 is also a chemorepellent for trochlear motor axons. *Cell*, *81*(4), 621–629. https://doi.org/10.1016/0092-8674(95)90083-7

Colman, H., Nabekura, J., & Lichtman, J. W. (1997). Alterations in synaptic strength preceding axon withdrawal. *Science (New York, N.Y.), 275*(5298), 356–361. https://doi.org/10.1126/science.275.5298.356

Crepel F, Mariani J, Delhaye-Bouchaud N. (1976). Evidence for a multiple innervation of Purkinje cells by climbing fibers in the immature rat cerebellum. *J. Neurobiol.* 7:567–78.

Chilton, J. K. (2006). Molecular mechanisms of axon guidance. *Developmental Biology*, *292*(1), 13–24. https://doi.org/10.1016/j.ydbio.2005.12.048

Defilippi, P., Di Stefano, P., & Cabodi, S. (2006). p130Cas: a versatile scaffold in signaling networks. *Trends in Cell Biology*, *16*(5), 257–263. https://doi.org/10.1016/j.tcb.2006.03.003

Dent, E. W., Gupton, S. L., & Gertler, F. B. (2011). The growth cone cytoskeleton in axon outgrowth and guidance. Cold Spring Harbor perspectives in biology, 3(3), a001800. https://doi.org/10.1101/cshperspect.a001800

Feldeim, D., & O'Leary, D. (2010). Visual map development: bidirectional and competition. *Cold Spring Harbor Perspectives in Biology*, *2:a001768*, 1–20.

Goodman, C. S., Bastiani, M. J., Doe, C. Q., du Lac, S., Helfand, S. L., Kuwada, J. Y., & Thomas, J. B. (1984). Cell recognition during neuronal development. *Science (New York, N.Y.)*, *225*(4668), 1271–1279. https://doi.org/10.1126/science.6474176

Govek, E. E., Newey, S. E., & Van Aelst, L. (2005). The role of the Rho GTPases in neuronal development. *Genes and Development*, *19*(1), 1–49. https://doi.org/10.1101/gad.1256405

Hamburger V, & Levi-Montalcini R. (1949). Proliferation, differentiation and degeneration in the spinal ganglia of the chick embryo under normal and experimental conditions. *Journal of Experimental Zoology, 111*, 457–501.

Harper, M. M., Ye, E. A., Blong, C. C., Jacobson, M. L., & Sakaguchi, D. S. (2010). Integrins contribute to initial morphological development and process outgrowth in rat adult hippocampal progenitor cells. *Journal of molecular neuroscience: MN*, *40*(3), 269–283. https://doi.org/10.1007/s12031-009-9211-x

Hensch, T. K. (2005). Critical period plasticity in local cortical circuits. *Nature Reviews Neuroscience*, *6*(11), 877–888. https://doi.org/10.1038/nrn1787

Hensch, T. K., & Bilimoria, P. M. (2012). Re-opening Windows: Manipulating Critical Periods for Brain Development. *Cerebrum : the Dana forum on brain science*, *2012*, 11.

Hindges, R., McLaughlin, T., Genoud, N., Henkemeyer, M., & O'Leary, D. D. M. (2002). EphB forward signaling controls directional branch extension and arborization required for dorsal-ventral retinotopic mapping. *Neuron*, *35*(3), 475–487. https://doi.org/10.1016/S0896-6273(02)00799-7

Hirotsune, S., Fleck, M. W., Gambello, M. J., Bix, G. J., Chen, A., Clark, G. D., Ledbetter, D. H., McBain, C. J., & Wynshaw-Boris, A. (1998). Graded reduction of Pafah1b1 (Lis1) activity results in neuronal migration defects and early embryonic lethality. *Nature Genetics*, *19*(4), 333–339. https://doi.org/10.1038/1221

Hong, K., Hinck, L., Nishiyama, M., Poo, M-M., Tessier-Levigne, M., & Stein, E. (1999). A ligand-gated association between cytoplasmic domains of UNC5 and DCC family recepors converts netrin-induced growth cone attraction to repulsion. *Cell*, *97*, 927–941. http://www.wormbase.org/db/misc/paper?name=WBPaper00003589

Huang, Z., Yazdani, U., Thompson-Peer, K. L., Kolodkin, A. L., & Terman, J. R. (2007). Crk-associated substrate (Cas) signaling protein functions with integrins to specify axon guidance during development. *Development*, *134*(12), 2337–2347. https://doi.org/10.1242/dev.004242

Hynes, R. O. (1996). Targeted mutations in cell adhesion genes: What have we learned from them? *Developmental Biology*, *180*(2), 402–412. https://doi.org/10.1006/dbio.1996.0314

Hynes R. O. (2002). Integrins: bidirectional, allosteric signaling machines. *Cell*, *110*(6), 673–687. https://doi.org/10.1016/s0092-8674(02)00971-6

Jaworski, A., & Tessier-Lavigne, M. (2012). Autocrine/juxtaparacrine regulation of axon fasciculation by Slit-Robo signaling. *Nature Neuroscience*, *15*(3), 367–369. https://doi.org/10.1038/nn.3037

Kennedy, T. E., Serafini, T., de la Torre, J. R., & Tessier-Lavigne, M. (1994). Netrins are diffusible chemotropic factors for commissural axons in the embryonic spinal cord. *Cell*, *78*(3), 425–435. https://doi.org/10.1016/0092-8674(94)90421-9

Kitsukawa, T., Shimizu, M., Sanbo, M., Hirata, T., Taniguchi, M., Bekku, Y., Yagi, T., & Fujisawa, H. (1997). Neuropilin-semaphorin III/D-mediated chemorepulsive signals play a crucial role in peripheral nerve projection in mice. *Neuron*, *19*(5), 995–1005. https://doi.org/10.1016/S0896-6273(00)80392-X

Koh, C. G. (2007). Rho GTPases and their regulators in neuronal functions and development. *NeuroSignals*, *15*(5), 228–237. https://doi.org/10.1159/000101527

Kolodkin, A. L., & Tessier-Lavigne, M. (2011). Mechanisms and molecules of neuronal wiring: A primer. *Cold Spring Harbor Perspectives in Biology*, *3*(6), 1–14. https://doi.org/10.1101/cshperspect.a001727

Kozulin, P., & Richards, L. (2016). Neuroscience in the 21st century: From basic to clinical, second edition. *Neuroscience in the 21st Century: From Basic to Clinical, Second Edition*, 202–222. https://doi.org/10.1007/978-1-4939-3474-4

Kuida, K., Haydar, T. F., Kuan, C.-Y., Gu, Y., Taya, C., Karasuyama, H., Su, M.S., Rakic, P., Flavell, R.A. (1998). Reduced apoptosis and cytochrome c-mediated caspase activation in mice lacking caspase 9. *Cell*, *94*, 325–337. https://www.cell.com/action/showPdf?pii=S0092-8674%2800%2981476-2

Landmesser, L., Dahm, L., Schultz, K., and Rutishauser, U. (1988). Distinct roles for adhesion molecules during innervation of embryonic chick muscle. *Develepmental Biology, 119*, 645–670.

Lanuza, M. A., Tomàs, J., Garcia, N., Cilleros-Mañé, V., Just-Borràs, L., & Tomàs, M. (2018). Axonal competition and synapse elimination during neuromuscular junction development. Current Opinion in Physiology, *4,* 25–31.

Levi-montalcini, R. (1987). The Nerve Growth Factor: thirty-five years later. *The EMBO Journal*, *6*(9), 2856.

Lewis, D. A., & Levitt, P. (2002). Schizophrenia as a disorder of neurodevelopment. *Annual Review of Neuroscience*, *25*, 409–432. https://doi.org/10.1146/annurev.neuro.25.112701.142754

Li, X., Saint-Cyr-Proulx, E., Aktories, K., & Lamarche-Vane, N. (2002). Rac1 and Cdc42 but not RhoA or Rho kinase activities are required for neurite outgrowth induced by the netrin-1 receptor DCC (deleted in colorectal cancer) in N1E-115 neuroblastoma cells. *Journal of Biological Chemistry*, *277*(17), 15207–15214. https://doi.org/10.1074/jbc.M109913200

Lim, J. W. C., Donahoo, A. L. S., Bunt, J., Edwards, T. J., Fenlon, L. R., Liu, Y., Zhou, J., Moldrich, R. X., Piper, M., Gobius, I., Bailey, T. L., Wray, N. R., Kessaris, N., Poo, M. M., Rubenstein, J. L. R., & Richards, L. J. (2015). EMX1 regulates NRP1-mediated wiring of the mouse anterior cingulate cortex. *Development (Cambridge)*, *142*(21), 3746–3757. https://doi.org/10.1242/dev.119909

Lin, D. M., and Goodman, C.S. (1994). Ectopic and increased expression of fasciclin II alters motoneuron growth cone guidance. *Neuron*, *13,* 507–523.

Lin, D. M., Fetter, R.D., Kopczynski, C., Grenningloh, G., and C. S. Goodman, C.S. (1994). Genetic analysis of fasciclin II in Drosophila: defasciculation, refasiculation, and altered fasciculation. *Neuron, 13*, 1055–1069.

Liu, G., Li, W., Gao, X., Li, X., Jürgensen, C., Park, H. T., Shin, N. Y., Yu, J., He, M. L., Hanks, S. K., Wu, J. Y., Guan, K. L., & Rao, Y. (2007). p130CAS is required for netrin signaling and commissural axon guidance. *Journal of Neuroscience*, *27*(4), 957–968. https://doi.org/10.1523/JNEUROSCI.4616-06.2007

Liu, X.-B. (2005). Stereotyped Axon Pruning via Plexin Signaling Is Associated with Synaptic Complex Elimination in the Hippocampus. *Journal of Neuroscience*, *25*(40), 9124–9134.

Lopresti, V., Macagno, E. R., & Levinthal, C. (1973). Structure and development of neuronal connections in isogenic organisms: cellular interactions in the development of the optic lamina of Daphnia. *Proceedings of the National Academy of Sciences of the United States of America*, *70*(2), 433–437. https://doi.org/10.1073/pnas.70.2.433

Low, L. K., Liu, X. B., Faulkner, R. L., Coble, J., & Cheng, H. J. (2008). Plexin signaling selectively regulates the stereotyped pruning of corticospinal axons from visual cortex. *Proceedings of the National Academy of Sciences of the United States of America*, *105*(23), 8136–8141. https://doi.org/10.1073/pnas.0803849105

Lowery, L. A., & Vactor, D. Van. (2009). The trip of the tip: Understanding the growth cone machinery. *Nature Reviews Molecular Cell Biology*, *10*(5), 332–343. https://doi.org/10.1038/nrm2679

Luo L, O'Leary DD (2005) Axon retraction and degeneration in development and disease. *Annual Reviews Neuroscience, 28*, 127–156.

Luxey, M., Jungas, T., Laussu, J., Audouard, C., Garces, A., & Davy, A. (2013). Eph: Ephrin-B1 forward signaling controls fasciculation of sensory and motor axons. *Developmental Biology*, *383*(2), 264–274. https://doi.org/10.1016/j.ydbio.2013.09.010

Mariani, J., & Changeux, J. P. (1981). Ontogenesis of olivocerebellar relationships. I. Studies by intracellular recordings of the multiple innervation of Purkinje cells by climbing fibers in the developing rat cerebellum. *J Neurosci*, *1*(7), 696–702.

Masuda, T., & Shiga, T. (2005). Chemorepulsion and cell adhesion molecules in patterning initial trajectories of sensory axons. *Neuroscience Research*, *51*(4), 337–347. https://doi.org/10.1016/j.neures.2005.01.007

Myers, J. P., Santiago-medina, M., & Gomez, T. M. (2012). *interactions*. *71*(11), 901–923. https://doi.org/10.1002/dneu.20931.Regulation

Nakamoto, T., Kain, K. H., & Ginsberg, M. H. (2004). Neurobiology: New Connections between Integrins and Axon Guidance. *Current Biology*, *14*(3), R121–R123. https://doi.org/10.1016/j.cub.2004.01.020

O'Leary, D. D. M., & Stanfield, B. B. (1985). Occipital cortical neurons with transient pyramidal tract axons extend and maintain collaterals to subcortical but not intracortical targets. *Brain Research*, *336*(2), 326–333.

O'Neill, G. M., Fashena, S. J., & Golemis, E. A. (2000). Integrin signaling: a new Cas(t) of characters enters the stage. *Trends in cell biology*, *10*(3), 111–119. https://doi.org/10.1016/s0962-8924(99)01714-6

Oppenheim RW. (1989). The neurotrophic theory and naturally occurring motoneuron death. *Trends Neuroscience, 12*: 252–55.

Ozaki, S., & Snider, W. D. (1997). Initial trajectories of sensory axons toward laminar targets in the developing mouse spinal cord. *The Journal of comparative neurology*, *380*(2), 215–229.

Pardo, C. A., & Eberhart, C. G. (2007). The neurobiology of autism. *Brain Pathology*, *17*(4), 434–447. https://doi.org/10.1111/j.1750-3639.2007.00102.x

Rakic, P., & Swaab, D. F. (1988). Defects of neuronal migration and the pathogenesis of cortical malformations. *Progress in Brain Research*, *73*(C), 15–37. https://doi.org/10.1016/S0079-6123(08)60494-X

Raper, J., & Mason, C. (2010). Cellular strategies of axonal pathfinding. *Cold Spring Harbor Perspectives in Biology*, *2*(9), 1–22. https://doi.org/10.1101/cshperspect.a001933

Riccomagno, M. M., Hurtado, A., Wang, H., Macopson, J. G., Griner, E. M., Betz, A., Brose, N., Kazanietz, M. G., & Kolodkin, A. L. (2012). The RacGAP β2-Chimaerin selectively mediates axonal pruning in the hippocampus. *Cell*, *149*(7), 1594–1606. https://doi.org/10.1016/j.cell.2012.05.018

Riccomagno, M. M., & Kolodkin, A. L. (2015). Sculpting Neural Circuits by Axon and Dendrite Pruning. *Annual Review of Cell and Developmental Biology*, *31*, 779–805. https://doi.org/10.1146/annurev-cellbio-100913-013038

Riccomagno, M. M., Sun, L. O., Brady, C. M., Alexandropoulos, K., Seo, S., Kurokawa, M., & Kolodkin, A. L. (2014). Cas adaptor proteins organize the retinal ganglion cell layer downstream of integrin signaling. *Neuron*, *81*(4), 779–786. https://doi.org/10.1016/j.neuron.2014.01.036

Roth, B. L. (2017). Use of DREADDS. *Neuron*, *89*(4), 683–694. https://doi.org/10.1016/j.neuron.2016.01.040.DREADDs

Sahin, M., Greer, P. L., Lin, M. Z., Poucher, H., Eberhart, J., Schmidt, S., Wright, T. M., Shamah, S. M., O'Connell, S., Cowan, C. W., Hu, L., Goldberg, J. L., Debant, A., Corfas, G., Krull, C. E., & Greenberg, M. E. (2005). Eph-dependent tyrosine phosphorylation of ephexin1 modulates growth cone collapse. *Neuron*, *46*(2), 191–204. https://doi.org/10.1016/j.neuron.2005.01.030

Sasaki, S., Mori, D., Toyo-oka, K., Chen, A., Garrett-Beal, L., Muramatsu, M., Miyagawa, S., Hiraiwa, N., Yoshiki, A., Wynshaw-Boris, A., & Hirotsune, S. (2005). Complete Loss of Ndel1 Results in Neuronal Migration Defects and Early Embryonic Lethality. *Molecular and Cellular Biology*, *25*(17), 7812–7827. https://doi.org/10.1128/mcb.25.17.7812-7827.2005

Shen, Y., Mani, S., Donovan, S. L., Schwob, J. E., & Meiri, K. F. (2002). Netrin-1 Is Required for Commissural Axon Guidanc. *Journal of Neuroscience*, *22*(1), 239–247.

Shekarabi, M., & Kennedy, T. E. (2002). The netrin-1 receptor DCC promotes filopodia formation and cell spreading by activating Cdc42 and Rac1. *Molecular and Cellular Neuroscience*, *19*(1), 1–17. https://doi.org/10.1006/mcne.2001.1075

Stanfield BB, O'Leary DD, Fricks C. (1982). Selective collateral elimination in early postnatal development restricts cortical distribution of rat pyramidal tract neurons. *Nature 298*, 371–73.

Stevens, A., & Jacobs, J. R. (2002). Integrins Regulate Responsiveness to Slit Repellent Signals. *Journal of Neuroscience*, *22*(11), 4448–4455. https://doi.org/10.1523/jneurosci.22-11-04448.2002

Tessier-Lavigne, M., & Goodman, C. S. (1996). The molecular biology of axon guidance. *Science (New York, N.Y.)*, *274*(5290), 1123–1133. https://doi.org/10.1126/science.274.5290.1123

Van Battum, E. Y., Brignani, S., & Pasterkamp, R. J. (2015). Axon guidance proteins in neurological disorders. *The Lancet Neurology*, *14*(5), 532–546. https://doi.org/10.1016/S1474-4422(14)70257-1

Watanabe M, Kano M. (2011). Climbing fiber synapse elimination in cerebellar Purkinje cells. *Eur. J. Neurosci. 34*, 1697–710.

Wiesel, T. N., & Hubel, D. H. (1963). Responses in Striate Deprived of Vision Cortex of One Eye. *Journal of Neurophysiology*, *26*(6), 1003–1017.

Wilson, I. A., Gallagher, M., Eichenbaum, H., & Tanila, H. (2006). Neurocognitive aging: prior memories hinder new hippocampal encoding. *Trends in neurosciences*, *29*(12), 662–670. https://doi.org/10.1016/j.tins.2006.10.002

Zhou, Y., Gunput, R. A., & Pasterkamp, R. J. (2008). Semaphorin signaling: progress made and promises ahead. *Trends in biochemical sciences, 33*(4), 161–170. https://doi.org/10.1016/j.tibs.2008.01.006

Yizhar, O., Fenno, L. E., Davidson, T. J., Mogri, M., & Deisseroth, K. (2011). Optogenetics in Neural Systems. *Neuron*, *71*(1), 9–34. https://doi.org/10.1016/j.neuron.2011.06.004

Chapter 2: Cas Adaptor Proteins Coordinate Sensory Axon Fasciculation

Tyler A. Vahedi-Hunter [a], Jason A. Estep [b], Kylee Rosette [c], Michael L. Rutlin [d], Kevin M. Wright [c], and Martin M. Riccomagno [a, b, *]

a. Neuroscience Program, Department of Molecular, Cell and Systems Biology, University of California, Riverside, CA 92521, USA.

b. Cell, Molecular and Developmental Biology Program, Department of Molecular, Cell and Systems Biology, University of California, Riverside, CA 92521, USA.

c. Vollum Institute, Oregon Health & Science University

d. Department of Neuroscience, Columbia University, New York, NY 10032

Abstract

Development of complex neural circuits like the peripheral somatosensory system requires intricate mechanisms to ensure axons make proper connections. While much is known about ligand-receptor pairs required for dorsal root ganglion (DRG) axon guidance, very little is known about the cytoplasmic effectors that mediate cellular responses triggered by these guidance cues. Here we show that members of the Cas family of cytoplasmic signaling adaptors are highly phosphorylated in central projections of the DRG as they enter the spinal cord. Furthermore, we provide genetic evidence that Cas proteins act DRG-autonomously to regulate fasciculation of sensory projections. These data establish an evolutionarily conserved requirement for Cas adaptor proteins during

peripheral nervous system axon pathfinding. They also provide insight into the interplay between axonal fasciculation and adhesion to the substrate.

Introduction

Precise assembly of the peripheral somatosensory system involves migration of neural crest cells (NCCs) to coalesce into sensory ganglia and subsequent guidance of axonal projections from these newly formed ganglia. The NCCs that give rise to the dorsal root ganglia (DRG) originate from the dorsal spinal cord and migrate ventro-medially between the neural tube and rostral somite (Serbedzija et al., 1989; Serbedzija et al., 1990). Upon reaching the DRG, these neural progenitors continue to proliferate before committing to a neuronal or glial fate (Frand and Sanes, 1991; Ma et al., 1986). The newly born sensory neurons then extend a central and a peripheral axon branch, acquiring the characteristic pseudounipolar morphology (Barber and Vaughn, 1986). The resulting central projections traverse towards the spinal cord and enter the central nervous system (CNS) through the Dorsal Root Entry Zone (DREZ), while the distal processes navigate long distances to innervate their peripheral targets Ozaki and Snider, 1997; Ramon y Cajal, 1909). Accurate guidance and fasciculation of these axons requires an intricately choreographed array of signaling cues acting on their cognate receptors (Kolodkin and Tessier-Lavigne, 2011; Wang et al., 2013). Although much is known about the ligand-receptor pairs required for axon trajectories, very little is known about the cytoplasmic effectors that allow these axons to respond to guidance cues.

Cas signaling adaptor proteins mediate a variety of biological processes including cell migration and changes in cell morphology (O'neill et al., 2000), and exhibit specific expression patterns during neural development in rodents (Merrill et al., 2004). Cas proteins interact with various classes of signaling proteins, including cytosolic tyrosine kinases (like Src and Fak). Upon phosphorylation, Cas proteins can provide docking sites for SH2-containing effectors, including Crk, which stimulate Rac1-mediated actin remodeling (Defilippi et al., 2006). We have recently uncovered an essential role for Cas family members during retinal ganglion cell migration (Riccomagno et al., 2014), yet our current understanding of Cas adaptor protein function during mammalian axon pathfinding *in vivo* is limited. One member of this family, p130Cas, has been proposed as a required downstream component of netrin-mediated commissural axon guidance in the chicken spinal cord (Liu et al., 2007). Interestingly, Drosophila Cas (dCas) has been shown to participate downstream of integrin receptors in axon fasciculation and guidance of peripheral motor axons (Huang et al., 2007). Whether Cas proteins play similar roles during mammalian peripheral nervous system (PNS) development is currently unknown.

Here we examine the requirement for Cas adaptor proteins during DRG axon pathfinding. Our genetic data supports a novel role for Cas adaptor proteins during the fasciculation and guidance of central DRG projections in the DREZ.

These data provide insight into the interplay between adhesion to the substrate and axon fasciculation.

Results

Cas adaptor proteins have been shown to participate in the formation of the neuronal scaffold of the mammalian retina (Riccomagno et al., 2014). In addition, dCas is required for integrin-mediated peripheral axon guidance and fasciculation in Drosophila (Huang et al., 2007). To investigate the role for Cas signaling adaptor proteins during mammalian PNS axon guidance, we started by assessing the expression pattern of *Cas* genes during embryonic development by *in situ* hybridization (Fig. 2.1a-l). *Cas* genes are broadly expressed in the DRG, but display specific regional expression in spinal cord (SC) at embryonic day (e)10.5 and e11.5 (Fig. 2.1a-f; 2.2a-c). P130Cas is mainly expressed in the mantle zone, with high levels of expression in the dorsal SC and ventral root (Fig. 2.1d). *CasL* expression in the spinal cord is primarily found in the dorsal SC and ventricular zone (Fig. 2.1e). *Sin/EFS* is also expressed around the ventricular zone of the SC, and subsets of DRG neurons (Fig. 2.1f). *p130Cas* and *Sin* continue to be expressed in the DRG at e12.5 and e14.5 (Fig. 2.1g, i, j, l). *CasL* DRG expression becomes weaker as development progresses, and becomes undetectable by e14.5 (Fig. 2.1b, e, h, k). All three *Cas* family members maintain expression in the spinal cord until at least e14.5 (Fig. 2.1d-l). At e 12.5, *p130Cas* maintains expression in the mantle zone, dorsal SC and ventral root, but also begins to be

expressed in the ventricular zone (Fig. 2.1g). A similar expansion in expression domain is observed for *Sin* (Fig. 2.1i), although the overall level of *Sin* expression is weaker than that of *p130Cas*. By e14.5 *p130Cas* and *Sin* appear to be broadly expressed in the SC, with stronger expression in the DREZ and ventral roots (Fig. 2.1j, l). At e12.5 and 14.5, *CasL* expression remains restricted to the ventricular zone (Fig. 2.1h, k). Sense negative control probes displayed negligible staining (Fig. 2.1m-o; 2.2d-f).

We next performed histological analyses of p130Cas protein expression in the developing spinal cord and DRG (Fig. 2.3a-c; 2.4). The expression pattern of p130Cas protein overlaps with that of *p130Cas* mRNA in DRG and spinal cord mantle zone cell bodies (Fig. 2.1g; 2.3a-c; 2.4a-d). In addition, p130Cas protein localizes to DRG central projections and spinal cord commissural axons, and is highly enriched in the DREZ and dorsal funiculus (Fig. 2.3a; 2.4a, c). Although there are some modest differences in the p130Cas mRNA and protein expression patterns inside the SC, these are likely due to the distinct subcellular distribution of these gene products. The overall pattern of expression was confirmed by utilizing a GENSAT BAC transgenic mouse line that expresses enhanced GFP (EGFP) under the control of *p130Cas* regulatory sequences (Gong et al., 2003; Heintz, 2004). This transgenic line allows for the detection of cells expressing *p130Cas* (Riccomagno et al., 2014). The *p130Cas-EGFP-Bac* spinal cord EGFP expression pattern is consistent with that of endogenous p130Cas protein and

mRNA in wild-type (WT) animals, with strong signal in dorsal SC, ventral root and DRG (Fig. 2.3d-f; 2.4; 2.5). As expected, no EGFP detection is observed in WT animals (Fig. 2.5c, f, i). As phosphorylation of Cas adaptor proteins mediates adhesion signaling during neural development (Riccomagno et al., 2014; Huang et al., 2007; Bourgin et al., 2007), we examined the localization of Phosphotyrosine-p130Cas (PY-Cas) in the developing spinal cord and DRG (Fig 2.3g-i). PY-Cas is present in the ventral funiculus and commissural axons in close proximity to the midline (Fig. 2.3g, h). Interestingly, PY-Cas is also enriched in the DREZ, DRG central projections and dorsal funiculus (Fig. 2.3g, i). Therefore, *Cas* mRNA, p130Cas protein, and phospho-tyrosine-p130Cas expression patterns are consistent with Cas involvement in DRG and commissural axon guidance.

In addition to expression of Cas genes in the SC and DRG, whole-mount in situ hybridization revealed the presence of *Cas* transcripts in the trigeminal ganglion and the nodose/petrosal complex at e10.5 and e11.5 (Fig. 2.1a-c; 2.6a-c). In situ hybridization on sections confirmed that *Cas* genes are broadly expressed in the trigeminal and nodose at e11.5 (Fig. 2.6d-i). Consistent with these results, p130Cas protein is found in cell bodies and projections of both ganglia from e10.5 to e12.5 (Fig. 2.6j-u), and overlaps with *p130Cas* mRNA expression at e11.5 (Fig. 2.6d, g). Expression of EGFP in *p130Cas-EGFP-Bac* animals confirmed the strong expression of *p130Cas* in trigeminal and nodose ganglia from

e10.5 to e12.5 (Fig. 2.7a-r). No EGFP expression was detected in WT nodose or trigeminal ganglia (Fig. 2.7c, f, i, l, o, r).

Given the expression and phosphorylation pattern of Cas adaptor proteins in the developing spinal cord and DRG, we next asked whether *Cas* genes are required for DRG and commissural axon pathfinding. Since the expression patterns of *Cas* genes during spinal cord development are highly overlapping and Cas adaptor proteins act redundantly during retina development (Riccomagno et al., 2014), we concurrently ablated all *Cas* genes from the dorsal spinal and DRG (dSC+DRG). Using *Wnt1Cre-2*a mice that expresses Cre recombinase in the dorsal spinal cord and neural-crest derived structures (Lewis et al., 2013) (Figs. 2.8 and 2.9), we ablated a conditional allele of *p130Cas* in a *CasL*$^{-/-}$*;Sin*$^{-/-}$ double null mutant genetic background (we refer to *p130Cas*$^{f/\Delta}$;*CasL*$^{-/-}$*;Sin*$^{-/-}$ mice as triple conditional knock-outs: "TcKO") (Riccomagno et al., 2014). We first confirmed the removal of functional Cas proteins by performing immunostaining for PY-Cas at e12.5: PY-Cas was almost completely absent in *Wnt1Cre;TcKO* SCs and DRGs (Fig. 2.8j). We next examined the overall projection pattern of DRG axons in *Wnt1Cre;TcKO* and control littermates. For this and all subsequent experiments *p130Cas* $^{f/+}$; *CasL*$^{-/-}$ and *Sin*$^{-/-}$embryos were used as controls. In control embryos, axons from DRG sensory neurons bifurcate and project along the anterior-posterior axis of the dorsal spinal cord as a tightly fasciculated bundle, as revealed by whole-mount immunohistochemistry at e12.5 (Fig. 2.10a, b). This is in stark

contrast to the DRG central projections of *Wnt1Cre;TcKO* embryos, which are highly defasciculated (Fig. 2.10c-d'), resulting in a highly significant increase in the number of "free" growth cones in the dorsal SC (Fig. 2.10e; two-tailed t-test p=9.06e-24). All other combinations of *Cas* family alleles display no overt phenotypes in DRG or other PNS axon tract guidance (data not shown). Interestingly, some of the defasciculated axons in *Wnt1Cre;TcKO* embryos appear to project towards the ventricular zone (Fig. 2.10c-d'). These phenotypes observed in *Wnt1Cre;TcKO* embryos are 100% penetrant (n=6).

To further explore the role of Cas proteins during DRG axon pathfinding, we examined in more detail the innervation of the SC gray matter by sensory axons in control and *Wnt1Cre;TcKO* mutants. DRG afferent axons project to the DREZ and then stall during a "waiting period" before innervating the spinal cord. In the mouse this period extends from e11 until e13.5 for proprioceptors, or e15 for nociceptors (Gu et al., 2003; Yoshida et al., 2006). In control e11.5 embryos, no sensory axons are detected medial to the DREZ and dorsal funiculus (Fig. 2.10f). However, there is a significant increase in the number of DRG axons that invade the gray matter of *Wnt1Cre;TcKO* embryos prematurely (Fig. 2.10g, h; two-tailed t-test p=3.82e-26). This suggests that Cas adaptor proteins are required for proper fasciculation of DRG axons at the dorsal funiculus, as well as preventing these axons from entering the SC gray matter prematurely.

Since Cas proteins are required for DRG axon fasciculation and guidance,

we hypothesized that Cas proteins may be required for pathfinding of other peripheral nerves. Could cranial nerves also require *Cas* gene function for proper fasciculation and guidance? Based on the strong expression of *Cas* genes in the nodose/petrosal complex and trigeminal ganglia (Figs. 2.6 and 2.7), we focused our attention on the vagal and trigeminal nerves. Normally, vagal nerve central projections join and fasciculate with descending axonal tracks coming from the midbrain (Fig. 2.11a) (Wright et al., 2012). Interestingly, in *Wnt1Cre;TcKO,* the vagal afferents overshoot the descending midbrain tracks and display a defasciculated phenotype (Fig. 2.11b). In addition to the vagal nerve, the trigeminal nerve also shows a distinct phenotype in *Wnt1Cre;TcKO* animals (Fig. 2.11c-f). The maxillary branch is highly defasciculated in *Wnt1Cre;TcKO* (Fig. 2.11d, f) compared to control littermates (Fig. 2.11c, e), which is a fully penetrant phenotype. Whereas the ophthalmic branch appears to be under-branched, this might be a result of a general developmental delay observed in *Wnt1Cre;TcKO* embryos by e12 (Fig. 2.11c-f): these embryos will die between e12.5 and e13. Overall, these data support a role for Cas adaptor proteins during peripheral nerve pathfinding.

A previous report using small interference RNA (siRNA) knock-down suggested that *p130Cas* is required for commissural axon guidance (Liu et al., 2007). We revisited this finding by taking advantage of our complete *Cas* loss of function mouse model (Fig. 2.12a-j). We labeled commissural axons using the

precrossing commissural axon marker Tag1 and the post-crossing marker L1 (Zou et al., 2000). A mild, yet significant reduction in the thickness of the ventral commissure was observed in *Wnt1Cre;TcKO* compared to control (Fig. 2.12 a-i; two tailed t-test p=0.004). This suggests that Cas genes might indeed play a conserved role in commissural axon guidance. Tag1 and L1 immunostaining also revealed a significant disorganization and reduction of the size of the DREZ in *Wnt1Cre;TcKO* animals compared to control (Fig. 2.12a, b, e, f, j; ; two tailed t-test p=6.22e-5). These results illustrate the essential and multifaceted role of Cas proteins during both CNS and PNS circuit assembly.

Basement membrane (BM) integrity is required for proper axon guidance (Wright et al., 2012). Thus, the abnormal fasciculation and guidance phenotypes observed at the DREZ in *Wnt1Cre;TcKO* embryos could be a secondary consequence of a disrupted basement membrane surface surrounding the spinal cord. To determine whether *Cas* genes are required for formation of the BM of the spinal cord, we analyzed its integrity in *Wnt1Cre;TcKO* animals. We visualized the BM using an antibody against laminin (Fig. 2.12e-h). The BM appears to be intact in *Wnt1Cre;TcKO* embryos, and is indistinguishable from control embryos (Fig. 2.12e-h). This suggests that *Cas* genes are dispensable for spinal cord BM formation, and that disruption of the basement membrane is unlikely to be responsible for axon pathfinding defects observed in *Wnt1Cre;TcKO* DRG central projections.

Selective ablation of *Cas* genes from the dorsal spinal cord and neural-crest derived PNS ganglia results in axon fasciculation and guidance defects (Fig. 2.10; 2.11); is there a DRG-autonomous requirement for Cas genes in axon pathfinding? To answer this question, we took advantage of a transgenic line that expresses Cre recombinase under control of the human tissue plasminogen activator promoter (Ht-PA). This *HtPACre* transgene is expressed in migratory neural crest cells and their derivatives, including DRG, trigeminal and nodose/petrosal ganglia (Pietri et al., 2003), but not in the dorsal neural tube (Fig. 2.8; 2.9). Consistent with the expression pattern of this Cre line (Fig. 2.8e-h), *HtPACre*-mediated ablation of *Cas* genes in *HtPACre*; *TcKO* embryos results in a notable reduction in PY-Cas signal in the DRGs and DREZ (Fig. 2.8i, k). PY-Cas can be still detected in commissural axons, and the ventral and lateral funiculus of *HtPACre*; *TcKO* embryos (Fig. 2.8k). We examined the DRG central and peripheral projections of control and *HtPACre*; *TcKO* embryos by whole-mount and section neurofilament immunofluorescence (Fig. 2.13a-f). Interestingly*, HtPACre*; *TcKO* animals (Fig. 2.13b) display aberrant defasciculation of DRG central projections compared to control littermates (Fig. 2.13a, e; two-tailed t-test p=1.26e-19). In addition, *HtPACre*; *TcKO* DRG axons invade the spinal cord gray matter prematurely (Fig 8c, d, f; two-tailed t-test p=1.76e-15). These abnormal defasciculation and pathfinding phenotypes look strikingly similar to those of *Wnt1Cre;TcKO* embryos (Fig. 2.10), suggesting that Cas genes act DRG-autonomously during central

projection fasciculation and guidance. However, *HtPACre*; *TcKO* vagal and trigeminal nerve projections look indistinguishable from controls (data not shown). This could be partially explained by the low level of recombination driven by the *HtPACre* transgene in these ganglia (Fig. 2.10).

The stereotyped innervation pattern of the limb by sensory axons provides an excellent model to analyze DRG peripheral projection branching and fasciculation (Pietri et al., 2004; Wickramasinghe et al., 2008). The early lethality of *Wnt1Cre;TcKO* animals (between e12 and e13) precluded us from performing analysis of limb innervation in those animals. Because *HtPACre*;*TcKO* animals survive at least until early adulthood, we explored hind-limb innervation in *HtPACre*;*TcKO* e14.5 embryos and control littermates using neurofilament 200 (NF200), a marker for mechanosensory aβ fibers (Fig. 2.13g, h). The innervation pattern in *HtPACre*;*TcKO* hind-limbs is abnormal compared to control limbs (Fig. 2.13g, h). Mechanosensory fibers stall prematurely and hyper-fasciculate in *HtPACre*;*TcKO* animals. These results demonstrate a requirement of *Cas* genes in a DRG-autonomous manner for the guidance and fasciculation of somatosensory peripheral and central projections.

Based on our results, we hypothesized that Cas adaptor proteins might regulate fasciculation at the DREZ by allowing the growing axons to distinguish between adhesion to the extracellular matrix (ECM) and to other axons. This distinction between cell-cell and cell-ECM adhesion will play a critical role at

choice-points like the DREZ, where axons must decide whether to join an axonal track or not (Raper and Mason, 2010). We first set out to ask whether altering the ECM environment results in changes to the fasciculation properties of DRG axons. We established a simple model to test for the axon-ECM vs. axon-axon adhesion choice: we cultured e13.5 DRG explants on a set concentration of Poly-D-lysine (0.1mg/ml) and a variable concentration of the ECM protein laminin (from 0 µg/ml to 5 µg/ml) (Fig. 2.14a-d). DRG axons plated on 5 µg/ml and 1 µg/ml laminin grew radially and display a characteristic sun-like morphology. Interestingly, when cultured on low (0.1 µg/ml) or no laminin, e13.5 DRG-explant axons fasciculate together forming a rim of axon bundles at a distance from the explant (Fig. 2.14c, d). This "cob-web" phenotype is observed in the great majority of explants cultured with low or no laminin (76.9% and 84.2%, respectively), but is never observed in explants cultured on 1 µg/ml or 5 µg/ml (Fig. 2.14a-e; Freeman-Halton extension of Fisher exact probability test, $p=4.94e-8$). The overall growth of DRG axons is also affected for explants grown on low- or no-laminin, as compared to axons grown on 5 µg/ml laminin (Fig. 2.15a; One-Way Anova, $p=1.11e-16$; Tukey HSD post-hoc test $p<0.00001$ for both pairwise comparisons). These results suggest that a modest change to the ECM composition can dramatically affect the fasciculation preferences and growth rate of DRG axons.

To investigate how Cas adaptor proteins participate in the fasciculation and defasciculation of axons at choice-points, we cultured DRG explants from control

and *HtPACre*; *TcKO* on 5 µg/ml laminin. Control DRG explants axons grew radially in a sun-like pattern, as described above (Fig. 2.14f). Interestingly, *HtPACre*; *TcKO* axons fasciculate together displaying the cob-web morphology (Fig. 2.14g, h). *HtPACre*; *TcKO* axons also display a reduced level of growth as compared to control (Fig. 2.15b; two tailed t-test, p=1.49e-7). The webbing phenotype was not observed in control DRG explants under the same conditions (Fig. 2.14f, h; Fisher Exact Probability test two-tailed p=7.47e-7), but is indistinguishable from the phenotype observed in WT explants cultured on no laminin (Fig. 2.14d, e, g, h; Fisher Exact Probability test one-tailed p=0.397; two-tailed p=0.613). This suggests that *HtPACre*; *TcKO* axons cultured on 5 µg/ml laminin behave as if there was no laminin in the environment. Importantly, the fact that *HtPACre; TcKO* DRG axons display a fasciculation phenotype in an isolated *in vitro* setting reinforces the idea of a cell-autonomous (or at least DRG-autonomous) function of *Cas* genes during DRG fasciculation. Overall, our data support a model whereby Cas proteins regulate DRG axon fasciculation *in vitro* and *in vivo* by allowing axons to sense the ECM.

Discussion

Here, we demonstrate an evolutionarily conserved requirement for Cas adaptor proteins during guidance and fasciculation of PNS axons. Our results in the mouse are consistent with the previously described role of *dCas* in Drosophila PNS development (Huang et al., 2007). In Drosophila, Cas phosphorylation and

function during PNS axon fasciculation and guidance is mainly regulated by integrins. Similarly, during mammalian retina migration, integrin-β1 appears to be the primary regulator of Cas function, as shown by the identical phenotype in their respective null mutants, and molecular epistasis results (Riccomagno et al., 2014). Whereas the peripheral innervation phenotypes in the developing limb are similar in *HtPACre;Itgb1$^{f/f}$* and *HtPACre;TcKO* mutants, the severe central projection phenotype observed in *Cas TcKO* mice was not observed in their *integrin-β1* counterparts (Pietri et al., 2004). This suggests that integrin-β1 is not the sole upstream regulator of Cas adaptor function during DRG central projection pathfinding. Whether integrins act redundantly to regulate Cas function or a different guidance cue- or adhesion-receptor is involved in this process remains to be investigated.

In addition to DRG pathfinding defects, *Wnt1Cre;TcKO* animals display aberrant trigeminal and vagal nerve fasciculation phenotypes. While the vagal nerve phenotype is very specific and fully penetrant, the under-branching trigeminal phenotypes could be likely attributed to a pleiotropic delay in embryonic development. Interestingly, *HtPACre*; *TcKO* vagal nerve central projections look indistinguishable from controls. The most plausible explanation for the lack of an abnormal phenotype in these mutants is that the *HtPACre* transgene is a poor driver of recombination in the nodose/petrosal complex (Fig. 2.9). Whereas *Wnt1Cre* expression results in strong recombination of a Cre reporter in both

nodose and trigeminal, *HtPACre* drives recombination in a very low number of nodosal cells (Fig. 2.9). Given this caveat, we cannot confirm or exclude the possibility that Cas genes might act in a cell-autonomous manner during the fasciculation of vagal projections.

In regards to Cas function during commissural axon guidance, it was reported that *p130Cas* mediates Netrin signaling during this pathfinding event (Liu et al., 2007). The single *Wnt1Cre*;*p130Cas*$^{f/f}$ mutants displayed no obvert axon guidance phenotypes (data not shown). The complete *Cas* loss-of-function mouse model (*Wnt1Cre;TcKO*) did show a significant thinning of the commissure by e11.5, although the phenotypes observed in the chicken knock-down experiments were much more striking [14]. Furthermore, the observed phenotype was notably milder than that of the *Netrin*$^{-/-}$ mice, which have almost no detectable ventral commissures (Serafini et al., 1996). This result suggests that if *Cas* genes indeed act downstream of Netrin during mouse commissural axon guidance, they would more likely serve as modulators than obligate-downstream effectors. Another possibility is that *Cas* genes might play a more general role during commissural axon fasciculation.

An unexpected discovery was the fact that *Cas-null* DRG axons displayed a different growth pattern on laminin than control explants, re-fasciculating with each other at a distance from the somas (Fig. 2.14). *Cas-null* DRG axons behave as if there was no laminin in the extracellular environment, even when cultured on

laminin. This result raises the intriguing possibility that *Cas* genes are required for neurons to distinguish between secreted adhesion molecules in the ECM (e.g. laminin) and neural adhesion molecules present in axons themselves. This environmental assessment will be particularly important at choice-points like the DREZ, and could offer a potential mechanism underlying the DRG central projection defasciculation phenotypes observed in *HtPACre*; *TcKO* and *Wnt1Cre;TcKO* embryos. Alternatively, Cas might be important for DRG axons to pause at the DREZ to sense repulsive and attractive cues on their way to finding their targets. In this regard it is interesting to note that some of the sensory phenotypes observed in *HtPACre*; *TcKO* and *Wnt1Cre;TcKO* embryos resemble aspects of *Robo/Slit* (Ma and Tessier-Lavigne, 2007; Dugan et al., 2011), *dystroglycan* (Wright et al., 2012), netrin (Varadarajan et al., 2017), and *Neuropilin-1* (Gu et al., 2003) mutants. Future studies will investigate the role of Cas adaptor proteins during the interplay between adhesion to the substrate and guidance cue signaling.

Materials and methods

Animals

The day of vaginal plug observation was designated as embryonic day 0.5 (e0.5) and the day of birth postnatal day 0 (P0). Control animals for all experiments were *p130Cas* $^{f/+}$; *CasL*$^{-/-}$ and *Sin*$^{-/-}$. Generation of the *HtPACre*, *Wnt1Cre*, *p130Cas*$^{f/f}$, *CasL*$^{-/-}$ and *Sin*$^{-/-}$ transgenic mouse lines has been described previously

(Riccomagno et al., 2014; Lewis et al., 2013; Pietri et al., 2003; Donlin et al., 2005; Seo et al., 2005). All animal procedures presented here were performed according to the University of California, Riverside's Institutional Animal Care and Use Committee (IACUC) guidelines. All procedures were approved by UC Riverside IACUC.

In situ Hybridization

In situ hybridization was performed on spinal cord frozen sections (20 µm thickness) using digoxigenin-labeled cRNA probes, as previously described (Giger et al., 2000). Whole-mount RNA in situ hybridization was performed as described (Matise et al., 1998). Generation of the *p130Ca*s, *CasL* and *Sin* cRNA probes has been described in (Riccomagno et al., 2014).

Immunofluorescence

Mice were perfused and fixed with 4% paraformaldehyde for 1 hour to O/N at 4°C, rinsed, and processed for whole-embryo staining or sectioned on a vibratome (75 μm). Whole-mount immunofluorescence was performed as described in (Huber et al., 2005). Immunohistochemistry of floating sections was carried out essentially as described (Polleux and Ghosh, 2002). For cryostat sections, following fixation, embryos were equilibrated in 30% sucrose/PBS and embedded in OCT embedding media (Tissue-Tek). Transverse spinal cord sections (20-40 μm) were obtained on a Leica CM3050 cryostat and blocked in 10% goat serum in 1 X PBS and 0.1% Triton-X100 for 1 hr at room temperature.

Sections were then incubated O/N at 4°C with primary antibodies.

Sections were then washed in 1 X PBS and incubated with secondary antibodies and TOPRO-3 (Molecular Probe at 1:500 and 1:2000, respectively). Sections were washed in PBS and mounted using vectorshield hard-set fluorescence mounting medium (Vector laboratories). Confocal fluorescence images were taken using a Leica SPE II microscope. Primary antibodies used in this study include: rabbit anti-p130Cas C terminal (Santa Cruz, 1:200), rabbit anti-p130Cas PY165 (Cell Signaling Technology, 1:100), rabbit anti-laminin (Sigma, 1:1000), rabbit anti-GFP (Lifescience Technologies, 1:500), chicken anti-GFP (AVES, 1:1000), mouse anti-Neurofilament (2h3, Developmental Studies Hybridoma Bank, 1:500), mouse anti-Tag1 (4D7, Developmental Studies Hybridoma Bank, 1:50), Rat anti-L1 (MAB5272, Millipore, 1:500) and rabbit anti-NF-200 (Millipore, 1:500).

Quantification of spinal cord ventral commissure and DREZ thickness

Thickness of the DREZ and ventral commissure were measured on L1-immunostained cryosections at e11.5 (20-µm sections). The thickness values for the ventral commissure were normalized to the distance between roof plate and floor plate for each section, as described previously (Hernandez-Enriquez et al., 2015; Jaworski et al., 2010). The maximal thickness of the DREZ for each hemi-spinal cord was recorded and normalized to the distance between the BM and the ventricular zone at the same dorso-ventral level. Thickness was measured at branchial levels. Five sections per embryo, from 3-5 embryos were analyzed.

Statistical differences for mean values between two samples were determined by two-tail Student's t-test for independent samples.

Quantification of growth cones invading the spinal cord

50-µm vibratome sections were stained with neurofilament (2H3) and the number of axons entering the spinal cord were quantified. "Free" growth cones per segment were quantified using high magnification images of cleared whole-mount embryos immunostained for 2H3. The number of free growth cones was determined by counting growth cones from the anterior end of a DRG to the anterior edge of the following DRG. Statistical differences for mean values between two samples were determined by two-tail Student's t-test for independent samples.

Tissue Culture

DRGs from e13.5 embryos were dissected in ice-cold L15 (Invitrogen). DRG explants were then plated on acid-washed glass coverslips previously coated with 0 to 5µg/ml laminin and 100µg/ml polyD-lysine. DRGs were then cultured for 18 hours in enriched Opti-MEM/F12 media containing 15ng/ml NGF, as previously described (Kolodkin et al., 1997). Live explants were stained with Calcein-AM (Invitrogen) and then imaged. For the Control vs. *HtPACre; TcKO* explant experiment a total of 12-15 explants from 3 independent experiments were analyzed.

Acknowledgements
We would like to thank Drs. Sachiko Seo and Mineo Kurokawa, and Dr. Konstantina Alexandropoulos for sharing the *CasL*$^{-/-}$ and *Sin*$^{-/-}$ mouse lines, respectively. The *p130Cas EGFP-Bac* line was generated by the GENSAT consortium. We also thank Drs. Garret Anderson and Randal Hand for helpful comments on the manuscript. This study was supported by Initial Complementary Funds from the University of California, Riverside.

Availability of data and materials
All data analyzed during this study are included in this article.

Authors Contributions
TAVH performed experiments and wrote the manuscript. JAE, KR, MLR and KMW designed and performed experiments. MLR and KMW also provided comments and suggestions for the manuscript. MMR conceived the project, designed and performed experiments, and wrote the manuscript.

Ethics approval
All animal procedures presented here were performed according to the University of California, Riverside's Institutional Animal Care and Use Committee (IACUC)-approved guidelines.

Competing interests
The authors declare that they have no competing interests.

References

Barber, R. P. & Vaughn, J. E. (1986). Differentiation of dorsal root ganglion cells with processes in their synaptic target zone of embryonic mouse spinal cord: a retrograde tracer study. *J Neurocytol 15*, 207-218.

Bourgin, C., Murai, K. K., Richter, M. & Pasquale, E. B. (2007). The EphA4 receptor regulates dendritic spine remodeling by affecting beta1-integrin signaling pathways. *J Cell Biol*, *178*, 1295-1307. doi:10.1083/jcb.200610139

Defilippi, P., Di Stefano, P. & Cabodi, S. p130Cas: a versatile scaffold in signaling networks. *Trends Cell Biol*, *16,* 257-263. doi:10.1016/j.tcb.2006.03.003

Dugan, J. P., Stratton, A., Riley, H. P., Farmer, W. T. & Mastick, G. S. (2011). Midbrain dopaminergic axons are guided longitudinally through the diencephalon by Slit/Robo signals. *Mol Cell Neurosci, 46*, 347-356. doi:10.1016/j.mcn.2010.11.003

Donlin, L. T., Danzl, N. M., Wanjalla, C. & Alexandropoulos, K. (2005). Deficiency in expression of the signaling protein Sin/Efs leads to T-lymphocyte activation and mucosal inflammation. *Mol Cell Biol, 25,* 11035-11046. doi:10.1128/MCB.25.24.11035-11046.2005

Frank, E. & Sanes, J. R. (1991). Lineage of neurons and glia in chick dorsal root ganglia: analysis in vivo with a recombinant retrovirus. *Development, 111*. 895-908.

Giger, R. J., Cloutier, J. F., Sahay, A., Prinjha, R. K., Levengood, D. V., Moore, S. E., Pickering, S., Simmons, D., Rastan, S., Walsh, F. S., Kolodkin, A. L., Ginty, D. D., & Geppert, M. (2000). Neuropilin-2 is required in vivo for selective axon guidance responses to secreted semaphorins. *Neuron*, *25*(1), 29–41. https://doi.org/10.1016/s0896-6273(00)80869-7

Gong, S. *et al.* (2003). A gene expression atlas of the central nervous system based on bacterial artificial chromosomes. *Nature 425*, 917-925. doi:10.1038/nature02033

Gu, C., Rodriguez, E. R., Reimert, D. V., Shu, T., Fritzsch, B., Richards, L. J., Kolodkin, A. L., & Ginty, D. D. (2003). Neuropilin-1 conveys semaphorin and VEGF signaling during neural and cardiovascular development. *Developmental cell*, *5*(1), 45–57. https://doi.org/10.1016/s1534-5807(03)00169-2

Heintz, N. (2004). Gene expression nervous system atlas (GENSAT). *Nat Neurosci 7*, 483. doi:10.1038/nn0504-483

Huang, Z., Yazdani, U., Thompson-Peer, K. L., Kolodkin, A. L. & Terman, J. R. (2007). Crk-associated substrate (Cas) signaling protein functions with integrins to specify axon guidance during development. *Development 134,* 2337-2347. doi:10.1242/dev.004242

Huber, A. B., Kania, A., Tran, T. S., Gu, C., De Marco Garcia, N., Lieberam, I., Johnson, D., Jessell, T. M., Ginty, D. D., & Kolodkin, A. L. (2005). Distinct roles for secreted semaphorin signaling in spinal motor axon guidance. *Neuron*, *48*(6), 949–964. https://doi.org/10.1016/j.neuron.2005.12.003

Hernandez-Enriquez, B., Wu, Z., Martinez, E., Olsen, O., Kaprielian, Z., Maness, P. F., Yoshida, Y., Tessier-Lavigne, M., & Tran, T. S. (2015). Floor plate-derived neuropilin-2 functions as a secreted semaphorin sink to facilitate commissural axon midline crossing. *Genes & development*, *29*(24), 2617–2632. https://doi.org/10.1101/gad.268086.115

Jaworski, A., Long, H. & Tessier-Lavigne, M. (2010). Collaborative and specialized functions of Robo1 and Robo2 in spinal commissural axon guidance. *J Neurosci 30*, 9445-9453. doi:10.1523/JNEUROSCI.6290-09.2010.

Kolodkin, A. L., Levengood, D. V., Rowe, E. G., Tai, Y. T., Giger, R. J., & Ginty, D. D. (1997). Neuropilin is a semaphorin III receptor. *Cell*, *90*(4), 753–762. https://doi.org/10.1016/s0092-8674(00)80535-8

Kolodkin, A. L. & Tessier-Lavigne, M. (2011). Mechanisms and molecules of neuronal wiring: a primer. *Cold Spring Harb Perspect Biol 3,* doi:10.1101/cshperspect.a001727

Lewis, A. E., Vasudevan, H. N., O'Neill, A. K., Soriano, P. & Bush, J. O. (2013). The widely used Wnt1-Cre transgene causes developmental phenotypes by ectopic activation of Wnt signaling. *Dev Biol 379*, 229-234. doi:10.1016/j.ydbio.2013.04.026

Liu, G., Li, W., Gao, X., Li, X., Jürgensen, C., Park, H.-T., Shin, N.-Y., Yu, J., He, M.-L., Hanks, S. K., Wu, J. Y., Guan, K.-L., & Rao, Y. (2007). p130CAS is required for netrin signaling and commissural axon guidance. *The Journal of Neuroscience*, *27*(4), 957-968. doi:10.1523/JNEUROSCI.4616-06.2007

Ma, L. & Tessier-Lavigne, M. (2007). Dual branch-promoting and branch-repelling actions of Slit/Robo signaling on peripheral and central branches of developing sensory axons. *J Neurosci 27*, 6843-6851. doi:10.1523/JNEUROSCI.1479-07.2007.

Ma, Q., Fode, C., Guillemot, F. & Anderson, D. J. (1999). Neurogenin1 and neurogenin2 control two distinct waves of neurogenesis in developing dorsal root ganglia. *Genes Dev 13,* 1717-1728.

Matise, M. P., Epstein, D. J., Park, H. L., Platt, K. A. & Joyner, A. L. (1998). Gli2 is required for induction of floor plate and adjacent cells, but not most ventral neurons in the mouse central nervous system. *Development 125,* 2759-2770.

Merrill, R. A., See, A. W., Wertheim, M. L. & Clagett-Dame, M. (2004).Crk-associated substrate (Cas) family member, NEDD9, is regulated in human neuroblastoma cells and in the embryonic hindbrain by all-trans retinoic acid. *Dev Dyn 231*, 564-575. doi:10.1002/dvdy.20159

O'Neill, G. M., Fashena, S. J. & Golemis, E. A. (2000). Integrin signalling: a new Cas(t) of characters enters the stage. *Trends Cell Biol 10*, 111-119.

Ozaki, S. & Snider, W. D. (1997). Initial trajectories of sensory axons toward laminar targets in the developing mouse spinal cord. *J Comp Neurol 380*, 215-229.

Pietri, T., Eder, O., Blanche, M., Thiery, J. P. & Dufour, S. (2003). The human tissue plasminogen activator-Cre mouse: a new tool for targeting specifically neural crest cells and their derivatives in vivo. *Dev Biol 259*, 176-187.

Pietri, T., Eder, O., Breau, M. A., Topilko, P., Blanche, M., Brakebusch, C., Fässler, R., Thiery, J. P., & Dufour, S. (2004). Conditional beta1-integrin gene deletion in neural crest cells causes severe developmental alterations of the peripheral nervous system. *Development (Cambridge, England)*, *131*(16), 3871–3883. https://doi.org/10.1242/dev.01264

Polleux, F., & Ghosh, A. (2002). The slice overlay assay: a versatile tool to study the influence of extracellular signals on neuronal development. *Science's STKE*, *2002*(136), pl9.

Ramon y Cajal, S. (1909). in *Histologie du système nerveux de l'homme & des vertébrés* Vol. 1 (ed L. Azoulay), 420-460.

Raper, J. & Mason, C. (2010). Cellular strategies of axonal pathfinding. *Cold Spring Harb Perspect Biol 2*, a001933. doi:10.1101/cshperspect.a001933

Riccomagno, M. M., Sun, L. O., Brady, C. M., Alexandropoulos, K., Seo, S., Kurokawa, M., & Kolodkin, A. L. (2014). Cas adaptor proteins organize the retinal ganglion cell layer downstream of integrin signaling. *Neuron*, *81*(4), 779–786. https://doi.org/10.1016/j.neuron.2014.01.036

Seo, S., Asai, T., Saito, T., Suzuki, T., Morishita, Y., Nakamoto, T., Ichikawa, M., Yamamoto, G., Kawazu, M., Yamagata, T., Sakai, R., Mitani, K., Ogawa, S., Kurokawa, M., Chiba, S., & Hirai, H. (2005). Crk-associated substrate lymphocyte type is required for lymphocyte trafficking and marginal zone B cell maintenance. *Journal of immunology (Baltimore, Md. : 1950)*, *175*(6), 3492–3501. https://doi.org/10.4049/jimmunol.175.6.3492

Serafini, T., Colamarino, S. A., Leonardo, E. D., Wang, H., Beddington, R., Skarnes, W. C., & Tessier-Lavigne, M. (1996). Netrin-1 is required for commissural axon guidance in the developing vertebrate nervous system. *Cell*, *87*(6), 1001–1014. https://doi.org/10.1016/s0092-8674(00)81795-x

Serbedzija, G. N., Bronner-Fraser, M. & Fraser, S. E. (1989). A vital dye analysis of the timing and pathways of avian trunk neural crest cell migration. *Development 106*, 809-816.

Serbedzija, G. N., Fraser, S. E. & Bronner-Fraser, M. (1990). Pathways of trunk neural crest cell migration in the mouse embryo as revealed by vital dye labelling. *Development 108*, 605-612.

Varadarajan, S. G., Kong, J. H., Phan, K. D., Kao, T. J., Panaitof, S. C., Cardin, J., Eltzschig, H., Kania, A., Novitch, B. G., & Butler, S. J. (2017). Netrin1 produced by neural progenitors, not floor plate cells, is required for axon guidance in the spinal cord. *Neuron*, *94*(4), 790–799.e3. https://doi.org/10.1016/j.neuron.2017.03.007

Wang, F., Julien, D. P. & Sagasti, A. (2013). Journey to the skin: Somatosensory peripheral axon guidance and morphogenesis. *Cell Adh Migr 7*, 388-394. doi:10.4161/cam.25000

Wickramasinghe, S. R., Alvania, R. S., Ramanan, N., Wood, J. N., Mandai, K., & Ginty, D. D. (2008). Serum response factor mediates NGF-dependent target innervation by embryonic DRG sensory neurons. *Neuron*, *58*(4), 532–545. https://doi.org/10.1016/j.neuron.2008.03.006

Wright, K. M., Lyon, K. A., Leung, H., Leahy, D. J., Ma, L., & Ginty, D. D. (2012). Dystroglycan organizes axon guidance cue localization and axonal pathfinding. *Neuron*, *76*(5), 931–944. https://doi.org/10.1016/j.neuron.2012.10.009

Yoshida, Y., Han, B., Mendelsohn, M. & Jessell, T. M. (2006). PlexinA1 signaling directs the segregation of proprioceptive sensory axons in the developing spinal cord. *Neuron 52,* 775-788. doi:10.1016/j.neuron.2006.10.032

Zou, Y., Stoeckli, E., Chen, H. & Tessier-Lavigne, M. (2000). Squeezing axons out of the gray matter: a role for slit and semaphorin proteins from midline and ventral spinal cord. *Cell*, *102,* 363-375.

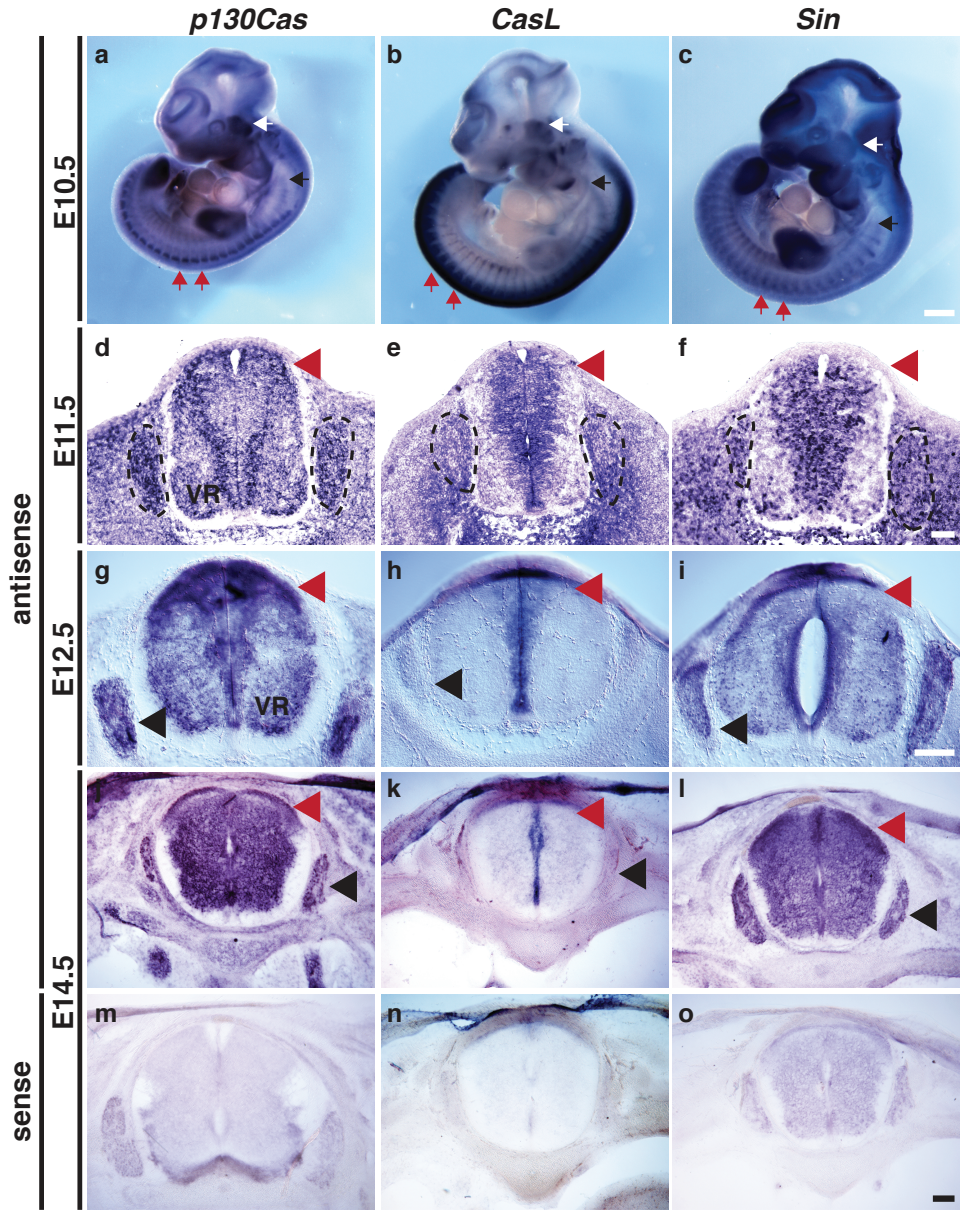

Figure 2.1. Expression of *Cas* genes in the developing dorsal root ganglia and spinal cord. (a-c) Whole-mount *in situ* hybridization for p*130Cas*, *CasL* and *Sin* in e10.5 embryos. White arrows mark the trigeminal ganglion, black arrows mark the nodose/petrosal compex, and red arrows point at DRG examples. **(d-o)** Transverse sections through embryonic spinal cords stained by in situ hybridization with probes against p*130Cas* (**d, g, j, m**), *CasL* (**e, h, k, n**) and *Sin* (**f, i, l, o**), at e11.5 (**d-f**), e12.5 (**g-i**), and e14.5 (**j-o**). *Cas* genes show overlapping expression in the DRGs (dotted line and black arrowhead) and dorsal spinal cord (red arrowheads). No staining was detected for the sense probes (**m-o**). Scale bars: 500 µm for **a-c**; 100 µm for **d-f**; 200 µm **g-i** and 100 µm **j-o**.

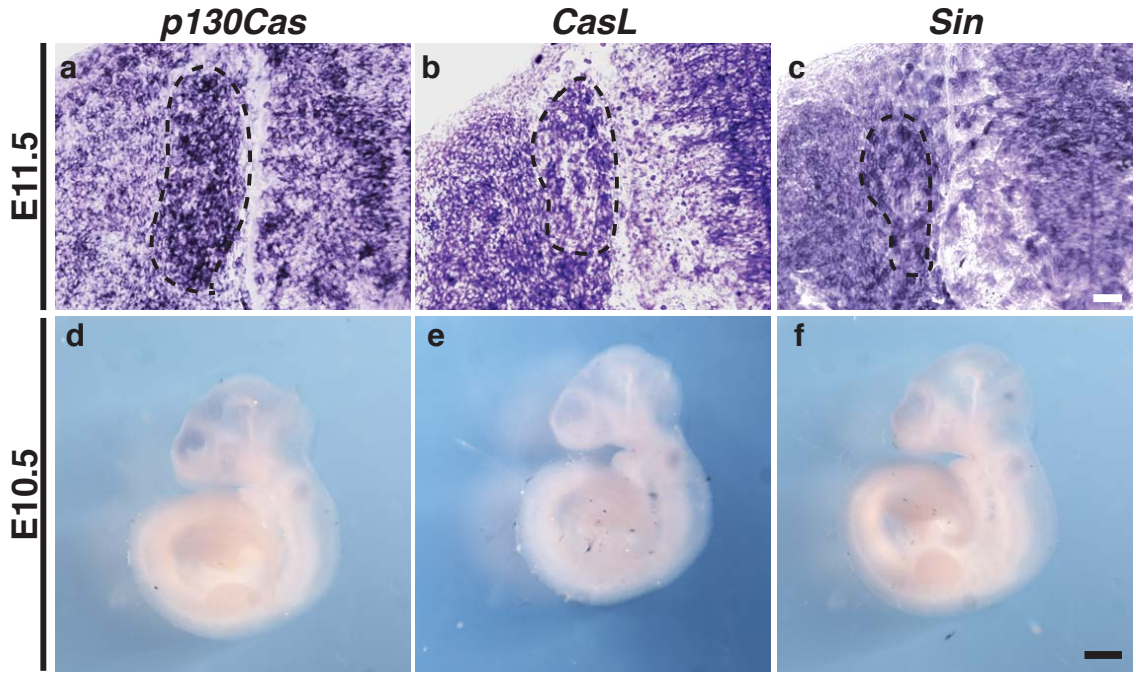

Figure 2.2. Expression of *Cas* mRNA in DRGs. (a-c) Transverse sections through embryonic SC and DRG stained by in situ hybridization with probes against p*130Cas* (**a**), *CasL* (**b**) and *Sin* (**c**) at e11.5. Dotted lines delineate the DRG. **(d-f)** Whole-mount *in situ* hybridization with sense control probes for p*130Cas*, *CasL* and *Sin* in e10.5 embryos. Scale bars: 50 µm for **a-c**; 500 µm for **d-f**.

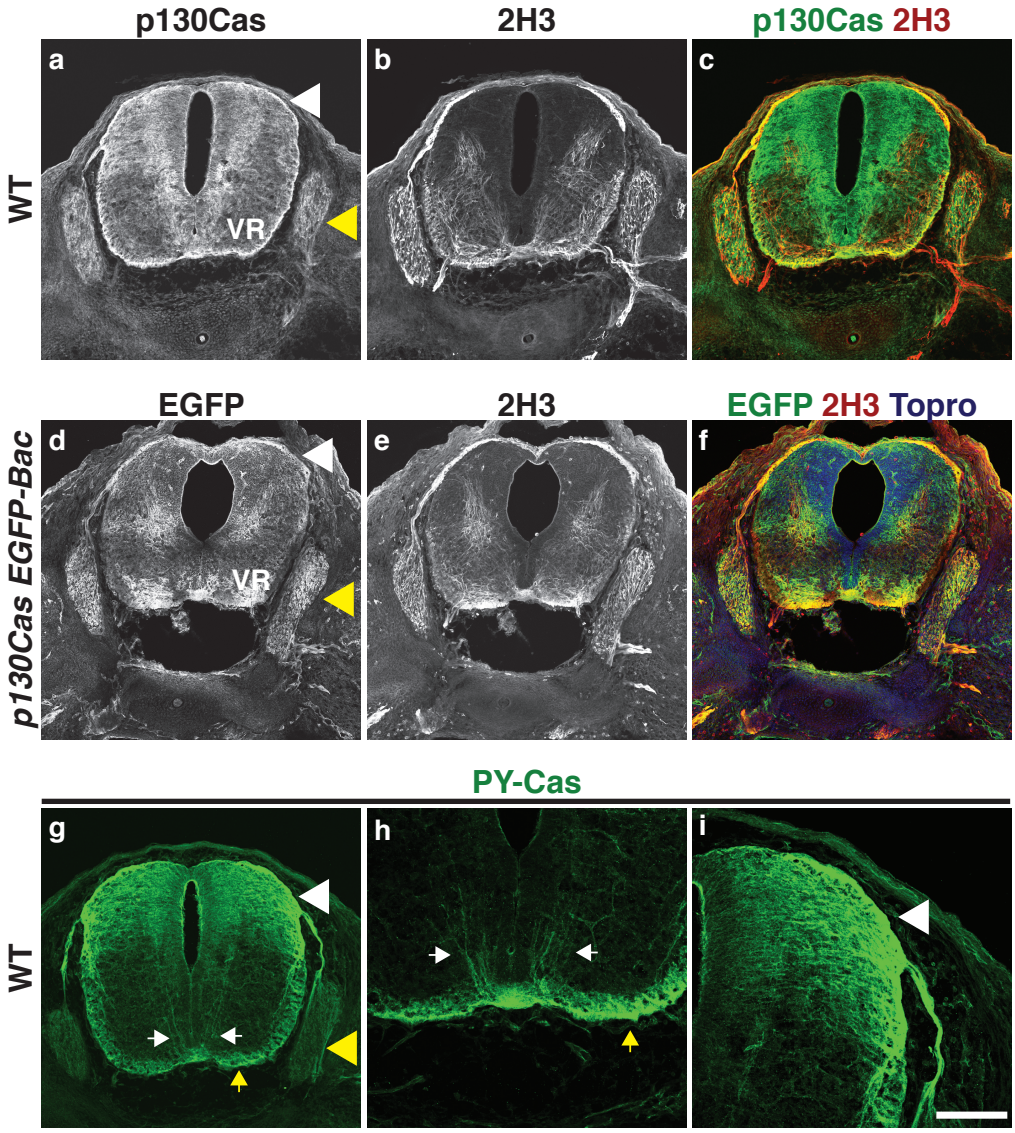

Figure 2.3. p130Cas is phosphorylated in commissural axons and DRG central projections. (**a-c**) Expression profile of p130Cas protein (green) in transverse sections through the mouse spinal cord at e12.5. Anti-Neurofilament (2H3, red) was used to reveal axons. (**d-f**) Immunofluorescence for EGFP (green) and 2H3 (red) in e12.5 *p130Cas EGFP-Bac* spinal cords. ToproIII (blue) was used to counterstain nuclei. (**g-i**) Expression of a phosophorylated-p130Cas (PY-Cas, green) in e12.5 spinal cord and DRGs. (**h**) PY-Cas is present in the ventral funiculus and commissural axons. (**i)** p130Cas phosphorylation is mainly found in the dorsal spinal cord and is enriched in DRG axons and DREZ. DRGs White arrowheads: DREZ; Yellow arrowheads: DRG; White arrows: commissural axons; Yellow arrows: ventral funiculus; VR: ventral roots. Scale bar: 200 µm for **a, b, d** and 100 µm for **c, e, f**.

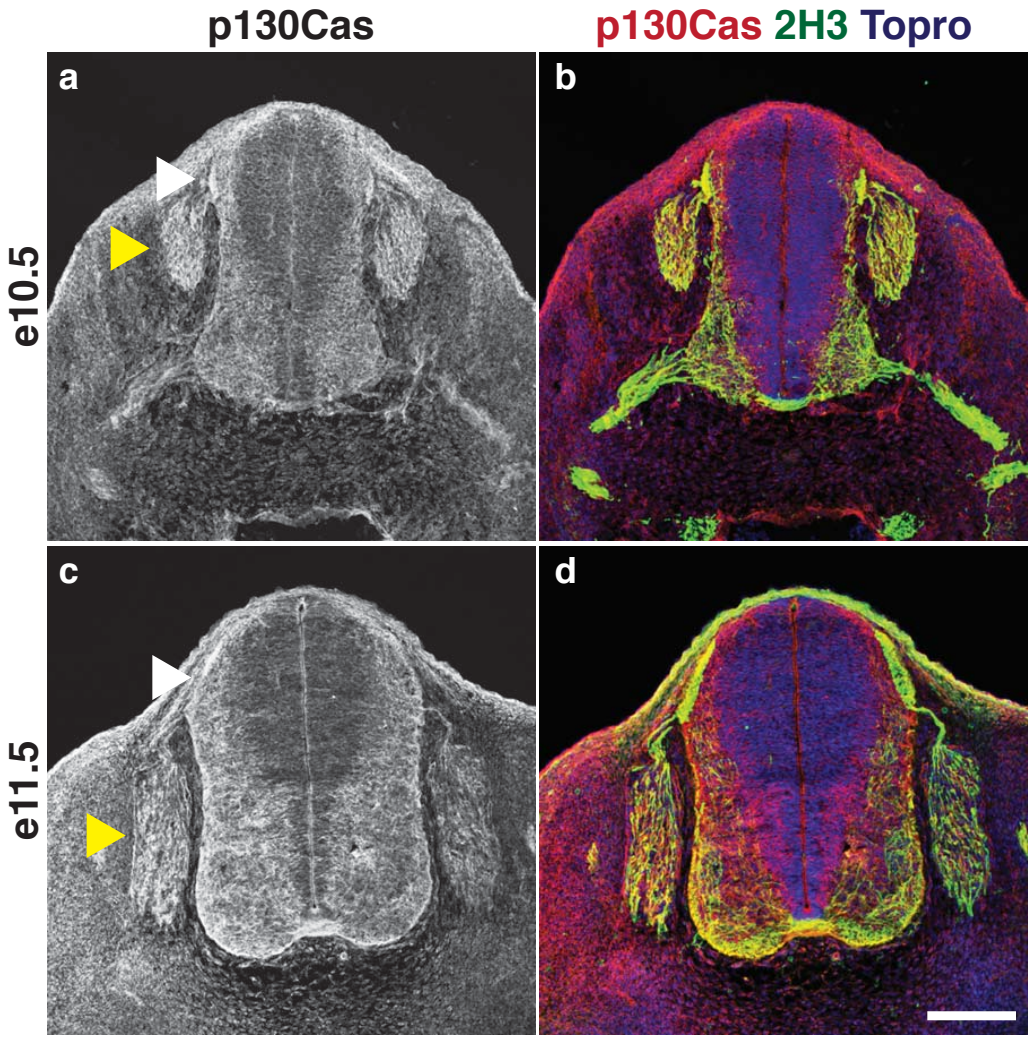

Figure 2.4. p130Cas expression in embryonic SC and DRG. (**a-d**) Expression profile of p130Cas protein (red) in transverse sections through the mouse spinal cord at e10.5 (**a, b**) and e11.5 (**c, d**). Anti-Neurofilament (2H3, green) was used to reveal axons. ToproIII (blue) was used to counterstain nuclei. White arrowheads: DREZ; Yellow arrowheads: DRG. Scale bar: 150 µm.

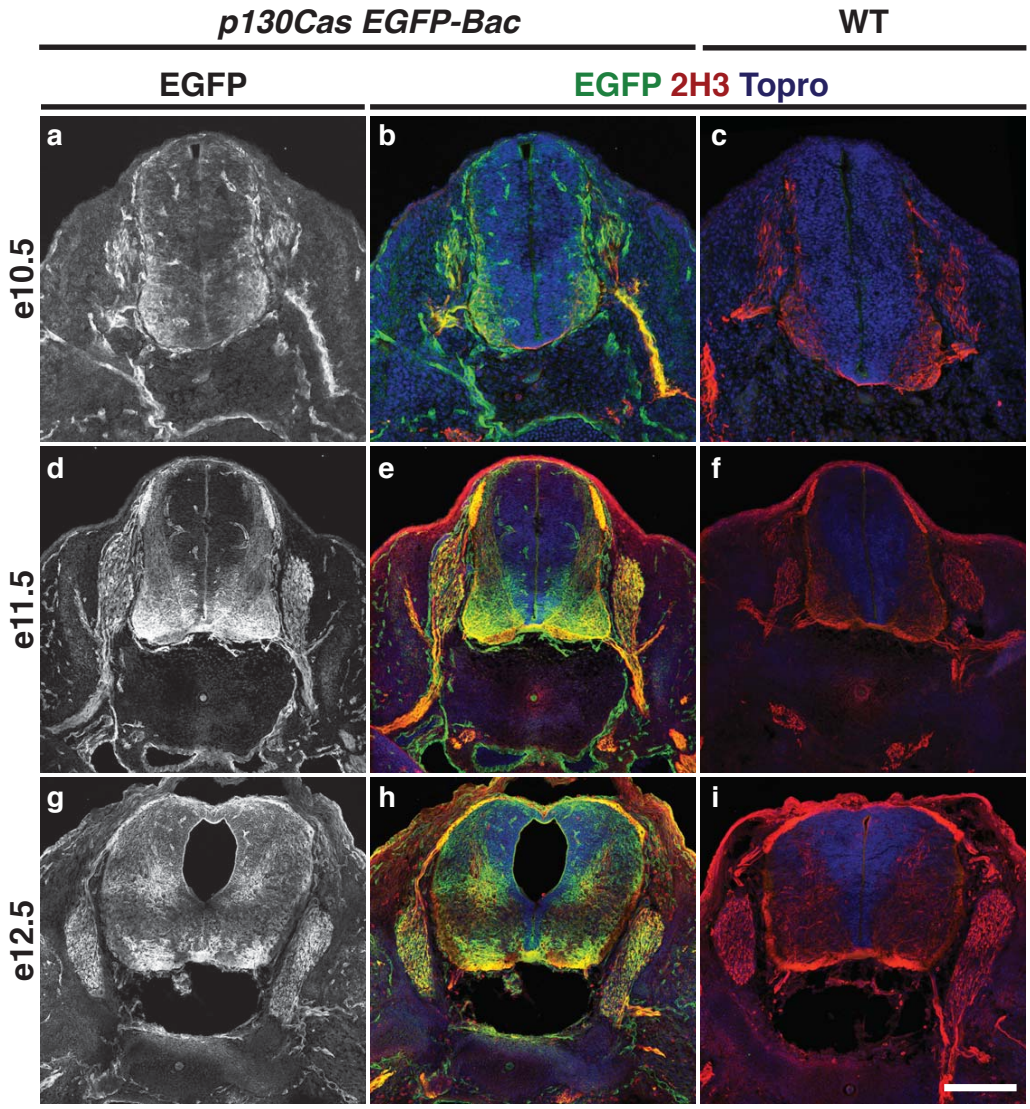

Figure 2.5. Expression analysis of *p130Cas EGFP-Bac* in developing SC. (**a-i**) Immunofluorescence for EGFP (green) and 2H3 neurofilament (red) on transverse sections from *p130Cas EGFP-Bac* (**a, b, d, e, g, h**) and WT **(c, f, i**) spinal cords at e10.5 **(a-c**), e11.5 (**d-f)** and e12.5 (**g-i).** ToproIII (blue) was used to counterstain nuclei. Note that *p130Cas*-driven EGFP expression is high in DRG, dorsal SC, DREZ and ventral roots. Panels **g** and **h** are also presented in Figure 2. Scale bar: 100 µm for **a-c**; 200 µm for **d-i.**

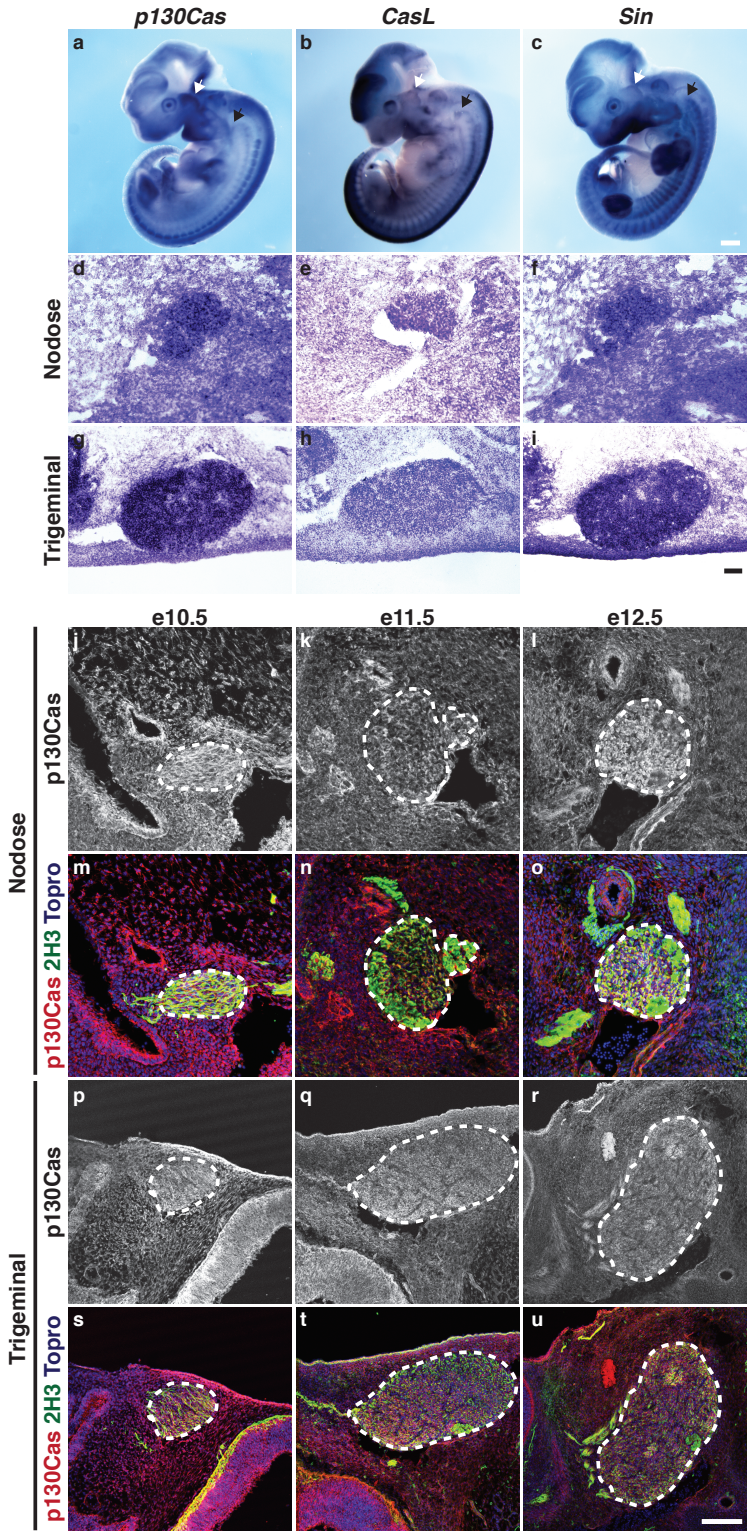

Figure 2.6. Expression of Cas mRNA and protein in trigeminal and nodose ganglia. (a-c) Whole-mount *in situ* hybridization for p*130Cas*, *CasL* and *Sin* in e11.5 embryos. White and black arrows mark the trigeminal ganglion and the nodose/petrosal complex, respectively. **(d-i)** In situ hybridization on transverse sections through the nodose (**d-f**) and trigeminal (**g-i**) of e11.5 embryos with probes against p*130Cas* (**d, g**), *CasL* (**e, h**) and *Sin* (**f, i,).** (**j-u**) Expression profile of p130Cas protein (red) in transverse sections through the nodose **(j-o**) and trigeminal (**p-u**) ganglia at various developmental stages. Anti-neurofilament (2H3, green) was used to visualize axon and ToproIII (blue) was used to counterstain nuclei. Dotted lines delineate the ganglia. Scale bars: 500 µm for **a-c,** 50 µm for **d-f**, 100 µm for **g-i,** 75 um for **j-o** and 150 um for **p-u**.

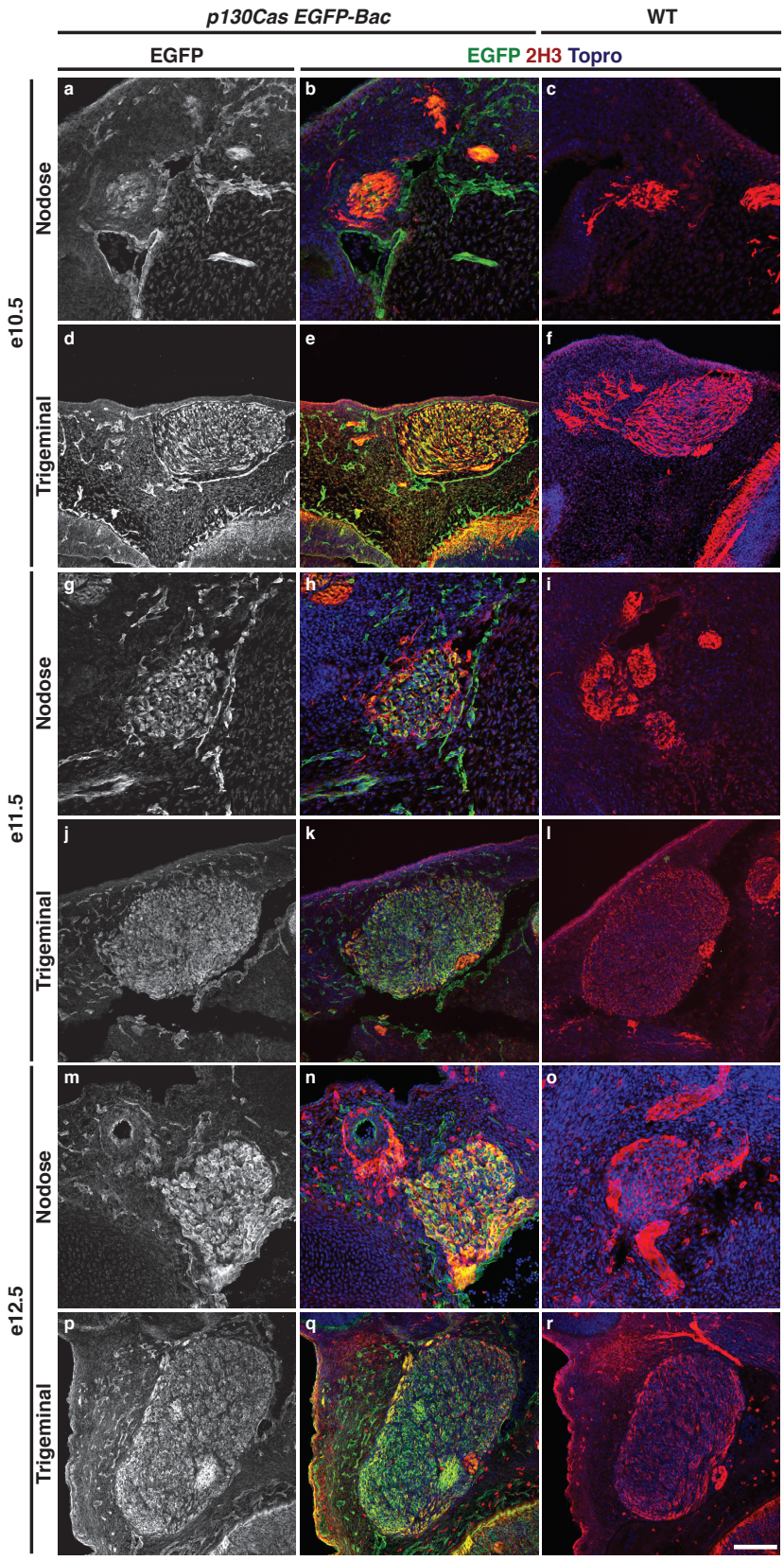

Figure 2.7. Expression analysis of *p130Cas EGFP-Bac* in cranial ganglia. (**a-r**) Immunofluorescence for EGFP (green) and 2H3 neurofilament (red) on transverse sections from *p130Cas EGFP-Bac* (**a, b, d, e, g, h, j, k, m, n, p, q**) and WT (**c, f, i, l, o, r**) embryos, through the nodose (**a-c, g-i, m-o**) and trigeminal (**d-f, j-l, p-r)** ganglia. ToproIII (blue) was used to counterstain nuclei. Note that *p130Cas*-driven EGFP expression is high throughout both ganglia. Scale bar: 75 um for **a-c**, **g-i** and **m-o**; 150 um **d-f**, **j-l** and **p-r.**

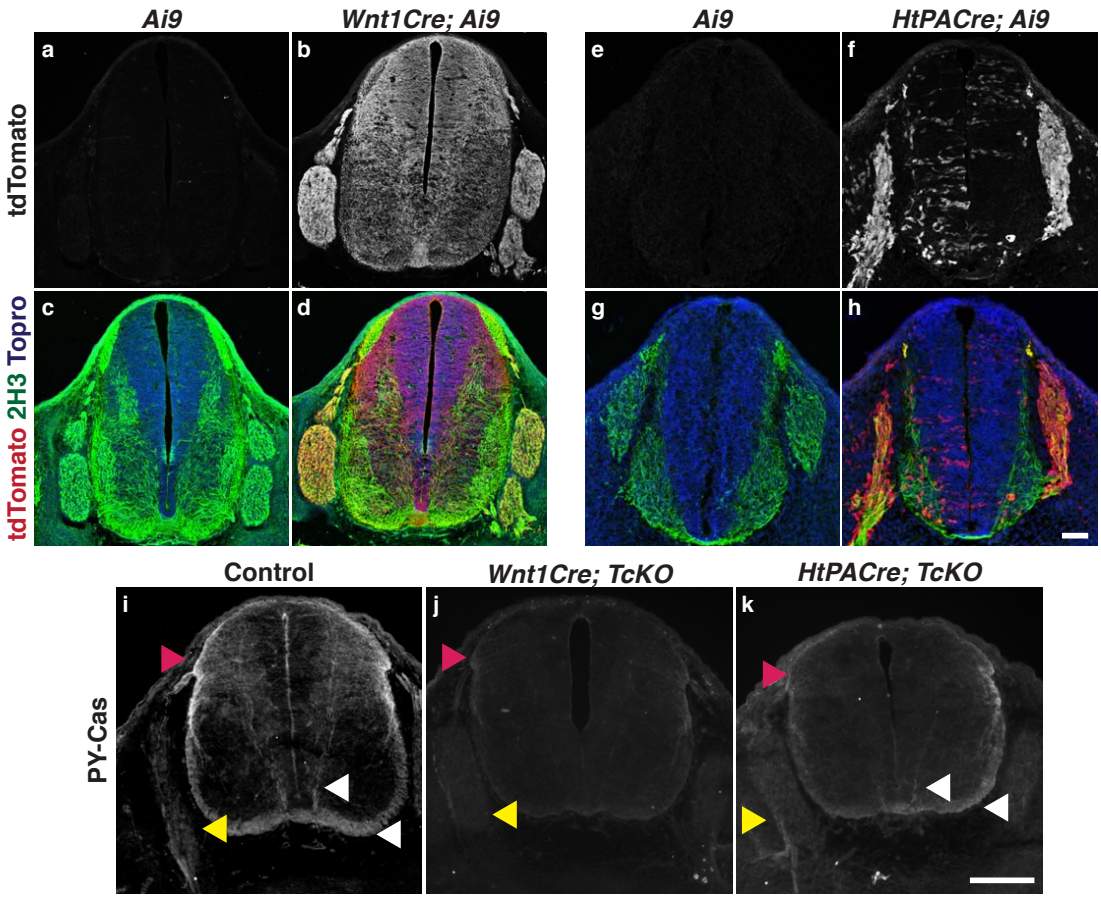

Figure 2.8. Recombination pattern of Cre lines in the spinal cord and DRG. (a-h) Cre activity as reported by tdTomato expression (red) in e12 control reporter animals (*Ai9*, **a, c, e, g**), *Wnt1Cre; Ai9* (**b, d**), and *HtPACre; Ai9* (**f, h**). Anti-2H3 (green) was used to visualize axons and ToproIII (blue) to label nuclei. *HtPACre; Ai9* displays some sparse labeling in the SC, which appears to be stochastic. **(i-k)** Immunostaining for PY-Cas in Control (**i**), *Wnt1Cre;TcKO* (**j**) and *HtPACre*; *TcKO* (**k**) e12.5 spinal cords. Note the efficient ablation of phosphorylated-Cas from DRG and DREZ in *Wnt1Cre;TcKO* and *HtPACre*; *TcKO* embryos. As expected, PY is still detected in the ventral funiculus and commissural axons of *HtPACre*; *TcKO* animals (**k**, white arrowheads). Yellow arrowheads: DRG; Red arrowheads: DREZ. Scale bars: 100 µm for **a-h**; 200 µm for **i-k**.

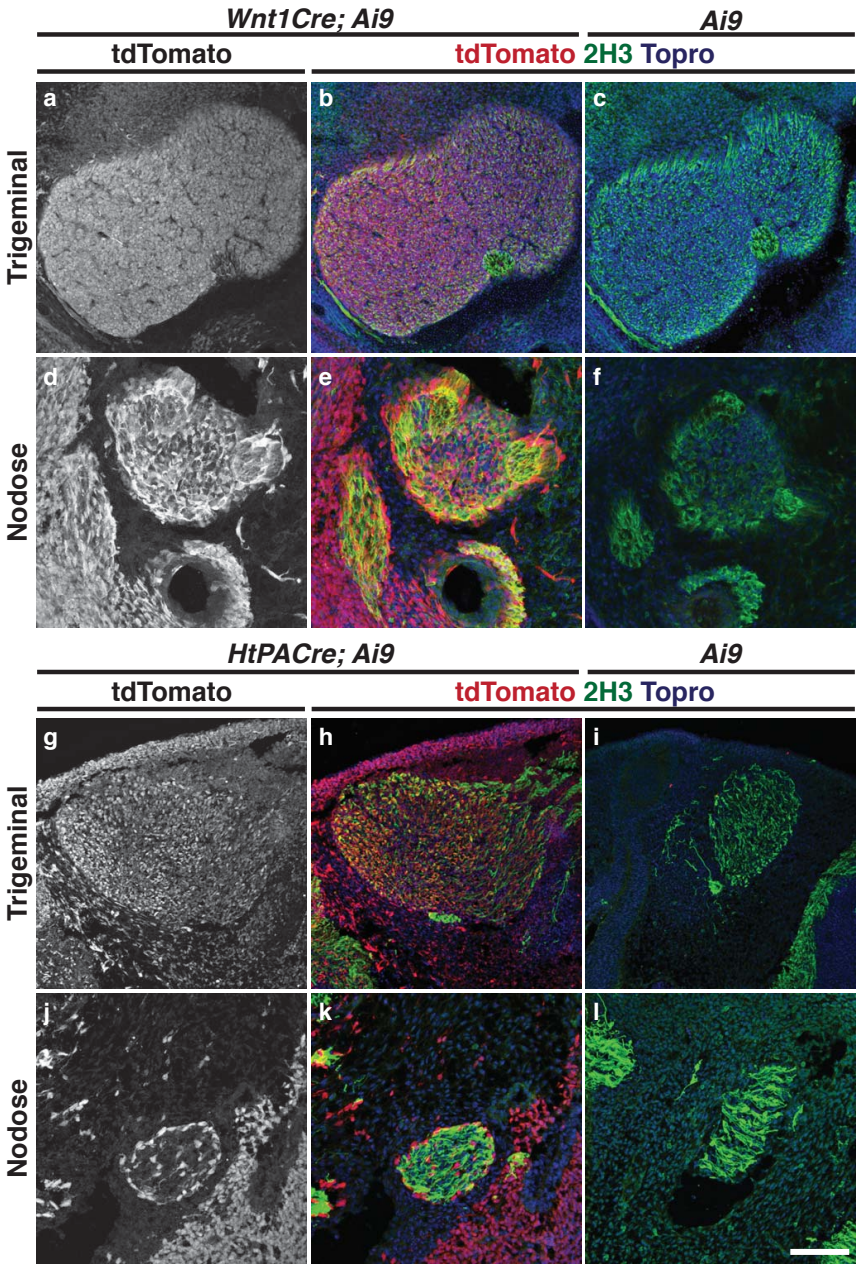

Figure 2.9. Recombination pattern of Cre lines in the nodose and trigeminal ganglion. (a-l) tdTomato expression (red) in *Wnt1Cre; Ai9* (a, b, d, e), *HtPACre; Ai9* (g, h, j, k), and *Ai9* control littermates (c, f , i ,l) at e11.5. Transverse sections through the trigeminal (a-c, g-i) and nodose (d-f, j-l) ganglia. Anti-2H3 (green) was used to label axons and ToproIII (blue) to label nuclei. *Wnt1Cre* (a, b, d, e) strongly drives recombination in the nodose and trigeminal ganglia. *HtPACre; Ai9* shows lower number of neurons expressing tdTomato in both ganglia, and appears to be a very inefficient driver of recombination in the nodose. Scale bar: 150 µm for a-c and g-i; 75 µm d-f, j-l.

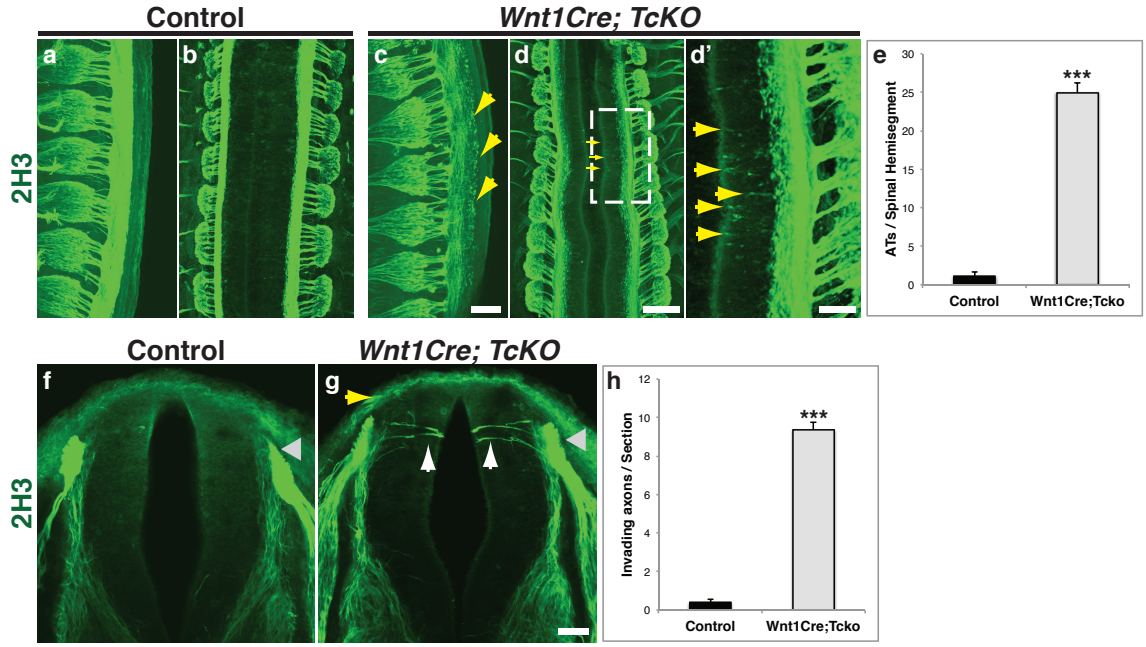

Figure 2.10. Cas adaptor proteins are required for the fasciculation of DRG central projections. (a-d') Whole embryo immunostaining for neurofilament (2H3, green) at e12.5, from a side view (**a, c**) or a dorsal view (**b, d, d'**). **d'** shows a higher magnification view of the dotted area in d. The centrally projecting DRG axons are severely defasciculated as they enter the spinal cord (yellow arrows). n=6 per gentoype; presented phenotypes displayed 100% penetrance. **(e)** Quantification of free growth cones (GCs) per spinal hemisegment, visualized from the side. Two-tailed t-student test ***, p=9.05e-24, 3-5 thoracic segments per animal, 6 animals for each genotype. **(f-g)** Transverse vibratome sections through e11.5 Control (**f**) and *Wnt1Cre; TcKO* (g) spinal cords at forelimb level stained using an antibody against neurofilament (2H3). Sensory axons invade the spinal cord gray matter prematurely in *Wnt1Cre; TcKO* animals (**g**, white arrows). Gray arrows: DREZ. **(h)** Quantification of number of growth cones (GCs) invading the spinal cord per section. Two-tailed t-student test ***, p= 3.82e-26. 5 sections per animal, 5 animals for each genotype. Error bars represent SEM. Scale bars: 100 µm for **a, c**; 200 µm **b, d**; 66.7 µm for **d'**; and 50 µm for **f, g**.

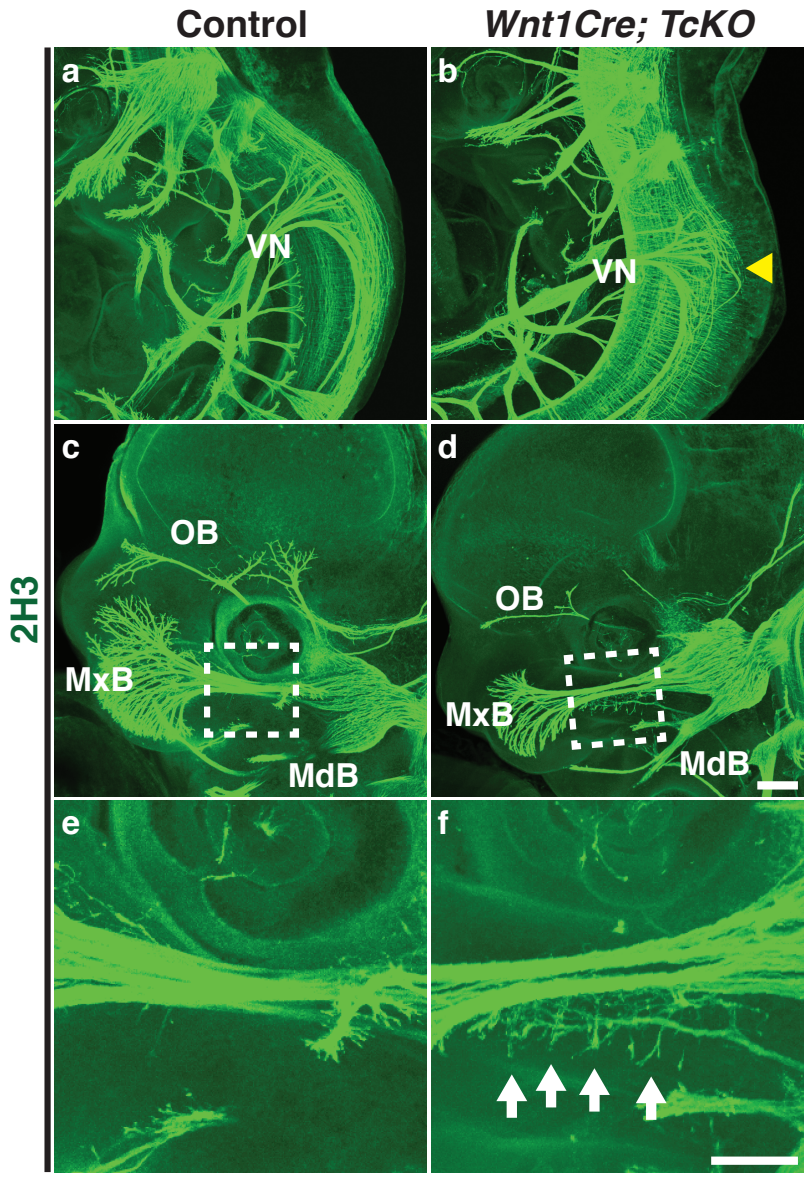

Figure 2.11. Cas adaptor proteins are essential for cranial nerve development. (a-f) Whole-mount immunostaining of Control (**a, c, e**) and *Wnt1Cre; TcKO* embryos (**b, d, f**) at e11.5 (**a,b**) and e12.5 (**c-f).** The central projections of the vagal nerve (VN) are severely defasciculated in *Wnt1Cre; TcKO* embryos (**b**, yellow arrowhead). The ophthalmic branch trigeminal nerve appears underbranched in *Wnt1Cre; TcKO* (**d**) embryos compared to controls **(c**). (**e-f**) Higher magnification view of white boxes in c and d reveals exuberant defasciculation of the maxillary branch of the trigeminal nerve in *Wnt1Cre; TcKO* embryos (**f,** white arrows). OB: Ophthalmic Branch; MxB: Maxillary Branch; MdB: Mandibular Branch. n=6, 100% penetrance. Scale bars: 200 µm for **a-d**; 100 µm for **e, f**.

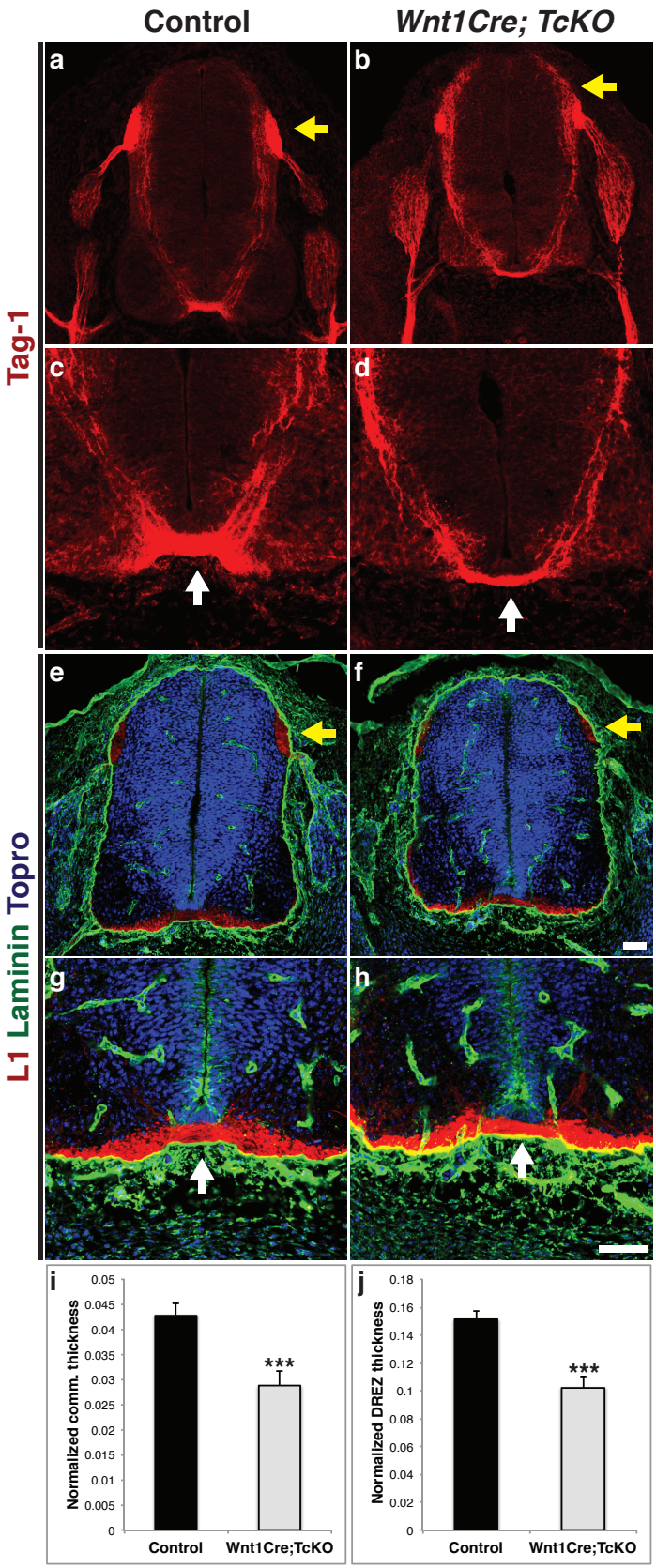

Figure 2.12. Cas mutants display a mild but significant commissural axon defect. (a-h) Transverse cryosections through control (**a, c, e, g**) and *Wnt1Cre;TcKO* (**b, d, f, h**) e11.5 spinal cords immunostained for Tag1 (**a-d**), L1Cam (**e-h**, red) and laminin (**e-h**, green). Sections in k-n were counterstained with Topro (blue). c-d, and g-h are higher magnification views of **a-b**, and **e-f**, respectively. The there is a mild reduction in the width of the ventral commissure (white arrows, **d, h**), and the DREZ is smaller and disorganized in *Wnt1Cre; TcKO* embryos (yellow arrows, **b, f**). **(i)** Quantification of the normalized commissure thickness in control and *Wnt1Cre;TcKO* embryos. Two-tailed t-student test ***, p= 0.0041. 5 branchial sections per animal, 4-5 animals for each genotype. **(j)** Quantification of the normalized DREZ thickness in control and *Wnt1Cre;TcKO* embryos. Two-tailed t-student test ***, p= 6.22e-5. 5 sections per animal, 5 animals for each genotype. Error bars represent SEM. Scale bars: 50 µm; Scale bar in **f** corresponds to **a,b, e, f**; scale bar in **h** for **c, d, g, h.**

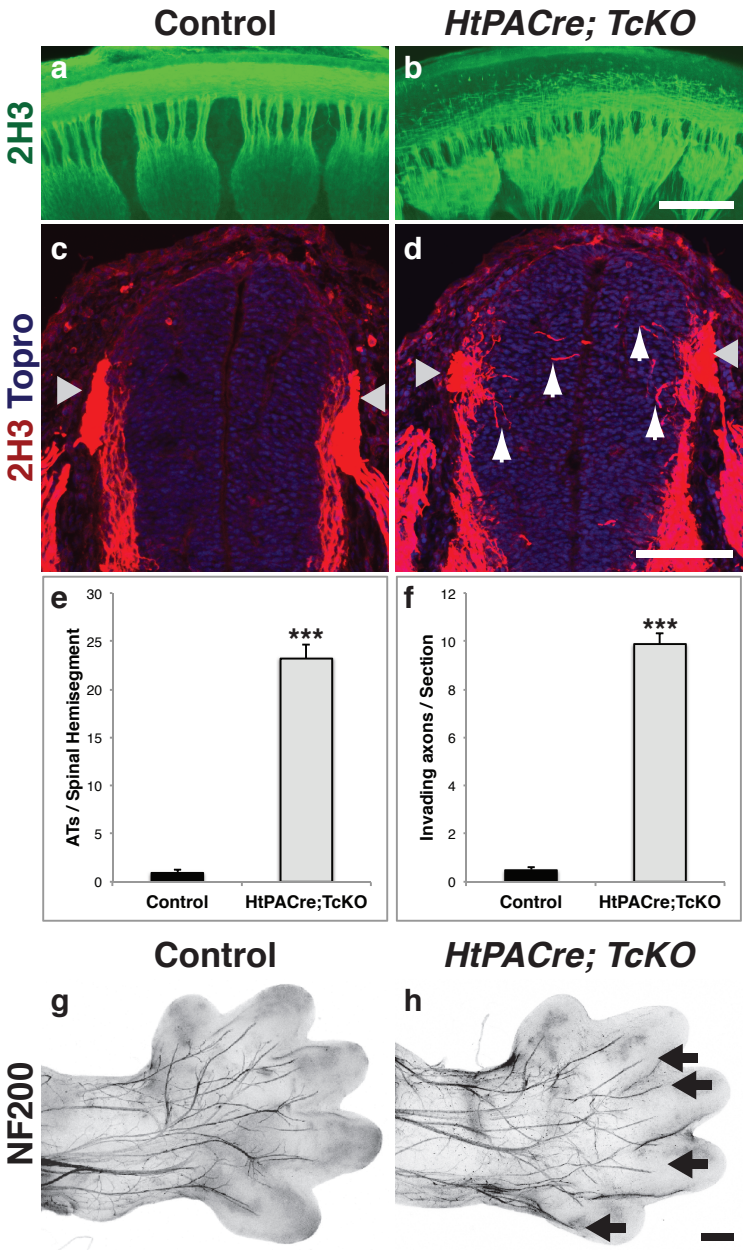

Figure 2.13. DRG-autonomous requirement for *Cas* genes. (a-b) Wholemount neurofilament immunostaing of control (**a**) and *HtPACre; TcKO* embryos (**b**). Sideview of e12.5 spinal cords stained with 2H3. The defasciculation of DRG central projection observed in *HtPACre; TcKO* embryos (**b**) resembles that of *Wnt1Cre; TcKO* embryos (Fig. 2.10). **(c-d)** Transverse vibratome sections through e11.5 Control (**c**) and *HtPACre; TcKO* (**d**) spinal cords at thoracic level stained using an antibody against neurofilament (2H3). Sensory axons prematurely invade the spinal cord gray matter of *HtPACre; TcKO* (**d**, white arrows) animals. Gray arrows: DREZ. **(e)** Quantification of free growth cones (GCs) per spinal hemisegment, visualized from the side. Two-tailed t-student test ***, p=1.26e-19 , 4-5 thoracic segments per animal, 5 animals for each genotype. **(f)** Quantification of number of growth cones (GCs) invading the spinal cord per section. Two-tailed t-student test ***, p= 1.76e-25. 5 thoracic sections per animal, 5 animals for each genotype. Error bars represent SEM. **(g-h)** Dorsal whole-mount view of e14.5 limbs stained with NF200. Select axonal branches that innervate the digits appear hyperfasciculated in *HtPACre; TcKO* (**h**) hindlimbs (black arrows). Fluorescent images were inverted to facilitate visualization. n=6 limbs per genotype. Scale bars: 200 µm for **a, b**; 100 µm for **c**, **d,** and 250 µm for **g, h**.

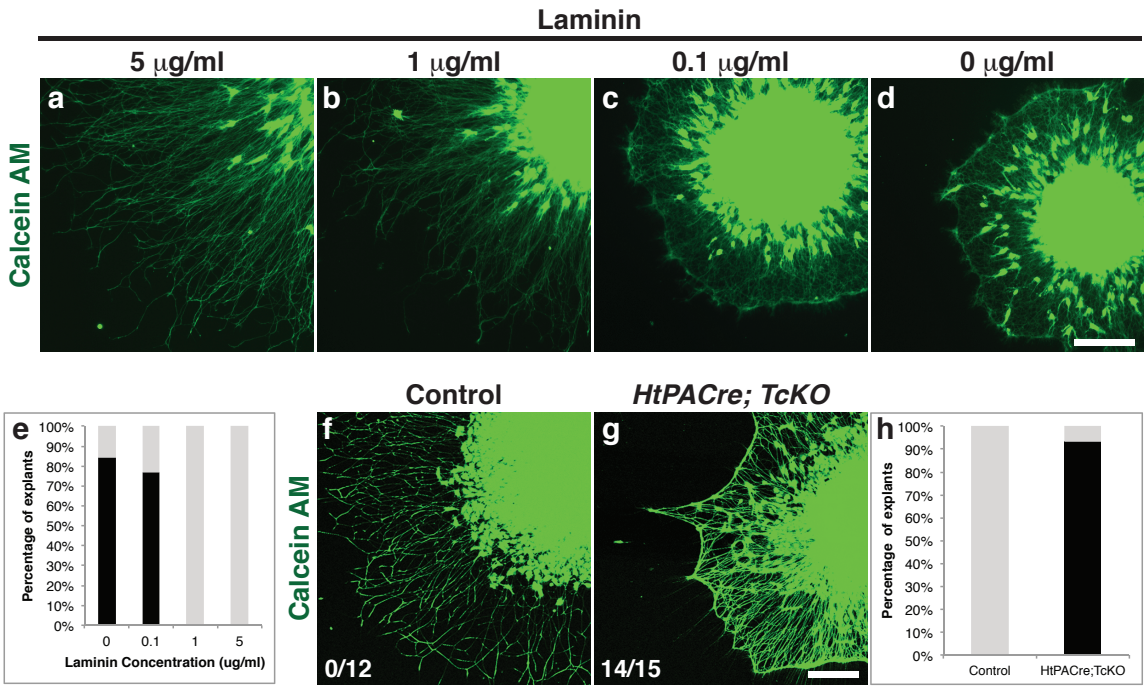

Figure 2.14. Cas genes are required for normal fasciculation *in vitro*. (a-d) e13.5 DRG explants from WT animals cultured on 100 μg/ml poly-D-lysine plus different concentrations of laminin. Cells were visualized using Calcein-AM. **(e)** Quantification of *in vitro* DRG phenotypes presented as percentage of explants that display webbing (black bars) vs. percentage of explants with normal morphology (gray bars). There is a significant difference in the webbing percentages under different culture conditions (Freeman-Halton extension of the Fisher exact probability test, p=4.94e-8; 9-16 explants for each condition). **(f-g)** DRG explants from control (**f**) and *HtPACre; TcKO* (**g**) embryos cultured on 100 μg/ml poly-D-lysine and 5 μg/ml laminin. Cells were visualized using Calcein-AM. The proportion of explants from each genotype displaying webbing is shown at the lower left corner of each panel. *HtPACre; TcKO* explants display an abnormal "cobweb" morphology (**g**), similar to WT explants cultured on poly-D-lysine alone (**d**). **(h)** Percentage of explants that display webbing (black bars) vs. percentage of explants with normal morphology (gray bars). The difference in the proportion of WT and *HtPACre; TcKO* explants that display the cob-web phenotype is highly significant (two-tailed Fisher exact test, p= 7.47e-7; 12-15 explants for each genotype). Scale bars 200 μm.

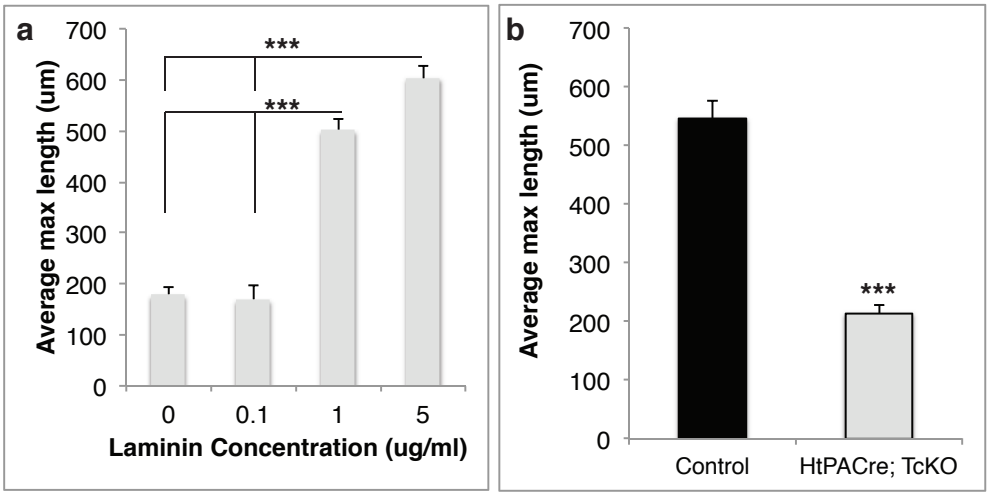

Figure 2.15. Axon growth of DRG explants. (a-b) Mean length of the longest neurite per explant as a measure of axon growth. (**a**) WT DRG axons grown on different concentrations of laminin. Axons grown on low-(0.1 µg/ml) or no-laminin grow significantly less than axons grown on 1 µg/ml or 5 µg/ml laminin (One-Way Anova p=1.1102e-16; n=15-16 explants per condition; *** Tukey HSD post-hoc test p<0.00001 vs. 0 and 0.1 µg/ml). (**b)** Quantification of Control and *HtPACre; TcKO* axon growth on 5 µg/ml laminin + 100 µg/ml poly-D-lysine. *HtPACre; TcKO* axons grow significantly less than control axons (*** two-tailed t-test p=1.489e-7, n=15 explants per genotype).

Chapter 3: ExBoX: a simple Boolean exclusion strategy to drive expression in neurons

Tyler Vahedi-Hunter*[1], Teresa Ubina*[1], Will Agnew-Svoboda[1], Wenny Wong[1], Akshay Gupta[1], Vijayalakshmi Santhakumar[1], Martin M. Riccomagno[1]

[1] Neuroscience Graduate Program, Department of Molecular, Cell & Systems Biology, University of California, Riverside, CA, USA

*Authors contributed equally to this work

Abstract

The advent of modern single-cell biology has revealed the striking molecular diversity of cell populations once thought to be more homogeneous. This newly appreciated complexity has made intersectional genetic approaches essential to understanding and probing cellular heterogeneity at the functional level. Here we build on previous knowledge to develop a simple AAV-based approach to define specific subpopulations of cells by Boolean exclusion logic (AND NOT). This Expression by Boolean Exclusion (ExBoX) system encodes for a gene of interest which is turned ON by a particular recombinase (Cre or FlpO) and turned OFF by another. ExBoX allows for the specific transcription of a gene of interest in cells

expressing only the activating recombinase, but not in cells expressing both. We show the ability of the ExBoX system to tightly regulate expression of fluorescent reporters both in vitro and in vivo, and further demonstrate the powerful adaptability of the system by achieving expression of a variety of virally-delivered coding sequences in the mouse brain. This simple strategy will expand the molecular toolkit available for cell- and time-specific gene expression in a variety of organisms and systems.

Introduction

Advancements in our understanding of the mechanisms underlying biological processes have been greatly dependent on the development of new genetic tools. A big breakthrough in mammalian genetics was the discovery and implementation of homologous recombination to generate loss-of-function alleles in mice (Capecchi, 1989). The introduction of recombinases as genetically encoded tools, in combination with conditionally targeted genetic alleles, made the control of genetic deletion in a tissue-specific manner possible (Gu et al, 1994; Tsien et al, 1996). With the availability of recombinase-dependent systems, region-specific gene knockouts and progenitor tracing have now become routine experimental strategies in mouse genetics (Branda & Dymecky, 2004).

Although cell diversity has always been appreciated in biology, single-cell profiling has revolutionized the way we think about certain organs by uncovering cell heterogeneity in populations that were once thought to display less complexity

(Darmanis et al, 2015). Our ability to appreciate cellular complexity is currently limited by the available tools to label and manipulate cells with increased specificity. One way to overcome this limitation is to simply expand the pool of tissue- and population-specific recombinase lines. This requires the generation and characterization of independent transgenic recombinase mouse lines for each newly discovered cell population. A complementary approach that can take advantage of preexisting transgenic lines is to incorporate genetically encoded intersectional approaches (Awatramani et al, 2003). In comparison to conventional transgenic strategies that select cellular targets based on expression of one particular promoter or driver, intersectional approaches provide tighter specificity by selecting targets based on the overlapping or sequential expression of multiple recombinases (Jensen & Dymecki, 2014). These intersectional strategies based on the combinatorial expression of two recombinase systems (Cre/lox and Flp/FRT) were first used in the mouse to perform fate mapping of previously elusive neural progenitors (Dymecki, Ray, & Kim 2010). Intersectional approaches are not only able to label subpopulations with greater specificity, but also make a variety of Boolean logic operations (AND, NOT, OR) available (Daigle et al., 2019; Plummer et al, 2015). With multiple recombinase systems driving the expression of reporter genes, targeting of subpopulations of cells can be achieved through intersectional (expressing all drivers) and subtractive (lacking expression of one or more drivers) strategies (Farago et al, 2006).

Viral vectors offer an alternative approach to driving conditional and intersectional expression (Schnütgen et al, 2003; Atasoy et al, 2008; Gradinaru, 2010; Fenno et al, 2014). Strictly genetically encoded strategies have clear advantages over surgically introduced viral vectors, like non-invasiveness and broad applicability in hard to reach tissues during otherwise inaccessible embryonic stages (Jensen & Dymecki, 2014). However, viral expression systems can be extremely powerful given the ease of generation and the additional level of control one can gain by selecting the region and time of injection (Zhang et al, 2007; Sternson et al, 2015). There are now multiple versions of recombinase-dependent AAVs for recombinases like Cre, Flp, and DRE (Atasoy et al, 2008; Saunders et al, 2012; Xue, Atallah, & Scanziani, 2014). More recently, systems for intersectional expression driven by AAVs have also been developed (Kakava-Georgiadou et al, 2019; Fenno et al, 2014). Combination of these viral and genetically-encoded approaches will ultimately be essential to understand whether newly discovered molecular diversity within cell populations amounts to any notable phenotypic difference in terms of cellular structure and function.

In addition to being able to parse out functional diversity, there is an interest in the field of developmental biology in being able to specifically turn genes ON and OFF during defined developmental windows or critical periods (Wiesel & Hubel,1963; Kozorovitskiy et al, 2012). Intersectional approaches using Boolean negation/exclusion could provide a solution to this problem: a gene of interest

could be turned ON by a particular recombinase at a particular time point, while turned OFF later (AND NOT) by a different recombinase (Table 3.1). Although a sophisticated system for AAV-driven expression using exclusion logic has been generated elsewhere (Fenno et al, 2014), the existing vectors have limitations in terms of being unnecessarily long and intricate in design, somewhat restricting their applicability. In this study we describe the design and characterization of an alternative expression system governed by Boolean exclusion logic and driven by a single AAV. The newly developed vectors are simpler in design and smaller in size, allowing for expression of longer genes of interest (GOI). As proof of principle, we validated the system in neuronal populations, and also generated tools for regulating neuronal activity in vivo.

Results

Design and construction of a combinatorial expression system using Boolean exclusion: CreOn-FlpOff ExBoX

To control expression and label subsets of cells with greater specificity using Cre and FLP recombinases, we set out to develop a simple AAV-based expression system governed by Boolean Exclusion logic (Expression by Boolean Exclusion or ExBoX). We first generated a system in which expression of a coding sequence of interest is turned ON by Cre recombinase and turned OFF by Flp recombinase: CreOn-FlpOff (Table 3.1). The CreOn-FlpOff vector was designed to contain a cassette with a coding sequence (CDS) of interest in-frame with a

hemagglutinin tag (HA), P2A site, and EGFP reporter inverted with respect to a promoter. The promoter chosen for these experiments was that of human Synapsin I, which is a well characterized postmitotic neuronal promoter (Glover et al., 2002). The inverted cassette is flanked by Frt sites, and double-lox sites (lox2722 and loxP) in inverse orientation (DIO) (Schnütgen et al., 2003) (Fig. 3.1A). Upon Cre-mediated recombination, an HA-tagged coding sequence of interest and EGFP get locked into the forward orientation, allowing for robust Cre-dependent expression in neurons. Conversely, in the presence of Flp the cassette is excised, resulting in abolishment of CDS and EGFP reporter expression (Fig. 3.1A). Thus, the CDS is expressed only in the presence of Cre AND NOT FlpO (Table 3.1).

For proof of concept, we first generated a plasmid carrying only EGFP in the reversible cassette of the CreOn-FlpOff system. The CreOn-FlpOff-EGFP plasmid was co-transfected with Cre recombinase, FlpO recombinase, or both Cre and FlpO in a neuroblastoma-derived cell line, Neuro2A (Fig. 3.1B, left). A plasmid driving mCherry under a constitutive promoter was co-transfected as transfection control. Upon transfection of the CreOn-FlpOff-EGFP plasmid alone, no EGFP expression is found in any cells. As expected, when CreOn-FlpOff-EGFP plasmid is co-transfected with Cre, the EGFP cassette is inverted to the correct orientation and 93.9%±0.3 of transfected cells express EGFP (Figure 3.1B). When CreOn-FlpOff-EGFP plasmid was co-transfected with Flp, or co-transfected with Cre and Flp, no cells expressed EGFP, suggesting that Flp can efficiently turn off reporter

expression (Fig. 3.1B). This confirms that expression from CreOn-FlpOff ExBoX vectors can be successfully manipulated through Boolean exclusion in N2A cells.

Design of a complementary system that is turned ON by Flp and turned OFF by Cre: FlpOn-CreOff ExBox

We next generated a complementary system that is turned on by Flp and off by Cre, FlpOn-CreOff (Table 3.1). FlpOn-CreOff was designed using a similar internal logic, where an expression cassette containing a CDS, an in-frame HA tag, P2A site, and TdTomato reporter, are inverted with respect to the promoter. This expression cassette is flanked by lox2722 sites, and a Flp controlled DIO switch (fDIO or fFLEX) (Xue et al, 2014) containing F14 and Frt sites (Figure 3.2A). In this system, Flp inverts the cassette, resulting in CDS and TdTomato reporter expression, while Cre excises the cassette, causing the abolishment of CDS and TdTomato reporter expression (Fig. 3.2A). Thus CDS expression should only occur when FlpO is present AND NOT Cre (Table 3.1).

As an initial proof-of-principle design, a FlpOn-CreOff vector driving simply a TdTomato fluorescent reporter was generated. FlpOn-CreOff-TdTomato plasmid was co-transfected with Cre, FlpO, or both Cre and FlpO. EGFP expressing plasmid was used as transfection control. When the FlpOn-CreOff-TdTomato plasmid was co-transfected with FlpO, approximately 85.8%±5.6 of transfected cells displayed TdTomato expression (Fig. 3.2B). When FlpOn-CreOff-TdTomato plasmid was co-transfected with Cre alone, there were no TdTomato expressing

cells. Finally, as expected, co-transfection of the FlpOn-CreOff-TdTomato plasmid with both Cre and FlpO resulted in no TdTomato reporter expression, confirming that Cre recombinase can abolish expression of this constructs even in the presence of Flp (Fig. 3.2B). Therefore, expression of the construct occurs only in the presence of Flp AND NOT Cre (Table 3.1).

Characterization of the ExBoX system in neurons

To test whether this newly developed system was able to drive expression in neurons, we tested these constructs in primary cortical cultures. We used the same plasmid combinations that were used in Neuro2A cells to perform ex-utero electroporation prior to plating. Primary neuronal cultures were observed at 3 days in vitro (DIV). Transfection of CreOn-FlpOff-EGFP plasmid alone resulted in no reporter expression (Fig. 3.3A). Notably, co-transfection of CreOn-FlpOff-EGFP plasmid with Cre resulted in 100%±0.0 of transfected neurons expressing EGFP as expected (Fig. 3.3A). When CreOn-FlpOff-EGFP plasmid was co-transfected with FlpO or with FlpO and Cre, we found no EGFP reporter expression in any transfected cells (Fig. 3.3A). Similarly, transfection of FlpOn-CreOff-TdTomato plasmid alone resulted in no reporter expression (Fig. 3.3B). Co-transfection of FlpOn-CreOff-TdTomato plasmid with FlpO resulted in 92.1%±2.0 of transfected cells expressing the TdTomato reporter, as expected (Fig. 3.3B). If FlpOn-CreOff-TdTomato plasmid is co-transfected with Cre alone, or Cre and FlpO, it is expected that there will be no TdTomato expression since Cre should excise the cassette.

As predicted, no cells transfected in this combination had any TdTomato expression (Fig. 3.3B).

We then tested the neuronal expression of the ExBoX system *in vivo.* Initial validation of CreOn-FlpOff was performed by *in utero* electroporation of CreOn-FlpOff-EGFP plasmid with Cre, with FlpO, or with Cre and FlpO into the lateral ventricle in E15.5 mice, followed by visualization 48 hours later. mCherry-expressing plasmids were used as electroporation controls. When the CreOn-FlpOff-EGFP plasmid was electroporated alone or with FlpO, we found no EGFP expression (Fig. 3.4A). Tissue co-transfected with CreOn-FlpOff-EGFP plasmid and Cre had robust expression of the EGFP reporter, resulting in labeling of 97.7%±0.9 of transfected cells (Fig. 3.4A). Co-electroporation of CreOn-FlpOff-EGFP plasmid with Cre and FlpO resulted in negligible EGFP expression (1.7%±0.9 of transfected cells, Fig. 3.4A).

To validate FlpOn-CreOff, we electroporated the FlpOn-CreOff-TdTomato plasmid alone and this resulted in no TdTomato expression. A plasmid driving EGFP under the pCAG promoter was used as electroporation control. Co-electroporation of FlpOn-CreOff-TdTomato plasmid with FlpO resulted in inversion of the cassette and detectable expression of TdTomato in 86.9%±3.1 of transfected cells (Fig. 3.4B). Co-electroporation of FlpOn-CreOff-TdTomato plasmid with Cre showed no TdTomato expression (Fig. 3.4B). Finally, no TdTomato expression was detected when the FlpOn-CreOff-TdTomato plasmid

was co-electroporated with FlpO and Cre, indicating successful AND NOT exclusion (Fig. 3.4B). These data suggest that FlpOn-CreOff and CreOn-FlpOff ExBoX work efficiently in neurons, *in vitro* and *in vivo*.

Validation of ExBoX AAVs in vivo

To generate tools that would be useful for manipulation of gene expression in the postnatal brain, we packaged the FlpOn-CreOff construct into AAV9. To validate that expression of the FlpOn-CreOff constructs is maintained in the virally-packaged form, we performed stereotactic injections to deliver FlpOn-CreOff-TdTomato AAV into the dentate gyrus (DG) of adult mice *in vivo*. FlpOn-CreOff-TdTomato AAV was co-injected with either AAV-EF1α-FlpO-WPRE (AAV-EF1α-FlpO), or with AAV-EF1α-FlpO and pENN.AAV.CamKII 0.4. Cre. SV40 (AAV-CamkII-Cre), and expression was observed after 3 weeks (Fig. 3.5). AAV expressing EGFP was co injected in WT and when Cre was injected to visualize the injection site. Similar to our previous findings with FlpOn-CreOff plasmids, robust TdTomato reporter expression was observed in DG neurons co-infected with AAV-FlpOn-CreOff-TdTomato and AAV-EF1α-FlpO (Fig. 3.5A, C), verifying that expression of the construct in the presence of the 'ON' recombinase was maintained in viral form. Furthermore, AAV-FlpOn-CreOff-TdTomato reporter expression was inactivated by CamkII-Cre even in the presence of AAV-EF1α-FlpO (Fig. 3.5B, D; 3.6). Thus, the FlpOn-CreOff construct works as expected when packaged into AAV9.

We next packaged the complementary CreOn-FlpOff construct into AAV9. To validate that expression of the CreOn-FlpOff construct is maintained in the virally-packaged form, we performed stereotactic injections to deliver CreOn-FlpOff-EGFP AAV into the dentate gyrus (DG) of adult mice *in vivo*. For validation for the viral CreOn-FlpOff construct we incorporated a genetically-encoded Cre recombinase driven by a transgene. The *Grik4-cre* mouse line was specifically chosen for providing robust Cre expression in the hippocampus, including the DG (Fig. 3.7). AAV-CreOn-FlpOff-EGFP was injected independently into *Grik4-Cre* mice or Cre-negative littermates (WT), or co-injected with AAV-EF1α-FlpO into *Grik4-Cre* animals (Fig. 3.8). AAV9 constitutively expressing TdTomato (pAAV-CAG-TdTomato) was co-injected in WT animals and with the AAV-EF1α-FlpO injection to visualize the injection site. When AAV-CreOn-FlpOff-EGFP was injected into WT (Cre-negative) animals, no EGFP reporter expression was observed (Fig. 3.8A, D, G). Conversely, injections into *Grik4-Cre* positive animals demonstrated robust EGFP reporter expression (Fig. 3.8B, E, H), verifying the Cre-dependent activation of the virally-packaged construct. Furthermore, in *Grik4-Cre* animals, co-injection of AAV-EF1α-FlpO resulted in inactivation of EGFP reporter expression (Fig. 3.8C, F; 3.6). These results suggest that the virally-packaged ExBoX constructs are successful at driving gene expression through the expected AND NOT Boolean operation.

Generation of Activity-modulating CreOn-FlpOff Viruses for Neuroscience

To further validate the ExBoX system using multiple different cargos, we next generated CreOn-FlpOff AAV constructs co-expressing EGFP and well-characterized modulators of neuronal firing or synaptic release. To reduce activity, we generated a CreOn-FlpOff virus that expresses Kir2.1 (AAV-CreOn-FlpOff-Kir2.1-EGFP), an inward-rectifying K+ channel that has been demonstrated to increase rheobase current and reduce resting membrane potential of neurons when overexpressed (Xue et al, 2014). In parallel, we cloned a version of Kir2.1 carrying three point mutations that render the channel in a non-functional state, referred to as Kir2.1Mut (AAV-CreOn-FlpOff-Kir2.1Mut-EGFP) (Xue et al, 2014), which can be used as a negative control for the Kir2.1 construct. We also designed a CreOn-FlpOff virus encoding mNaChBac (AAV-CreOn-FlpOff-mNaChBac-EGFP). This bacterial Na^+ ion channel has been demonstrated to increase firing of neurons when overexpressed by reducing action potential threshold and rheobase (Xue et al, 2014). To serve as negative control for mNaChBac in neural circuit experiments, we cloned a non-conducting mNaChBac mutant referred to as mNaChBacMut into the CreOn-FlpOff vector (AAV-CreOn-FlpOff-mNaChBacMut-EGFP) (Xue et al, 2014). Finally, we generated CreOn-FlpOff encoding tetanus toxin (AAV-CreOn-FlpOff-TeTN-EGFP) to block synaptic transmission (Sweeney et al, 1995).

We validated reporter expression of these five viral constructs in adult mice using stereotactic injection to deliver each independently or in combination with AAV-EF1α-FlpO into the DG of adult Grik4-Cre mice or WT (Cre-negative) littermates (Fig. 3.9). To visualize the injection site pAAV-CAG-TdTomato was co-injected in WT, or when AAV-EF1α-FlpO was injected. As expected, injection of any of the viral constructs into Cre-negative animals produced no EGFP reporter expression (Fig. 3.9A, E, I, M, Q). Conversely, each virus was able to produce robust EGFP reporter expression in DG neurons when injected into Grik4-Cre positive animals (Fig. 3.9B, F, J, N, R), demonstrating expression of these viral constructs is Cre-dependent. Furthermore, in *Grik4-Cre* mice injection of AAV-EF1α-FlpO prevented EGFP reporter expression (Figure 3.9C, D, G, H, K, L, O, P, S, T, and 3.10). Thus, despite the larger cargo size, expression of these activity-modulating CreOn-FlpOff viral constructs was similar to that of the CreOn-FlpOff-EGFP viral construct (Fig. 3.8). Overall, our data suggest that the ExBoX system can be used to efficiently control expression of multiple genes of interest in a Cre- and Flp-dependent manner through AND NOT Boolean operations.

Discussion

Design of a simpler, more space-efficient Boolean exclusion expression system

The ability to identify and characterize specific cell types and subpopulations has been challenging in part because, until recently, cell targeting strategies have been limited to populations defined by expression of a single marker or reporter. In order to solve this issue and increase specificity of target selection, a number of intersectional strategies have been developed (Atasoy et al, 2008; Fenno et al, 2014; Gradinaru et al, 2010; Jensen & Dymecki, 2014; Plummer et al, 2015; Schnütgen et al, 2003). A previous study described the generation of an expression system using Boolean logical operations, all governed by a single AAV vector (Fenno et al., 2014). This system, called INTERSECT, incorporated a modular intron-containing system capable of driving transcription using multiple Boolean logical operations such as AND, NOT, AND NOT, XOR, and NAND (Fenno et al., 2014). While extremely elegant, the design for the AND NOT constructs was constrained by the fact that it followed the same internal logic as the AND INTRSECT constructs. As a result of this constraint the currently existing AND NOT system has a couple of shortcomings. The first limitation is that this system adds two introns that make the constructs longer by 194 base-pairs. This is not a serious concern when expressing from a plasmid, but it becomes relevant when dealing with viruses with limited packaging capacity like AAV (Dong et al., 1996). Another concern with the use of introns is that they make the design and cloning of other coding sequences into these vectors more difficult and

cumbersome. In this study, we generated an alternative system aimed at solving these constraints. Thus, by design, the ExBoX system has two clear advantages over previous systems: it provides more cargo room and has a simpler design, allowing for replacement of the CDS cassette in a simple cloning step.

The ExBoX system allows for robust expression only in the presence of the respective ON switch, which can be reliably inactivated in the presence of the OFF switch (Table 3.1). This is true for both plasmid (Figs. 3.1-3.4) and viral constructs (Figs. 3.5-3.10) as validated by a battery of *in vitro* and *in vivo* experiments in embryonic and postnatal tissues. Altogether, these experiments demonstrate that the ExBoX system is effective in delivering strong recombinase-dependent expression in a variety of settings.

A Boolean system to control expression with temporal and cell-type specificity

Boolean logic AND-NOT operations made available by ExBoX can be used to study previously inaccessible subpopulations. In situations where there is no suitable specific driver for a subpopulation of interest, the ExBoX system can be used to drive expression of a gene of interest or reporter in said subpopulation, provided there is a recombinase driver available for a broader neuronal population, and one for the cells to be excluded (Fig. 3.11). For example, the AND NOT logic of the ExBoX system could be utilized to label or genetically manipulate 5HTR3a^{+};VIP^{-} interneurons in the cortex (Tremblay et al., 2016). This could be done by turning on expression of a CreOn-FlpOff construct with *HTR3a-Cre*, while

excluding inhibitory neurons expressing *VIP-FlpO* (Fig. 8A) (Che et al., 2018; He et al., 2017; Gerfen et al., 2013).

In addition to cell-specificity, these intersectional approaches can be used to achieve temporal control. This is particularly important when studying developmental events or degenerative diseases with defined critical periods. Using ExBoX one could take advantage of the expression of a recombinase to provide cell-type specificity, and a second recombinase to turn OFF expression at the desired time (Fig. 3.11B). For example, expression of a gene of interest in the DG can be turned ON by injecting ExBoX AAVs at a desired developmental time point into *Grik4-Cre* mice, and later turned OFF with Flp, thus creating a window of expression.

The tissue- and temporal-specificity conferred by the ExBoX system will make developmental studies that were previously limited by the pre-existing tools possible. With this in mind, we generated ExBoX vectors encoding for neuronal activity and synaptic transmission modulators, which will allow for tight control of these functional manipulations in time and space. These activity-modulating tools, although well characterized in a variety of circuits (see Bando et al., 2016; Burrone et al., 2002; Johns et al., 1999; Lin et al., 2010; Okada and Matsuda, 2008; Priya et al., 2018; Sim and Antolin et al., 2013; Sweeney et al, 1995; Xue et al, 2014 for examples), will need to be validated in each particular setting and/or system. To facilitate studies where the timing of CDS expression is critical, we are currently

generating AAV vectors driving expression of a tamoxifen-dependent FlpO (data not shown) (Goodrich et al, 2018). This AAV-FlpOERT2 could be delivered at the same time as the ExBoX AAVs and used to turn OFF expression by orally providing tamoxifen at a later timepoint.

Expanding the toolkit to study gene function

Due to the ExBoX's simple design, the system can be easily modified to incorporate alternative and/or additional recombinase systems. For example, inclusion of the Dre-Rox recombinase system, in addition to Cre-lox and Flp-frt, would provide even greater intersectional specificity (Plummer et al, 2015). In addition to Dre-ON and OFF intersectional AND NOT systems, this could theoretically enable AND-NOT-NOT Boolean logic operations, permitting an even greater expanse of possibilities. In addition, by using other promoters in the AAV constructs this system can be used to drive expression in any cell-type or organ of interest. The broad applicability and exquisite specificity of the system would make the use of these vectors particularly useful for gene therapy applications.

In summary, we designed and generated a new set of viral tools to drive expression using Boolean exclusion logic, ExBoX. ExBoX AAVs allow for tight spatial and temporal control of transcription. These new tools are simple and can be easily modified to express any desired gene of interest. Our design also increases the space available for other coding sequences of interest, even if this increase in capacity is somewhat small (194 bps). As proof of concept, we

generated a variety of vectors encoding for neuronal activity and synaptic transmission regulators that will be readily available to the neuroscience community. Based on its simplicity, we believe the ExBoX system will help universalize the use of combinatorial expression approaches. Combining these newly developed tools with genetically encoded Cre and FlpO lines, in addition to a growing variety of viral tools, will allow for cell-specific gene expression in a variety of systems.

Materials and Methods

Animals

The ICR mouse strain was purchased from Taconic. The *Grik-4-Cre* transgenic mouse strain was purchased from The Jackson Laboratory. Generation of the *Grik4-cre* transgenic mouse line has been described previously (Nakazawa et al., 2002). Mice were housed in a controlled environment maintained at approximately 22*C on a 12-hour light/dark cycle. Mouse chow and water were provided ad libitum. The day of vaginal plug observation was designated as embryonic day 0.5 (E0.5), and the day of birth as postnatal day 0 (P0). All animal procedures presented were performed according to the University of California Riverside's Institutional Animal Care and Use Committee (IACUC) guidelines and approved by UC Riverside IACUC.

Viral constructs

The CreOn-FlpOff and FlpOn-CreOff ExBoX viral constructs were designed

using ApE (https://jorgensen.biology.utah.edu/wayned/ape/) and Vector Builder (vectorbuilder.com) free software. The plasmids were synthesized and assembled by Vector Builder. Plasmid DNA was purified using the Qiagen Maxi Prep kit (Qiagen Cat#10023). AAVs were also packaged by Vector Builder into AAV2/9. pENN.AAV.CamKII 0.4. Cre. SV40 (AAV5) (Addgene viral prep #105558-AAV5; http://n2t.net/addgene:105558; RRID:Addgene_105558), pAAV-CAG-TdTomato (AAV5) (Addgene viral prep#59462-AAV5; http://n2t.net/addgene:59462; RRID:Addgene_59462) and pCAG-FLEX-EGFP-WPRE (AAV9) (Addgene viral prep #51502-AAV9; http://n2t.net/addgene:51502; RRID:Addgene_51502) were obtained from Addgene (Oh, S.W., Harris, J.A., Ng, L., et al., 2014). rAAV5/AAV-EF1α-FlpO-WPRE and rAAV9/CAG-GFP were obtained from the UNC GTC Vector Core.

In utero electroporation

Pregnant ICR mice at E15.5 were anesthetized with isoflurane and an abdominal incision was made to expose the uterus. Pups were visualized through the uterine wall. Plasmids diluted in fast green and phosphate buffered saline (PBS) (3 µg/µl) were injected through sharpened glass capillary needles into the lateral ventricle. 5mm paddles were used to deliver five 40V pulses of 50ms each with 950ms intervals across the hemispheres. Uterine horns were repositioned inside the female and the abdominal cavity was filled with 5x penicillin/streptomycin (pen/strep) in sterile PBS. Pups were collected at E17.5 via transcardial perfusion

with PBS and 4% paraformaldehyde (PFA) and fixed in 4% PFA for four hours at 4°C, rinsed with PBS, and sectioned coronally at 150um on a vibrating microtome (VT100S; Leica). Immunohistochemistry was performed as described (Polleux & Ghosh, 2002). Nuclei were visualized with DAPI (10g/ml) and primary antibodies used were chicken anti-GFP (1:500, Aves Labs Cat# GFP-1010) and rabbit anti-dsRed (1:500, Takara Bio Cat# 632475) with secondary antibodies goat anti-chicken 488 (1:1000, Thermo Fisher Scientific Cat# A-11039) and goat anti-rabbit 546 (1:1000, Abcam Cat# ab60317). Sections were mounted on glass microscope slides with Fluoro Gel (Electron Microscopy Sciences Cat# 1798502) and imaged with a laser-scanning confocal microscope (Leica SPEII).

Ex utero electroporation

Ex utero electroporation was performed similarly as *in utero* electroporation. Pregnant ICR mice at E14.5 were cervically dislocated, uterine horns were removed, and pups were dissected out in Complete HBSS on ice. Plasmids were injected bilaterally and 5mm paddles were used to deliver five 40V pulses of 50ms each with 950 ms intervals across each hemisphere. After electroporation, cortices were removed for primary cortical culture.

Primary Cortical Neuron Culture

Primary cortical neurons were isolated from E14.5 ICR mouse embryos as described (Kim & Magrané, 2011) using growth media as described (Polleux and

Ghosh 2010). 12mm circular coverslips were treated with 12M HCL overnight and thoroughly neutralized with deionized water. Acid-treated coverslips were stored in a glass petri dish with 70% to 100% Ethanol. The coverslips were fire-sterilized prior to use and coated with laminin and poly-D-lysine (8.3ug/mL) in sterile water in a 24-well sterile culture plate. *Ex utero* electroporation was performed prior to dissection in Complete Hanks Balanced Salt Solution (HBSS, 2.5mM HEPES pH7.4, 2.5mM D-glucose, 1mM $CaCl_2$, 1mM $MgSO_4$, 2.5mM $NaHCO_3$). Neurons were plated at a density of $2.6x10^5$cells/cm^2 and maintained in Complete Neurobasal (Neurobasal media, pen/strep, Glutamax, B27) in 5% CO_2 at 37°C. 50% of the media was exchanged with fresh media 48 hours after plating. Neurons were collected after 72 hours and fixed in 4% PFA for 5 minutes, then rinsed with PBS 3x for 5 min. Cells were incubated in blocking buffer (PBS, 1% goat or donkey serum, 0.1% Triton-X) for 30 minutes at RT, rinsed with PBS 1x, then incubated in primary antibodies (chicken anti-GFP (1:1000, Aves Labs Cat# GFP-1010) and/or rabbit anti-dsRed (1:1000, Takara Bio Cat# 632475) in antibody dilution buffer (PBS, 0.1% goat or donkey serum) at 4°C overnight. The following day cells were rinsed in PBS 4x for 5min, and were incubated in secondary antibodies (goat anti-chicken 488 (1:1000, Thermo Fisher Scientific Cat# A-11039) and goat anti-rabbit 546 (1:1000, Abcam Cat# ab60317)) and DAPI (1ug/mL) in antibody dilution buffer for 2 hours, then rinsed with PBS 4x for 10min. Coverslips were mounted on glass slides with Fluoro Gel and imaged with a confocal microscope.

Neuro2A Cell Culture

Neuro2A (N2A) cells from ATCC were maintained in DMEM with pen/strep and 10% fetal bovine serum and incubated in 5% CO_2 at 37°C. Cells were plated on laminin and poly-D-lysine (8.3µg/ml) coated 12mm coverslips in a 24-well plate at $7.8x10^4$cells/cm^2. Cells were transfected 24 hours later with Metafectene PRO (Biontex Cat# T040-1.0) according to manufacturer's suggested protocol with a 1:4 DNA to Metafectene ratio. Cells were fixed 48 hours after transfection with 4% PFA for 5 min, rinsed with PBS, stained with DAPI (1 µm/mL) for one hour, then rinsed again with PBS 3x for 5min. Coverslips were mounted with Fluoro Gel onto a glass slide and examined with confocal microscopy.

Stereotaxic Injections

Stereotaxic injections were performed as described previously (Osten et al., 2007) in P30 mice. Mice were put under anesthesia for the duration of the procedure using isoflurane. Injections for AAV-FlpOn-CreOff-TdTomato expression experiments were performed in CD1 mice targeting the DG of the Hippocampus (coordinates: A/P -1.70 mm; M/L ±1.90 mm; D/V, -1.70 mm). Right hemisphere injections received a 400nl viral cocktail of AAV-FlpOn-CreOff-TdTomato ($6.55x10^{12}$ GC/mL), rAAV5/EF1α-FlpO-WPRE, pENN.AAV.CamKII 0.4. Cre. SV40, and pCAG-FLEX-EGFP-WPRE in a 1:1:1:1 ratio, whereas the contralateral hemisphere received a 200nl viral cocktail containing FlpOn-CreOff-TdTomato ($6.55x10^{12}$ GC/mL), EF1α-FlpO-WPRE, in a 1:1 ratio. Titers for

commercially available AAVs were as follows: pENN.AAV.CamKII 0.4. Cre. SV40 (2.4 x 10^{13} GC/ml), pCAG-FLEX-EGFP-WPRE (3.3 x 10^{13} GC/ml), pAAV-CAG-TdTomato (1.2 x 10^{13} GC/ml), rAAV5/EF1α-FlpO-WPRE (2.6 x 10^{12} GC/ml), and rAAV9/CAG-GFP (2 x 10^{12} GC/ml). FlpO-negative controls were injected with a viral cocktail of FlpOn-CreOff-TdTomato and pAAV-CAG-GFP. For viral CreOn-FlpOff-EGFP construct experiments, injections were performed in *Grik4-Cre* mice. Right hemisphere injections received 200nl of desired CreOn-FlpOff construct, whereas the contralateral left hemisphere received a 500nl viral cocktail containing the construct, rAAV5/EF1α-FlpO-WPRE, and pAAV-CAG-TdTomato in a 2:2:1 ratio (respectively). Viral CreOn-FlpOff-EGFP constructs co-expressing following GOIs were tested: Kir2.1 (3.34x10^{13} GC/ml), Kir2.1-mutant (4.6x10^{13} GC/ml), NaChBac (2.98x10^{12} GC/ml), NaChBac-mutant (4.93x10^{13} GC/ml), and TeTN (2.52x10^{12} GC/ml). Three weeks after injections, mice were perfused and fixed with 4% paraformaldehyde O/N at 4 °C, rinsed in PBS x1, and sectioned coronally on a vibratome (150 µm). Sections were incubated in 4',6-diamidino-2-phenylindole (DAPI) and mounted onto slides with Fluoro Gel fluorescence mounting medium (Electron Microscopy Sciences Cat# 1798502). Expression was observed via confocal microscopy.

Image analysis

N2A and primary cortical neuron image analysis was performed with FIJI (Schindelin et al., 2012). GFP+ and RFP+ cells were all manually counted. DAPI

counts were obtained by thresholding the DAPI channel, image was made binary, then the watershed function was used and finally the analyze particles function to count nuclei with a size between 20-2000 pixels^2 and 0.2-1.0 circularity. Transfection efficiency was calculated as $\frac{\#RFP\ or\ \#GFP}{\#DAPI} \times 100$. Percentage of transfected cells in which recombinase activity resulted in fluorescent reporter (RFP or GFP) expression were calculated as $\frac{\#GFP\ or\ RFP}{\#\ transfected} \times 100$. Images obtained from *in utero* electroporations were counted manually, avoiding the ventricular zone where it became impossible to distinguish individual cells. Percentage of ON cells were calculated the same as in N2A and primary cortical neurons. The N2A, primary cortical culture, and intrauterine electroporation datasets were tested for normality with the Shapiro-Wilk test and QQ plot. A One-way ANOVA with Tukey's multiple comparisons test was done for N2A transfection and intrauterine electroporation data (Figures 1,2,4). Unpaired t-test was performed on viral injection data (Figures S1 and S3). The data set for primary cortical cell counts failed to meet normality and thus Fisher's exact test was performed (Figure 3). Image analysis for viral constructs was performed with ImageJ. A region of interest in granule cell layer of the DG and defined by the site of injection was selected. Mean pixel intensity of the viral reporter fluorophore in the ROI was measured. An uninjected region of the hippocampus was simultaneously selected and measured for fluorescence intensity, and defined as background fluorescence. Background fluorescence was then subtracted from the mean pixel intensity of the ROI. The

percentage of viral reporter expression maintained when the OFF recombinase was co-injected was calculated as $\frac{mean\ pixel\ intensity\ OFF}{mean\ pixel\ intensity\ ON} \times 100$ for each animal, and was averaged across samples (n=3) for each viral construct.

Acknowledgements
We would like to thank Drs. Edward Zagha and Kevin Wright for critically reading the manuscript and providing helpful comments. We would like to thank the University of North Carolina Chapel Hill Gene Therapy Center Vector Core for packaging of viral constructs. pENN.AAV.CamKII 0.4.Cre.SV40 was a gift from James M. Wilson, pCAG-FLEX-EGFP-WPRE was a gift from Hongkui Zeng, and pAAV-CAG-TdTomato and pAAV-CAG-GFP were a gift from Edward Boyden. AAV-EF1α-FlpO-WPRE was a gift from Karl Deisseroth.

Competing interests
The authors declare no competing financial interests.

Funding sources
This work was supported by grants from the National Institutes of Health (R21MH118640 and R01NS104026 to M.M.R.; R01NS069861 and R01NS097750 to V.S) and a Hellman Foundation Fellowship to M.M.R.

References

Antón-bolaños, N., Sempere-ferràndez, A., Guillamón-Vivancos, T., Martini, F. J., Pérez-Saiz, L., Gezelius, H., Filipehuk, A., Valdeolmillos, M., López-Bendito, G. (2019). Prenatal activity from thalamic neurons governs the emergence of functional cortical maps in mice. *Science*, 364(6444), 987–990. https://doi.org/10.1126/science.aav7617

Atasoy, D., Aponte, Y., Su, H. H., & Sternson, S. M. (2008). A FLEX switch targets channelrhodopsin-2 to multiple cell types for imaging and long-range circuit mapping. *Journal of Neuroscience*, *28*(28), 7025–7030. https://doi.org/10.1523/JNEUROSCI.1954-08.2008

Awatramani, R., Soriano, P., Rodriguez, C., Mai, J. J., & Dymecki, S. M. (2003). Cryptic boundaries in roof plate and choroid plexus identified by intersectional gene activation, *Nat. Genet.*, *35*(1), 70–75. https://doi.org/10.1038/ng1228

Bando, Y., Irie, K., Shimomura, T., Umeshima, H., Kushida, Y., Kengaku, M., Fujiyoshi, Y., Hirano, T., Tagawa, Y. (2016). Control of spontaneous Ca2+ transients is critical for neuronal maturation in the developing neocortex. *Cerebral Cortex, 26*(1), 106–117. https://doi.org/10.1093/cercor/bhu180

Branda, C. S., & Dymecki, S. M. (2004). Talking about a revolution: the impact of site-specific recombinases on genetic analyses in mice. *Developmental Cell*, *6*, 7–28.

Burrone, J., O'Byrne, M., & Murthy, V. N. (2002). Multiple forms of synaptic plasticity triggered by selective suppression of activity in individual neurons. *Nature*, 420(6914), 414–418. https://doi.org/10.1038/nature01242

Capecchi, M. (1989). Altering the genome by homologous recombination. *Science*, *244*(4910), 1288–1292. https://doi.org/10.1126/science.2660260

Che, A., Babij, R., Iannone, A. F., Fetcho, R. N., Ferrer, M., Liston, C., Fishell, G., De Marco Garcia, N. V. (2018). Layer I interneurons sharpen sensory maps during neonatal development. *Neuron*, 99(1), 98–116. https://doi.org/10.1016/j.neuron.2018.06.002.Layer

Daigle, T. L., Madisen, L., Hage, T. A., Valley, M. T., Knoblich, U., Larsen, R. S., Li, L. (2019). A suite of transgenic driver and reporter mouse lines with enhanced brain cell type targeting and functionality. *Cell*, 174(2), 465–480. https://doi.org/10.1016/j.cell.2018.06.035.A

Darmanis, S., Sloan, S. A., Zhang, Y., Enge, M., Caneda, C., Shuer, L. M., Hayden Gephart, M. G., Barres, B. A., & Quake, S. R. (2015). A survey of human brain transcriptome diversity at the single cell level. *Proceedings of the National Academy of Sciences*, 112(23), 7285–7290. https://doi.org/10.1073/pnas.1507125112

Dong, J., Fan, P., & Frizzell, R. A. (1996). Quantitative analysis of packaging capacity of recombinant adeno-associated virus. *Human Gene Therapy*, 7, 2101–2112.

Dymecki, S. M., Ray, R. S., & Kim, J. C. (2010). Mapping Cell Fate and Function Using Recombinase-Based Intersectional Strategies. Guide to Techniques in Mouse Development, Part B: Mouse Molecular Genetics. *Methods Enzymol.* (2nd ed., Vol. 477). https://doi.org/10.1016/S0076-6879(10)77011-7

Fenno, L. E., Mattis, J., Ramakrishnan, C., Hyun, M., Lee, S. Y., He, Tucciarone, J., Selimbeyoglu, A., Berndt, A., Grosenick, L., Zalocusky, K.A., Bernstein, H., Swanson, H., Perry, C., Diester, I., Boyce, F.M., Bass, C., Neve, R., Huang, Z.J., & Deisseroth, K. (2014). Targeting cells with single vectors using multiple-feature Boolean logic. *Nature Methods, 11*, 763–772. https://doi.org/10.1038/nmeth.2996

Garcıa-Garcia, M. J., Eggenschwiler, J. T., Caspary, T., Alcorn, H. L., Wyler, M. R., Huangfu, D., Rakeman, A.S., Lee, J.D., Feinberg, E.H., Timmer, J.R., & Anderson, K. V. (2005). Analysis of mouse embryonic patterning and morphogenesis by forward genetics. *PNAS*, *5*(7), 5913–5919. www.pnas.org/cgi/doi/10.1073/pnas.0501071102

Gerfen, C. R., Paletzki, R., & Heintz, N. (2013). GENSAT BAC cre-recombinase driver lines to study the functional organization of cerebral cortical and basal ganglia circuits. *Neuron*, 80(6), 1368–1383. https://doi.org/10.1016/j.neuron.2013.10.016

Glover, C. P., Bienemann, A. S., Heywood, D. J., Cosgrave, A. S., & Uney, J. B. (2002). Adenoviral-mediated, high-level, cell-specific transgene expression: a SYN1-WPRE cassette mediates increased transgene expression with no loss of neuron specificity. *Molecular therapy: the journal of the American Society of Gene Therapy*, *5*(5 Pt 1), 509–516. https://doi.org/10.1006/mthe.2002.0588

Goodrich, M. M., Talhouk, R., Zhang, X., & Goodrich, D. W. (2018). An approach for controlling the timing and order of engineered mutations in mice. *Genesis* (New York, N.Y.: 2000*), 56*(8), e23243. https://doi.org/10.1002/dvg.23243

Gordon, J., & Ruddle, F. (1981). Integration and stable germ line transmission of genes injected into mouse pronuclei. *Science*, 214(4526), 1244–1246. https://doi.org/10.1126/science.6272397

Gradinaru, V., Zhang, F., Ramakrishnan, C., Mattis, J., Prakash, R., Diester, I., Goshen, I., Thompson, K. R., Deisseroth, K. (2010). Molecular and cellular approaches for diversifying and extending optogenetics. *Cell*, *141*(1), 154–165. https://doi.org/10.1016/j.cell.2010.02.037

Gu, H., Marth, J. D., Orban, P. C., Mosmann, H., & Rajewsky, K. (1994). Deletion of a DNA polymerase β gene segment in T cells using cell type-specific gene targeting. *Science*, *265*(5168), 103–106. https://doi.org/10.1126/science.8016642

He, M., Tucciarone, J., Lee, S., Nigro, M. J., Kim, Y., Levine, J. M., Kelly, S.M., Krugikov, I., Wu, P., Chen, Y., Gong, L., Hou, Y., Osten, P., Rudy, B., Huang, Z. J. (2016). Strategies and tools for combinatorial targeting of GABAergic neurons in mouse cerebral cortex. *Neuron*, *91*(6), 1228–1243. https://doi.org/10.1016/j.neuron.2016.08.021.

Hogan, B., & Williams, J. (1981). Integration of foreign genes into the mammalian germ line: Genetic engineering enters a new era. *Nature*, *294*(5836), 9–10. https://doi.org/10.1038/294009a0

Jaenisch, R., & Mintz, B. (1974). Simian Virus 40 DNA sequences in DNA of healthy adult mice derived from preimplantation blastocysts injected with viral DNA. *Proceedings of the National Academy of Sciences*, *71*(4), 1250–1254. https://doi.org/10.1073/pnas.71.4.1250

Jensen, P., & Dymecki, S. M. (2014). Essentials of recombinase-based genetic fate mapping in mice. *Methods Mol Biol*, *1092*, 437–454. https://doi.org/10.1007/978-1-60327-292-6

Johns, D. C., Marx, R., Mains, R. E., O'Rourke, B., & Marbán, E. (1999). Inducible genetic suppression of neuronal excitability. *Journal of Neuroscience*, *19*(5), 1691–1697. https://doi.org/10.1523/jneurosci.19-05-01691.1999

Kakava-georgiadou, N., Zwartkruis, M. M., Bullich-vilarrubias, C., Adan, R. A. H., & Marti, F. (2019). An intersectional approach to target neural circuits with cell- and projection-type specificity: validation in the mesolimbic dopamine system. *Frontiers in Molecular Neuroscience*, *12*(February), 1–9. https://doi.org/10.3389/fnmol.2019.00049

Kim H.J., Magrané J. (2011) Isolation and culture of neurons and astrocytes from the mouse brain cortex. In: Manfredi G., Kawamata H. (eds) Neurodegeneration. Methods in Molecular Biology (Methods and Protocols), vol 793. Humana Press, Totowa, NJ

Kozorovitskiy, Y., Saunders, A., Johnson, C. A., Lowell, B. B., Sabatini, B. L., Israel, B., & Medical, D. (2012). Recurrent network activity drives striatal synaptogenesis. *Nature*, *485*(7400), 646–650. https://doi.org/10.1038/nature11052.

Kristianto, J., Johnson, M. G., Zastrow, R. K., Radcliff, A. B., & Blank, R. D. (2017). Spontaneous recombinase activity of Cre-ERT2 in vivo. *Transgenic research*, 26(3), 411–417. https://doi.org/10.1007/s11248-017-0018-1

Lin, C. W., Sim, S., Ainsworth, A., Okada, M., Kelsch, W., & Lois, C. (2010). Genetically increased cell-intrinsic excitability enhances neuronal integration into adult brain circuits. *Neuron*, 65(1), 32–39. https://doi.org/10.1016/j.neuron.2009.12.001

Madisen, L., Garner, A. R., Carandini, M., Zeng, H., & Cheng, A. (2015). Transgenic mice for intersectional targeting of neural sensors and effectors with high specificity and performance. *Neuron, 85*, 942–958. https://doi.org/10.1016/j.neuron.2015.02.022

Merte, J., Wang, Q., Vander Kooi, C. W., Sarsfield, S., Leahy, D. J., Kolodkin, A. L., & Ginty, D. D. (2010). A forward genetic screen in mice identifies Sema3A^{K108N}, which binds to Neuropilin-1 but cannot signal. *Journal of Neuroscience*, *30*(16), 5767-5775. https://doi.org/10.1523/JNEUROSCI.5061-09.2010

Nakazawa, K., Quirk, M.C., Chitwood, R. A., Watanabe, M., Yeckel, M. F., Sun, L.D., Kato, A., Carr, C. A., Johnston, D., Wilson, M. A., Tonegawa, S. (2002). Requirement for hippocampal CA3 NMDA receptors in associative memory recall. *Science, 297*(5579): 211-218.

Nusslein-Volhard, C., & Wieschaus, E. (1980). Mutations affecting segment number and polarity in Drosophila. *Nature*, *287*(October), 795–801. https://doi.org/10.1038/287795a0

Oh, S. W., Harris, J. A., Ng, L., Winslow, B., Cain, N., Mihalas, S., Wang, Q., Lau, C., Kuan, L., Henry, A. M., Mortrud, M. T., Ouellette, B., Nguyen, T., Sorensen, S. A., Slaughterbeck, C., Wakeman, W., Li, Y., Feng, D., … Anh Zeng, H. (2014). A mesoscale connectome of the mouse brain. Nature, 508(7495), 207–214. https://doi.org/10.1038/nature13186

Okada, M., & Matsuda, H. (2008). Chronic lentiviral expression of inwardly rectifying K+ channels (Kir2.1) reduces neuronal activity and downregulates voltage-gated potassium currents in hippocampus. *Neuroscience*, *156*(2), 289–297. https://doi.org/10.1016/j.neuroscience.2008.07.038

Osten, P., Cetin, A., Komai, S., Eliava, M., & Seeburg, P. H. (2007). Stereotaxic gene delivery in the rodent brain. *Nature Protocols*, *1*(6), 3166–3173.

Plummer, N. W., Evsyukova, I. Y., Robertson, S. D., Marchena, J. De, Tucker, C. J., & Jensen, P. (2015). Expanding the power of recombinase-based labeling to uncover cellular diversity. *Development, 142*, 4385–4393. https://doi.org/10.1242/dev.129981

Polleux, F., & Ghosh, A. (2002). The slice overlay assay: a versatile tool to study the influence of extracellular signals on neuronal development. *Science's STKE*, *2002*(136), pl9.

Priya, R., Paredes, M. F., Karayannis, T., Yusuf, N., Liu, X., Jaglin, X., Graef, I., Alvarez-Buylla A., Fishell, G. (2018). Activity regulates cell death within cortical interneurons through a calcineurin-dependent mechanism. *Cell Reports*, 22(7), 1695–1709. https://doi.org/10.1016/j.celrep.2018.01.007

Rubin, G., & Spradling, A. (1982). Genetic transformation of Drosophila with transposable element vectors. *Science*, *218*(4570), 348–353. https://doi.org/10.1126/science.6289436

Sauer, B., & Mcdermott, J. (2004). DNA recombination with a heterospecific Cre homolog identified from comparison of the pac-c1 regions of P1-related phages. *Nucleic Acids Research, 32*(20), 1–10. https://doi.org/10.1093/nar/gkh941 1–10 doi:10.1093/nar/gkh941

Saunders, A., Johnson, C. A., Sabatini, B. L., & Miyamichi, K. (2012). Novel recombinant adeno-associated viruses for Cre activated and inactivated transgene expression in neurons. *Frontiers in Neural Circuits*, *6*(47), 1–10. https://doi.org/10.3389/fncir.2012.00047

Schindelin, J., Arganda-Carreras, I., Frise, E., Kaynig, V., Longair, M., Pietzsch, T., Preibisch, S., Rueden, C., Saalfeld, S., Schmid, B., Tinevez, J.-Y., White, D. J., Hartenstein, V., Eliceiri, K., Tomancak, P., & Cardona, A. (2012). Fiji: An open-source platform for biological-image analysis. *Nature Methods*, 9(7), 676–682.

Schnütgen, F., Doerflinger, N., Calléja, C., Wendling, O., Chambon, P., & Ghyselinck, N. B. (2003). A directional strategy for monitoring Cre-mediated recombination at the cellular level in the mouse. *Nature Biotechnology, 21*, 562–565. https://doi.org/10.1038/nbt811

Sim, S., Antolin, S., Lin, C. W., Lin, Y. X., & Lois, C. (2013). Increased cell-intrinsic excitability induces synaptic changes in new neurons in the adult dentate gyrus that require Npas4. *Journal of Neuroscience*, 33(18), 7928–7940. https://doi.org/10.1523/JNEUROSCI.1571-12.2013

Sternson, S. M., Atasoy, D., Betley, J. N., Henry, F. E., & Xu, S. (2016). An emerging technology framework for the neurobiology of appetite. *Cell Metabolism*, *23*(2), 234–253. https://doi.org/10.1016/j.cmet.2015.12.002

Sweeney, S.T., Broadie, K., Keane, J., Niemann H., O'Kane, C.J. (1995). Targeted expression of tetanus toxin light chain in Drosophila specifically eliminates synaptic transmission and causes behavioral defects. *Neuron* 14, 341–351.

Tremblay, R., Lee, S., & Rudy, B. (2016). GABAergic interneurons in the neocortex: from cellular properties to circuits. *Neuron*, 91(2), 260–292. https://doi.org/10.1016/j.neuron.2016.06.033

Tsien, J. Z., Chen, D. F., Gerber, D., Tom, C., Mercer, E. H., Anderson, D. J., Mayford, M., Kandel, E. R., & Tonegawa, S. (1996). Subregion- and cell type–restricted gene knockout in mouse brain. *Cell*, 87(7), 1317–1326. https://doi.org/10.1016/S0092-8674(00)81826-7

Wright, K. M., Lyon, K., Leung, H., Leahy, D. J., Ma, L., & David, D. (2013). Dystroglycan organizes axon guidance cue localization and axonal pathfinding. *Neuron*, *76*(5), 931–944. https://doi.org/10.1016/j.neuron.2012.10.009.

Xue, M., Atallah, B. V., & Scanziani, M. (2014). Equalizing excitation-inhibition ratios across visual cortical neurons. *Nature*, *511*(7511), 596–600. https://doi.org/10.1038/nature13321

Zhang, F., Aravanis, A.M., Adamantidis, A., Lecea, L., and Deisseroth, K. (2007). Circuit-breakers: optical technologies for probing neural signals and systems. *Nature Reviews Neuroscience* 8(August), 577–581. https://doi:10.1038/nr n2192

	No Recombinase	Cre Only	FlpO Only	Cre and FlpO
Cre = ON **FlpO = OFF**	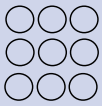	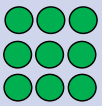	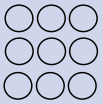	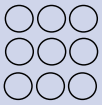
FlpO = ON **Cre = OFF**			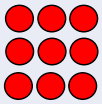	

Table 1. Conceptual basis for the Expression by Boolean Exclusion (AND NOT) system using multiple recombinases. Expression of a gene of interest (GOI) can be spatially and temporally manipulated through the use of multiple recombinases. In this model, expression of a GOI depends on the presence of an ON recombinase, and is prevented by the presence of an OFF recombinase. Thus, gene expression only occurs in cells where the ON recombinase is present AND NOT the OFF recombinase. Controlling where and when the ON and OFF recombinases are expressed provides a high level of specificity for targeting cell populations.

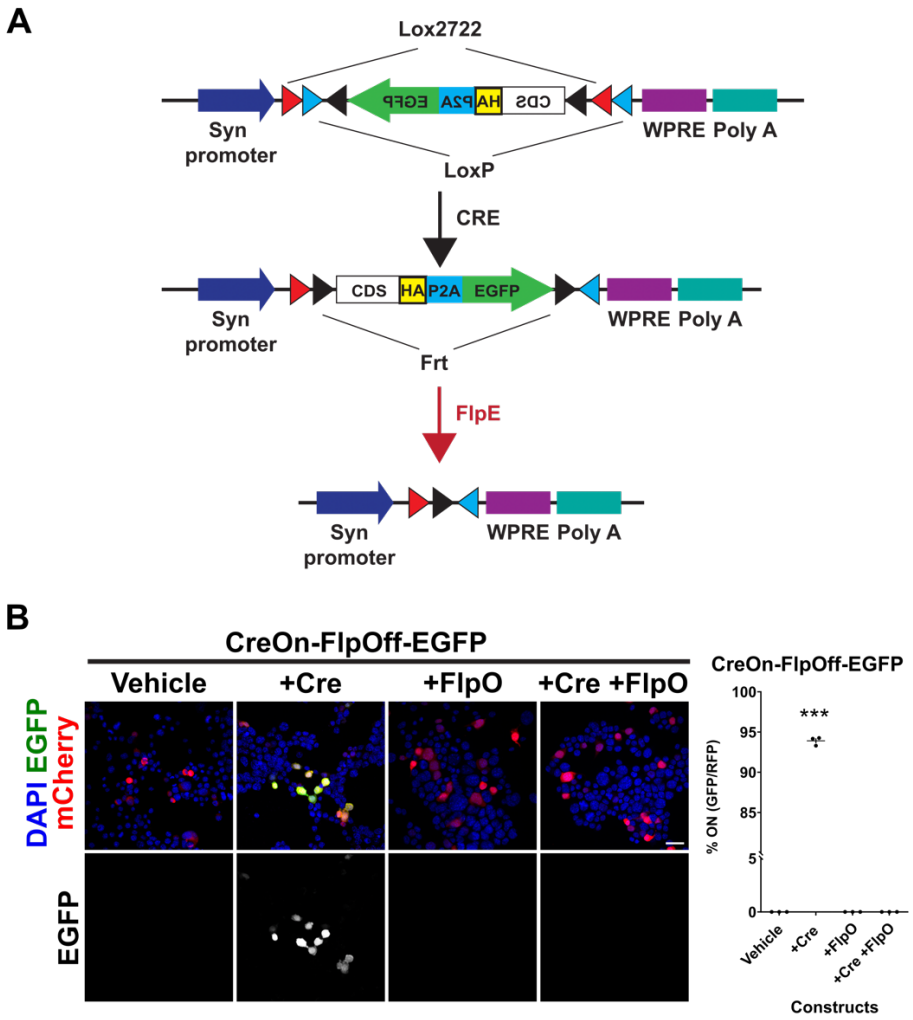

Figure 3.1. Design and proof of concept for CreOn-FlpOff constructs. (A) Schematic representation of the CreOn-FlpOff construct. It is composed of an inverted expression cassette encoding for a coding sequence (CDS) fused to an HA tag, a P2A site, and EGFP, which is flanked by Frt, lox2722, and loxP sites. Presence of Cre recombinase results in inversion of the cassette and expression. Presence of FlpO results in removal of the cassette. **(B)** Expression of fluorescent reporter proteins in Neuro2A cells transfected with CreOn-FlpOff-EGFP construct (green) and pCAG-mCherry (red, loading control). Co-transfection with pCAG-Cre plasmid causes inversion of the cassette into the "ON" position and EGFP expression. Co-transfection of pCAG-FlpO deletes the cassette and abolishes EGFP expression. (**B**, right panel) Quantification of N2A cell transfections. Upon transfection with Cre, the CreOn-FlpOff-EGFP construct results in 93.9%±0.3 of transfected cells expressing EGFP, while co-transfection with FlpO results in abolishment of EGFP expression. N=3 independent experiments, error bars ±SEM. ANOVA $p<0.001$; Tukey post-hoc test *** $p<0.0001$ vs. all other transfections. Scale bar 30µm.

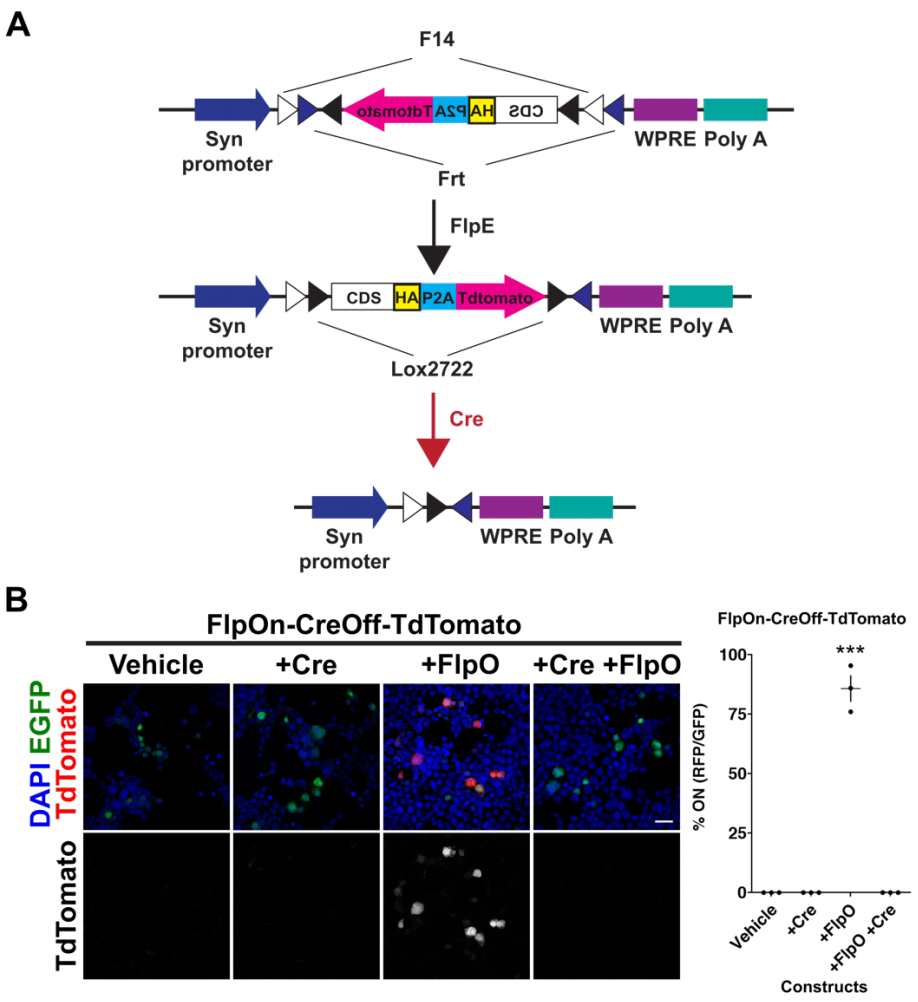

Figure 3.2. Design and proof of principle for FlpOn-CreOff constructs. (A) Schematic representation of the FlpOn-CreOff construct. The inverted expression cassette is flanked by lox2722, F14, and Frt sites. Presence of Flp recombinase results in inversion of the cassette and expression. Presence of Cre results in removal of the cassette. **(B)** Expression of fluorescent reporters in Neuro2A cells transfected with FlpOn-CreOff-TdTomato construct (red) and pCAG-EGFP (green, transfection control) in Neuro2A cells. Co-transfection with pCAG-FlpO causes inversion of the cassette into the "ON" position and TdTomato expression. Transfection with pCAG-Cre removes the cassette and abolishes TdTomato expression. Upon transfection with FlpO, the FlpOn-CreOff-TdTomato construct results in detectable expression of reporter in 85.8%±5.6 of transfected cells, while co-transfection with Cre results in abolishment of TdTomato expression (right panel). N=3 independent experiments, error bars ±SEM. ANOVA $p<0.01$; Tukey post-hoc test *** $p<0.0001$ vs. all other transfections. Scale bar 30µm.

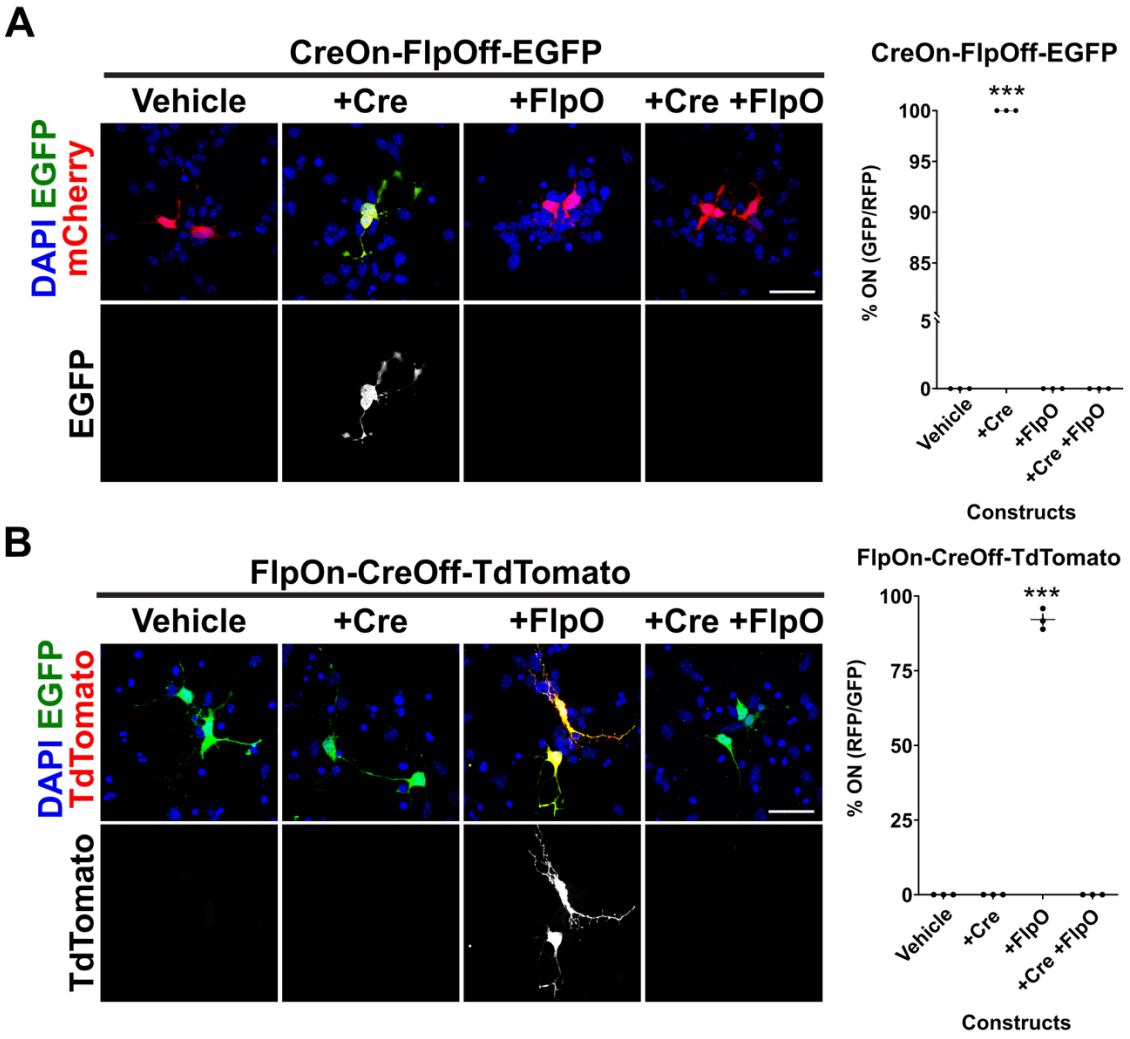

Figure 3.3. Validation of CreOn-FlpOff in primary cortical neurons. (A) Primary cortical neurons transfected with CreOn-FlpOff and Cre results in 100%±0.0 of transfected cells expressing EGFP. Without Cre or in the presence of FlpO there is no EGFP expression in any neurons. pCAG-mCherry was co-transfected as transfection control. **(B)** Primary cortical neurons transfected with FlpOn-CreOff-TdTomato and FlpO results in detectable TdTomato expression in 92.1%±2.0 of transfected cells (right). pCAG-EGFP was co-transfected as transfection control. Without FlpO, or in the presence of Cre, there is no TdTomato expression in any neurons. N=3, error bars ±SEM. Fisher's exact test ***p<0.0001. Scale bar 30µm.

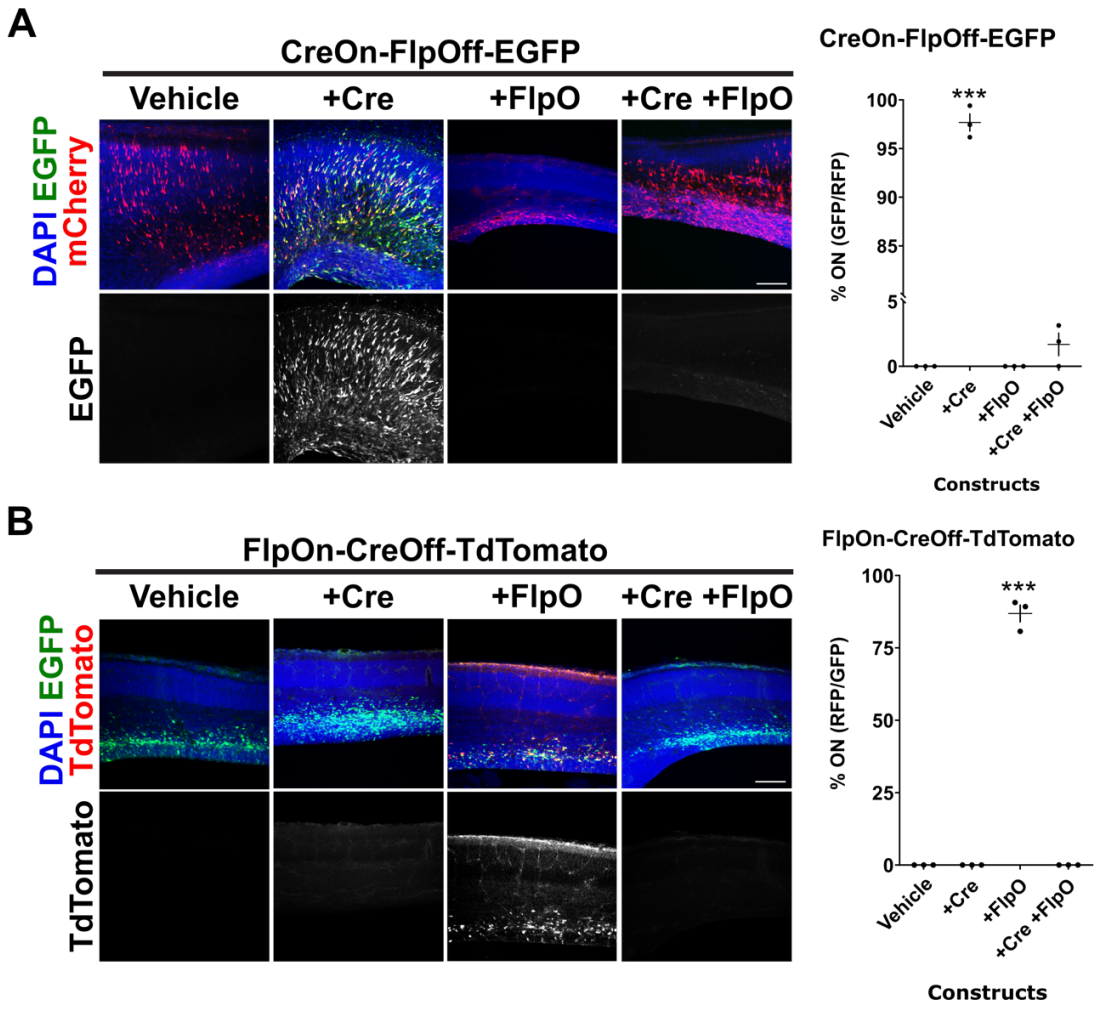

Figure 3.4. *In vivo* validation of CreOn-FlpOff and FlpOn-CreOff vectors via *in utero* electroporation (IUE). (A) Co-electroporation of CreOn-FlpOff-EGFP with mCherry reporter, Cre + pCAG-mCherry, FlpO-mCherry, or Cre + FlpO-mCherry in e15.5 ICR mouse embryos. Electroporation of CreOn-FlpOff-EGFP with Cre results in 97.7%±0.9 of transfected cells expressing EGFP (right). Electroporation with FlpO results in no expression and electroporation with Cre and FlpO results in only 1.7%±0.9 of cells still expressing EGFP. mCherry expression serves as electroporation control. **(B)** Co-electroporation of FlpOn-CreOff-TdTomato with pCAG-IRES-EGFP reporter, Cre-IRES-EGFP, FlpO, or Cre-IRES-EGFP + FlpO in e15.5 Swiss-Webster embryos. pCAG-IRES-EGFP expression was used as electroporation control.Electroporation of FlpOn-CreOff-TdTomato with FlpO results in 86.9%±3.1 of transfected cells expressing TdTomato (right). Co-electroporation with Cre, or with Cre and FlpO, results in no cells expressing TdTomato. N=3, error bars ±SEM. ANOVA $p<0.001$ for both sets of experiments; Tukey post-hoc test: *** $p<0.0001$ vs. all other transfections. Scale bar 100µm.

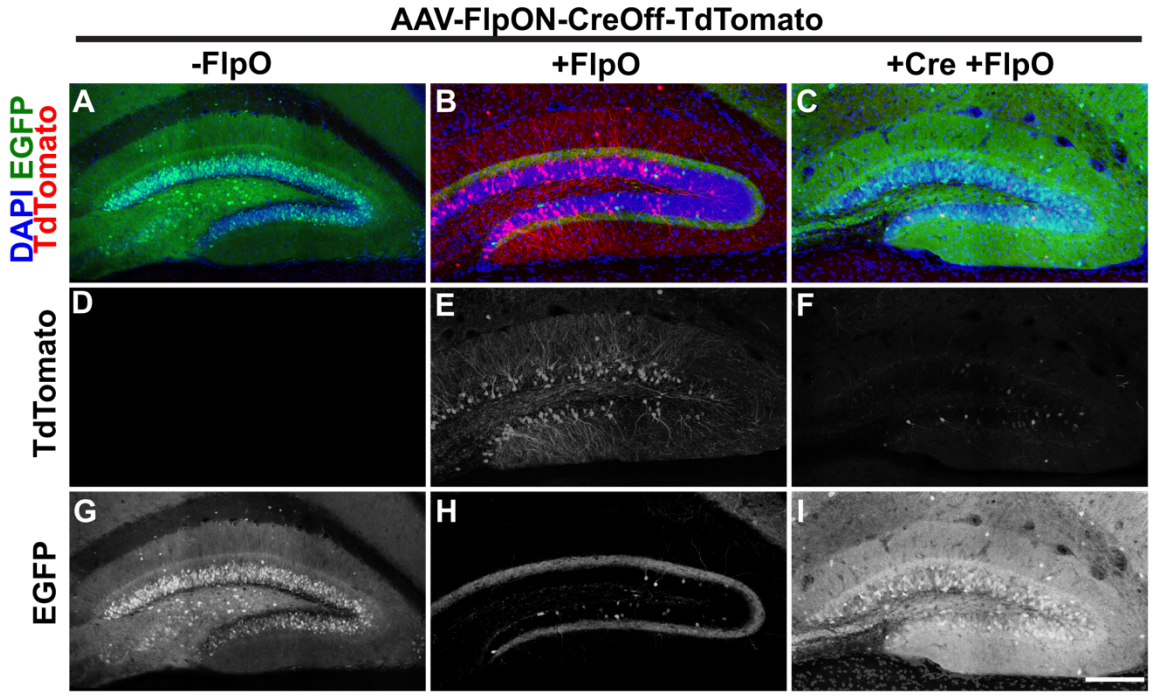

Figure 3.5. *In-vivo* validation of FlpOn-CreOff AAV by stereotactic injection in postnatal DG neurons. (A-I) Expression of viral FlpOn-CreOff-TdTomato construct (red) in WT animals co-injected with pAAV-CAG-GFP **(A, D, G)**, with AAV-EF1α-FlpO-WPRE **(B, E, H),** or AAV-EF1α-FlpO-WPRE + AAV-CamKII-Cre + AAV-CAG-FLEX-EGFP **(C, F, I)**. EGFP expression is used to visualize the injection site in the absence of TdTomato expression. Even in the presence of FlpO, Cre injection resulted in inactivation of TdTomato reporter expression (**C**, **F**). DAPI (blue) was used to visualize nuclei. Scale bar: 150 µm.

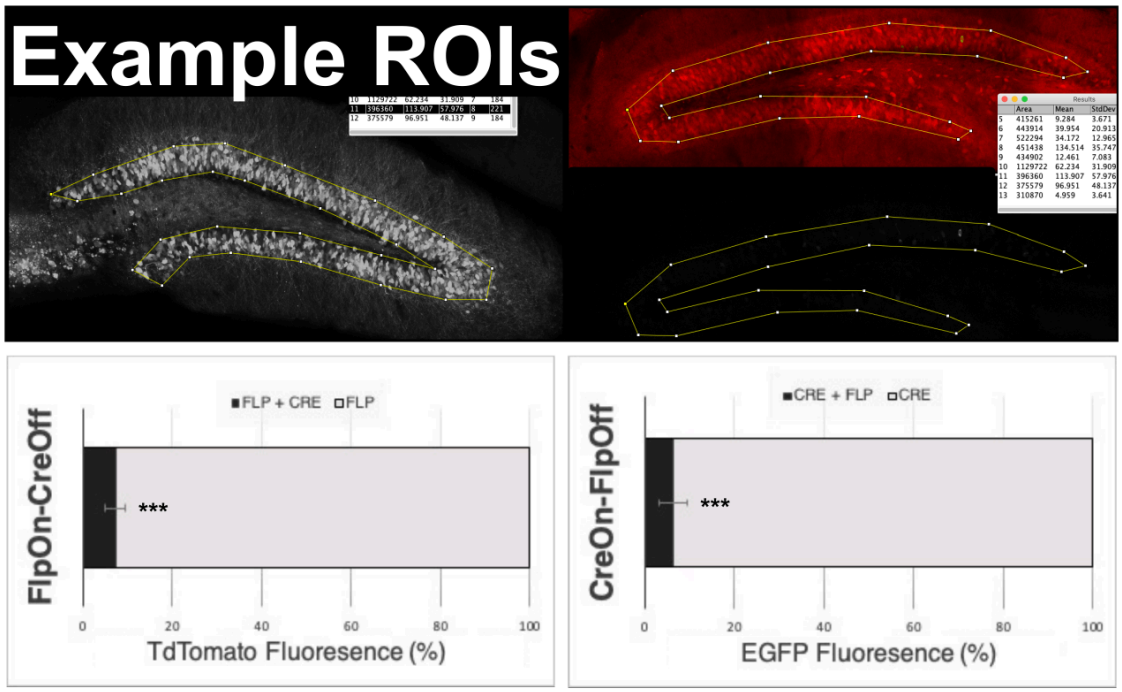

Figure 3.6. Example ROIs and quantification of fluorescent expression for AAV-FlpOn-CreOff-TdTomato and AAV-CreOn-FlpOff-EGFP injected animals. Top: The injected region of dentate gyrus granule cell layer was selected and measured for mean pixel intensity. Top right: To pick an accurate ROI when inactivated expression was indiscernible, the co-injected reporter was used to define the ROI boundary and the selection was applied. Bottom: Mean percentage of AAV-FlpOn-CreOff-TdTomato and AAV-CreOn-FlpOff-EGFP reporter fluorescence remaining when exposed to both ON and OFF recombinases (black) in comparison to fluorescence observed in the presence of the ON recombinase (gray). Unpaired t-test ***p<0.001. Error bars ±SEM.

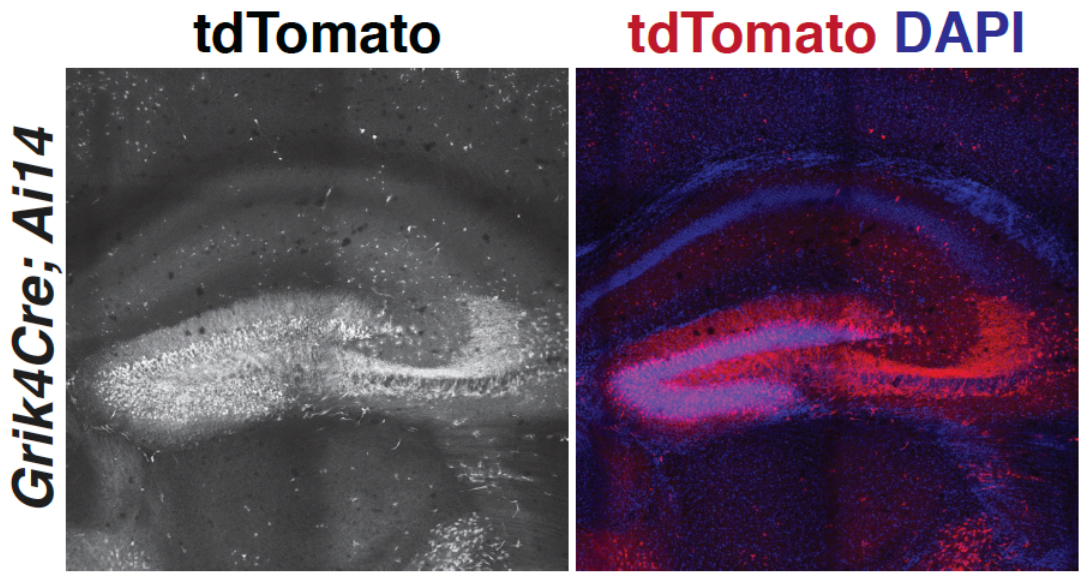

Figure 3.7. Expression of *Grik4-Cre* in the dentate gyrus. When crossed to a TdTomato reporter mouse (*Ai14*), robust labeling in the DG is observed.

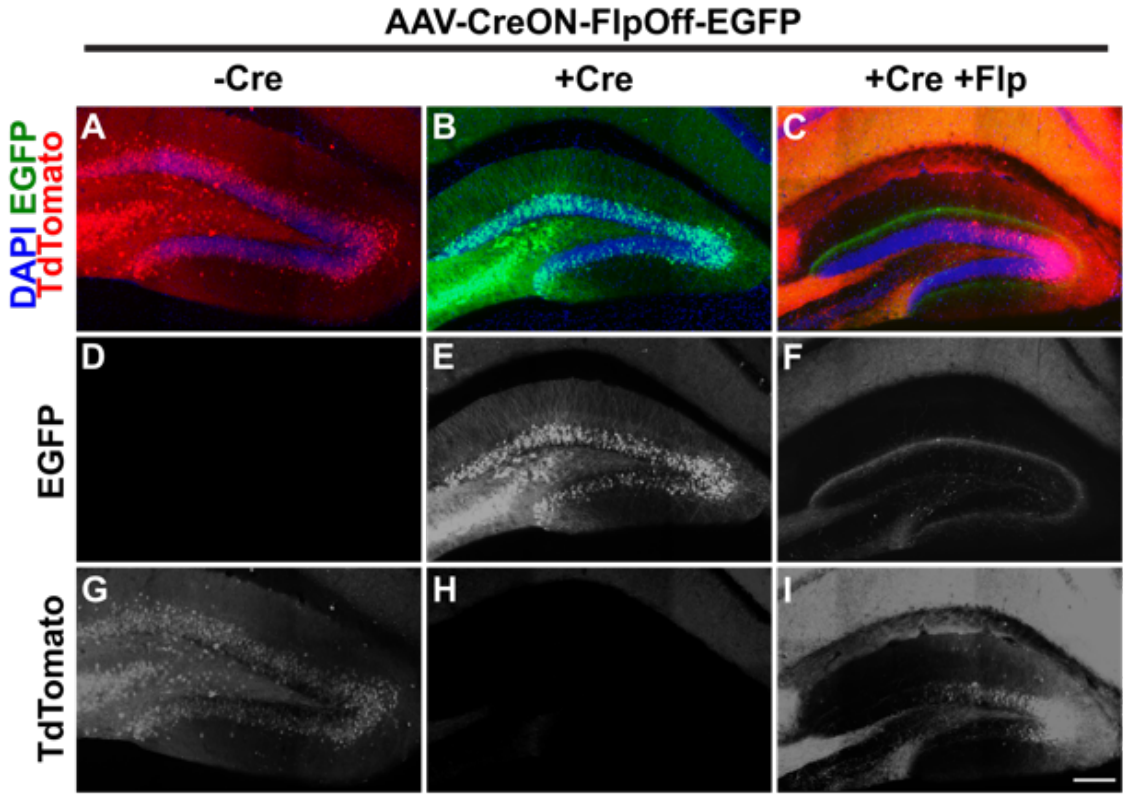

Figure 3.8. In-vivo validation of CreOn-FlpOff AAV in the dentate gyrus of postnatal mice. (A-I) Expression of viral CreOn-FlpOff-EGFP construct (green) in WT animals (**A, D, G**), in Grik4-Cre animals (**B, E, H**), and in Grik4-Cre mice co-injected with AAV-EF1α-FlpO-WPRE (**C, F, I**). pAAV-CAG-TdTomato (red) was co-injected when necessary to visualize the injection site. Even in the presence of Cre, FlpO injection resulted in inactivation of reporter expression by the CreOn-FlpOff-EGFP virus **(C, F**). EGFP labeling in the molecular layer of AAV-EF1α-FlpO injected animals (**C,F**) is from axonal projections from the contralateral side. DAPI (blue) was used to visualize nuclei. Scale bar: 150 µm.

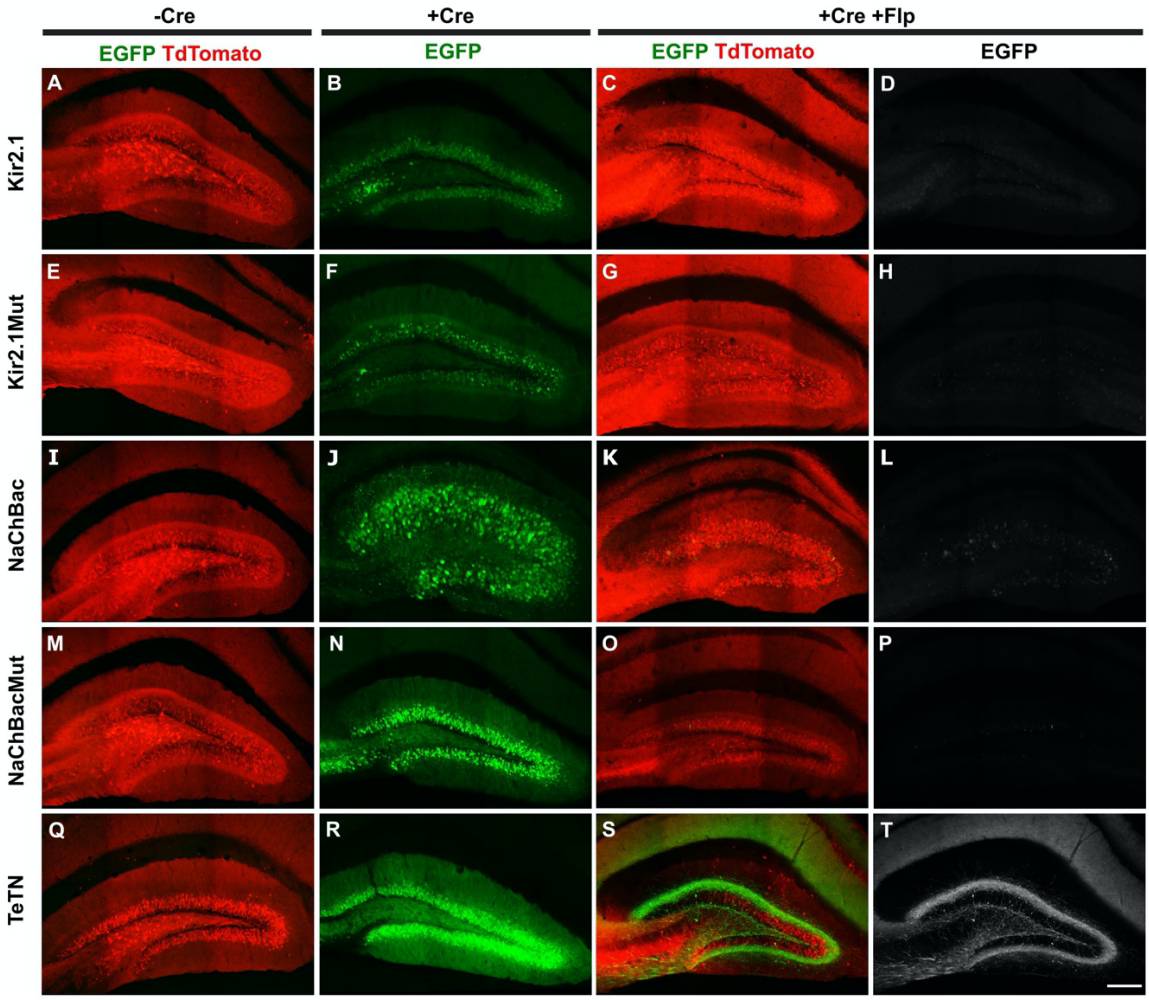

Figure 3.9. *In-vivo* validation of CreOn-FlpOff AAV constructs to manipulate neuronal activity. (A-T) Expression of fluorescent reporter by CreOn-FlpOff AAVs (green) co-expressing (**A-D)** Kir2.1, (**E-H**) Kir2.1-Mutant, (**I-L**) NaChBac, (**M-P**) NaChBac-mutant, and (**Q-T**) TETN in WT (**A, E, I, M, Q**) , *Grik4-Cre* animals **(B, F, J, N, R)** and *Grik4-Cre* animals co-injected with AAV-EF1α-FlpO-WPRE (**C, D, G, H, K, L, O, P, S, T).** Injections delivering AAV-EF1α-FlpO included pAAV-CAG-TdTomato (red) in order to visualize infected cells. In the presence of Cre and FlpO, expression of the CreOn-FlpOff virus was inactivated (**C, D, G, H, K, L, O, P, S, T).** EGFP labeling in the molecular layer of TeTN/FlpO injected animals (**T)** is from axonal projections from the contralateral side. Scale bar: 150 µm.

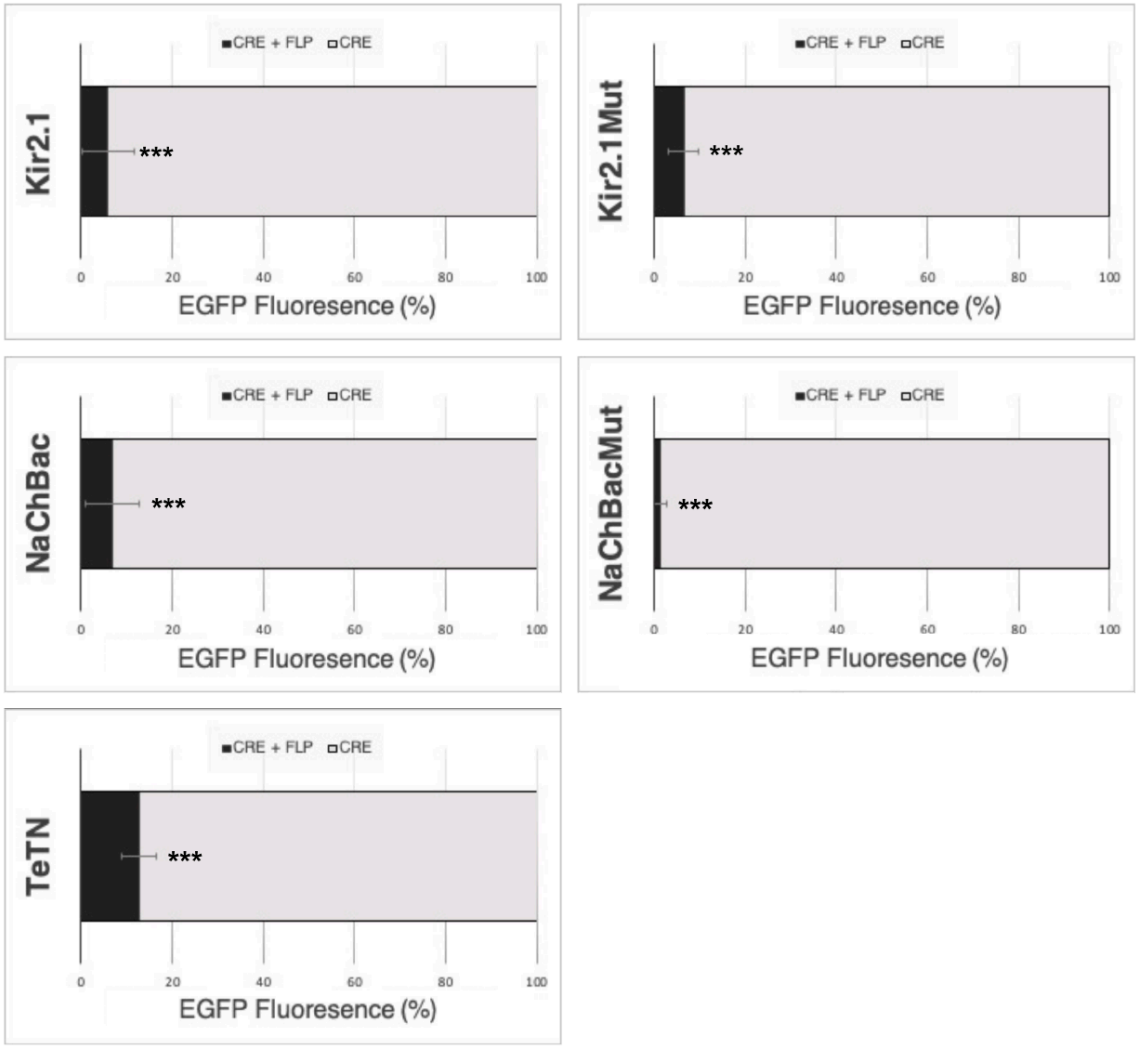

Figure 3.10. Quantification of fluorescence for AAV-CreOn-FlpOff-EGFP constructs expressing activity-modifying GOIs. Mean percentage of reporter fluorescence remaining when exposed to both ON and OFF recombinases (black) in comparison to fluorescence observed in the presence of the ON recombinase alone (gray). Unpaired t-test ***$p<0.0001$. Error bars ±SEM.

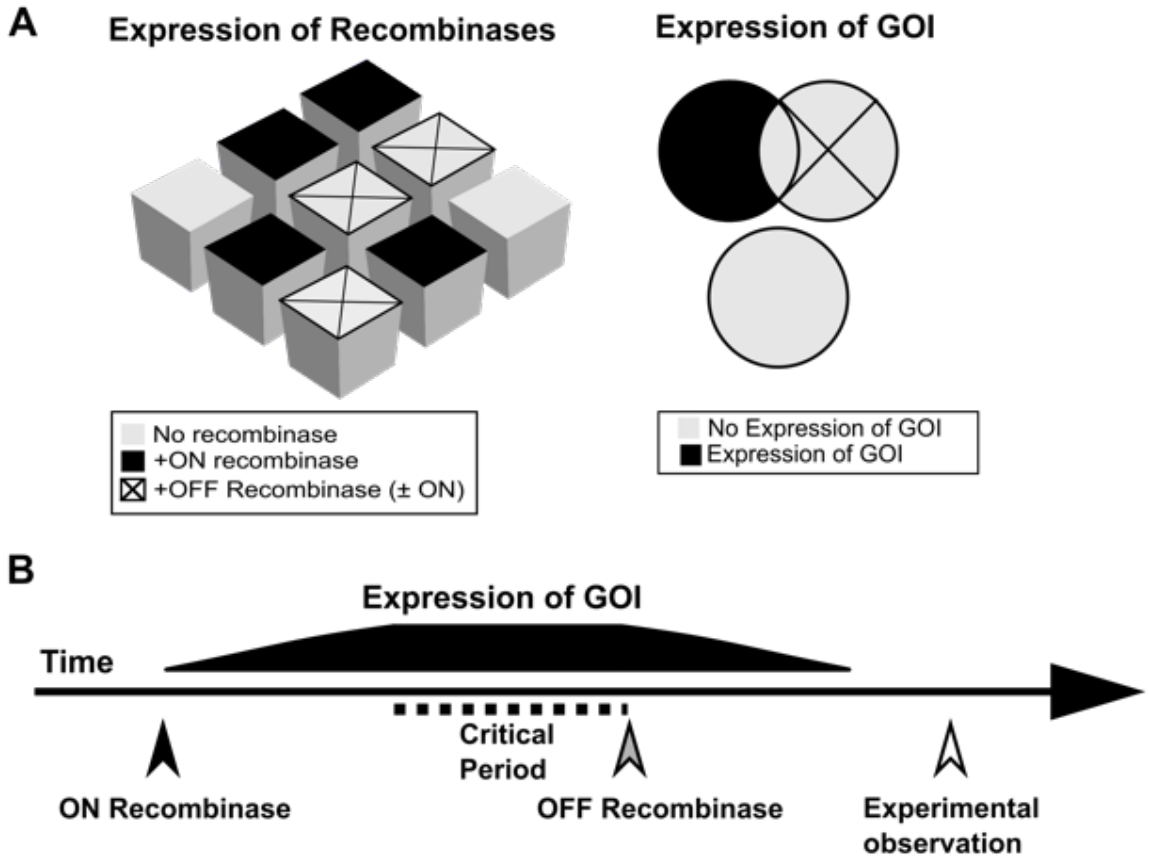

Figure 3.11. The ExBoX system can be utilized in multiple ways. (A) Expression of a gene of interest (GOI) can be restricted to a specific subpopulation of cells. Only the subpopulation of cells expressing the ON recombinase, but not the OFF recombinase, will express the GOI. **(B)** ExBoX can also be used for temporal control of expression. In this scheme, activation of the ON recombinase is used just prior to a critical period of interest. Introduction or activation of the OFF recombinase at the end of this critical period will turn off expression of the GOI. This serves to reduce confounding factors during later experimental observation, as GOI expression is no longer present.

Chapter 4

General Conclusions & Future Directions

Although the aims of these studies were very different, they were both able to address particular needs within the field of circuit development. The first Aim focuses on understanding the molecular mechanism of axon fasciculation as sensory axons enter the spinal cord. Our data suggest that Cas signaling adaptor proteins are required for fasciculation of growing DRG axons at the DREZ choice point. The loss of these proteins during peripheral sensory circuit building events demonstrates the importance of proper signal transduction in response to guidance cues. The second Aim centered around the design of the ExBoX Boolean viral system to turn expression of genes on and off at will. This system will make possible investigations of developmental events with enhanced cell-type and temporal specificity.

Cas adaptor proteins in axon fasciculation

While very little is known about the cytoplasmic proteins that allow axons to respond to guidance cues, our investigation of the Cas family of adaptor proteins was able to elucidate much about their role during guidance and fasciculation of vertebrate PNS axons. Our findings demonstrated that Cas adaptor proteins are expressed in the DRG central projections, and are required neuronal-autonomously for proper fasciculation of these projections at the DREZ choice point. Our *TcKO* Cas mutants demonstrated both fasciculation and defasciculation

phenotypes, suggesting that these proteins are required to regulate the decision of adherence by allowing axons to sense the extracellular substrate. We were able to support this notion by demonstrating an inability of cultured *TcKO* DRG explants to detect and grow over laminin, instead choosing to fasciculate with other axons in a cob-web phenotype. Ultimately, our results support the role of Cas effector proteins in regulating DRG axon fasciculation by allowing axons to detect the cues of the ECM substrate.

Although a great deal of investigation is still required to elucidate the exact roles of Cas proteins during mammalian axon guidance signaling, these findings establish a foothold for further advancement. Subsequent investigation should determine the upstream activators of Cas proteins at the DREZ choice point. Integrin receptors are known regulators of axon adhesion to the substrate, and a key candidate for upstream activation of Cas proteins at the DREZ. Roles for Cas proteins in the transduction of integrin signaling have been observed in axon fasciculation events in Drosophila (Huang et al., 2007), yet whether or not this receptor is the key upstream trigger of Cas proteins at the DREZ in mammals is unknown. Our DRG explant fasciculation assay in response to laminin offers strong support for Cas protein involvement in the detection of integrin binding partners. However, the observed role of Cas proteins in fasciculation of DRG peripheral projections adds complexity to this story. In contrast to the projections that converge at the DREZ requiring Cas proteins for fasciculation, the afferent

projections that innervate the periphery seem to require Cas proteins for defasciculation. While this could also be due to altered integrin signaling, the possibility of distinct fasciculation signaling pathways requiring Cas proteins exists. An investigation to delineate the upstream activators of Cas proteins at these two different choice points will be necessary to fully comprehend the role of these proteins in axon guidance and fasciculation. The study of the proteins recruited downstream of Cas activation will be equally interesting. Cas adaptor proteins have been shown to activate a member of the RhoGTPase family, Rac1 (Liu et al., 2007). Whether that role is conserved at the DRG choice points or a novel downstream effector is recruited needs to be revealed. As has been described (Koh et al., 2006), effector proteins such as those of the RhoGTPase family can have opposing effects on regulation of cytoskeletal rearrangement and axon adhesion. It is therefore pertinent to not only know what the signal of activation is, but to characterize the final effector proteins recruited as well.

ExBoX: cell specificity and temporal control of gene expression

Advancements in our understanding of the mechanisms underlying biological processes have been greatly dependent on the development of genetic tools. Once homologous recombination became widely available to generate loss-of-function alleles in mice (Capecchi, 1989), the next challenge became to control genetic deletion in a tissue specific manner. The introduction of recombinases as genetically encoded tools, in combination with conditionally targeted genetic

alleles, made overcoming the hurdle of tissue-specific deletion possible (Gu et al, 1994; Tsien et al, 1996). With the availability of recombinase-dependent systems, tissue- and region-specific gene knockouts, and progenitor tracing have now become routine experimental strategies in developmental genetics (Branda & Dymecky, 2004). A current limitation is the degree of specificity available in labeling particular pools of cells. Taking advantage of preexisting transgenic lines, intersectional approaches provide tighter specificity by selecting targets based on the overlapping or sequential expression of multiple recombinases (Jensen & Dymecki, 2014). The viral delivery of intersectional targeting strategies (Schnütgen et al, 2003; Atasoy et al, 2008; Gradinaru, 2010; Fenno et al, 2014) further adds to the control one can gain by selecting the region and time of injection (Zhang et al, 2007; Sternson et al, 2015). We designed a novel AAV-based intersectional approach to define and target specific subpopulations of cells via Expression by Boolean Exclusion (ExBoX). ExBoX uses AND NOT logic to control the expression of a coding sequence: a gene of interest is turned on by a particular recombinase and turned off by a different one. Thus, this strategy allows for the specific transcription of a gene of interest in cells expressing the single activating recombinase, but not in cells expressing both.

In addition to parsing out functional diversity, there is an interest in the field of developmental biology in being able to specifically turn genes ON and OFF during defined developmental windows or critical periods (Wiesel & Hubel,1963;

Kozorovitskiy et al, 2012). Viral Intersectional approaches using Boolean negation/exclusion could provide a solution to this problem: a gene of interest could be turned ON by a particular recombinase at a particular time point, while turned OFF later (AND NOT) by a different recombinase. Similarly, an apparent roadblock in the investigation of activity-dependent circuit refinement events is the need for tools that can manipulate the activity of circuitry and be activated or deactivated at a particular time of interest. While DREADDs and optogenetics offer possible solutions to this problem, they do so with many drawbacks and limitations. The ExBoX Boolean viral system offers another potential solution to regulate expression of reporters and activity manipulations. With activity manipulations driven by ExBoX, the investigation of circuit refinement events requiring manipulation of activity during limited windows are now more feasible than with the tools previously available. For example, a subset of projections that undergoes pruning during a specific time window can be specifically labeled and manipulated based on expression of one recombinase, and the activity manipulation can be turned OFF after said time window has elapsed with application of a second recombinase. DREADDs and Optogenetics would require the continuous upkeep of the manipulation with frequent drug application or light stimulation, respectively; and manipulations conferred by DREADDs and optogenetics can be inconsistent between dosing. In contrast, ExBoX requires only one activation and deactivation achieved via application or activation of the appropriate recombinase. As

demonstrated by this example, a key advantage of the ExBoX system over the previous tools is that expression of manipulations will be consistently maintained throughout the duration of the developmental event of interest.

One specific future application of the ExBoX system would be to investigate the requirement of activity in the refinement of mediodorsal thalamic (MD) projections to the medial prefrontal cortex (mPFC). While our preliminary unpublished work has confirmed the presence of a refinement event and a coinciding spike of activity during the refinement window, the requirement of activity in refinement of these projections is unknown. Using ExBoX to drive expression of activity-modulating transgenes such as *Kir2.1* and *NacBaCh* to increase or decrease activity, respectively, we can target specific projections for manipulation (such as those coming from the MD thalamus) based on genetic expression of one recombinase, and control the duration of the manipulation to coincide with the refinement window by inactivating the manipulation with expression of the second recombinase.

Significance

In summary, our studies have contributed original observations pertaining to axon fasciculation during neural circuit development, and have generated an efficient and universal tool to drive tightly controlled expression using Boolean exclusion logic. While our Cas findings add to the knowledge base of signal transduction during axon guidance, the importance of ExBoX in driving science

forward resides not only in adding new tools to the kit, but in making them easier to use, easier to build upon, easier to disseminate, and easier to adapt to different animal models and organs. We believe that our findings pertaining to Cas proteins during axon fasciculation will pave the way for many investigations of axon guidance in years to come. We also believe that the ExBoX tool will have a significant impact not only on the field of Neuroscience, but also on the fields of Cell and Developmental Biology, and Molecular Genetics.

References

Atasoy, D., Aponte, Y., Su, H. H., & Sternson, S. M. (2008). A FLEX Switch targets channelrhodopsin-2 to multiple cell types for imaging and long-range circuit mapping. *Journal of Neuroscience*, *28*(28), 7025–7030. https://doi.org/10.1523/JNEUROSCI.1954-08.2008

Branda, C. S., & Dymecki, S. M. (2004). Talking about a revolution: the impact of site-specific recombinases on genetic analyses in mice. *Developmental Cell*, *6*, 7–28.

Capecchi, M. (1989). Altering the genome by homologous recombination. *Science*, *244*(4910), 1288–1292. https://doi.org/10.1126/science.2660260

Fenno, L. E., Mattis, J., Ramakrishnan, C., Hyun, M., Lee, S. Y., He, Tucciarone, J., Selimbeyoglu, A., Berndt, A., Grosenick, L., Zalocusky, K.A., Bernstein, H., Swanson, H., Perry, C., Diester, I., Boyce, F.M., Bass, C., Neve, R., Huang, Z.J., & Deisseroth, K. (2014). Targeting cells with single vectors using multiple-feature Boolean logic. *Nature Methods, 11*, 763–772. https://doi.org/10.1038/nmeth.2996

Gradinaru, V., Zhang, F., Ramakrishnan, C., Mattis, J., Prakash, R., Diester, I., Goshen, I., Thompson, K. R., Deisseroth, K. (2010). Molecular and cellular approaches for diversifying and extending optogenetics. *Cell*, *141*(1), 154–165. https://doi.org/10.1016/j.cell.2010.02.037

Gu, H., Marth, J. D., Orban, P. C., Mosmann, H., & Rajewsky, K. (1994). Deletion of a DNA polymerase β gene segment in T Cells using cell type-specific gene targeting. *Science*, 265(5168), 103–106. https://doi.org/10.1126/science.8016642

Huang, Z., Yazdani, U., Thompson-Peer, K. L., Kolodkin, A. L., & Terman, J. R. (2007). Crk-associated substrate (Cas) signaling protein functions with integrins to specify axon guidance during development. *Development*, *134*(12), 2337–2347. https://doi.org/10.1242/dev.004242

Jensen, P., & Dymecki, S. M. (2014). Essentials of recombinase-based genetic fate mapping in mice. *Methods Mol Biol*, *1092*, 437–454. https://doi.org/10.1007/978-1-60327-292-6

Kozorovitskiy, Y., Saunders, A., Johnson, C. A., Lowell, B. B., Sabatini, B. L., Israel, B., & Medical, D. (2012). Recurrent network activity drives striatal synaptogenesis. *Nature*, *485*(7400), 646–650. https://doi.org/10.1038/nature11052.

Koh, C. G. (2007). Rho GTPases and their regulators in neuronal functions and development. *NeuroSignals*, *15*(5), 228–237. https://doi.org/10.1159/000101527

Liu, G., Li, W., Gao, X., Li, X., Jürgensen, C., Park, H. T., Shin, N. Y., Yu, J., He, M. L., Hanks, S. K., Wu, J. Y., Guan, K. L., & Rao, Y. (2007). p130CAS is required for netrin signaling and commissural axon guidance. *Journal of Neuroscience*, *27*(4), 957–968. https://doi.org/10.1523/JNEUROSCI.4616-06.2007

Schnütgen, F., Doerflinger, N., Calléja, C., Wendling, O., Chambon, P., & Ghyselinck, N. B. (2003). A directional strategy for monitoring Cre-mediated recombination at the cellular level in the mouse. *Nature Biotechnology, 21*, 562–565. https://doi.org/10.1038/nbt811

Sternson, S. M., Atasoy, D., Betley, J. N., Henry, F. E., & Xu, S. (2016). An emerging technology framework for the neurobiology of appetite. *Cell Metabolism*, *23*(2), 234–253. https://doi.org/10.1016/j.cmet.2015.12.002

Tsien, J. Z., Chen, D. F., Gerber, D., Tom, C., Mercer, E. H., Anderson, D. J., Mayford, M., Kandel, E. R., & Tonegawa, S. (1996). Subregion- and cell type–restricted gene knockout in mouse brain. *Cell*, 87(7), 1317–1326. https://doi.org/10.1016/S0092-8674(00)81826-7

Wiesel, T. N., & Hubel, D. H. (1963). Responses in striate deprived of vision cortex of one eye. *Journal of Neurophysiology*, *26*(6), 1003–1017.

Zhang, F., Aravanis, A.M., Adamantidis, A., Lecea, L., and Deisseroth, K. (2007). Circuit-breakers: optical technologies for probing neural signals and systems. *Nature Reviews Neuroscience* 8(August), 577–581. https://doi:10.1038/nr n2192